CRANFIELD UNIVERSITY

Lulu Zhou

Toxicity evaluation and medical application of multi-walled carbon nanotubes

Centre for Biomedical Engineering

PhD
Academic Year: 2011 - 2015

Supervisor: Dr Yi Ge & Prof Joe Lunec
January 2015

CRANFIELD UNIVERSITY

Centre for Biomedical Engineering

PhD

Academic Year 2011 - 2015

Lulu Zhou

Toxicity evaluation and medical application of multi-walled carbon nanotubes

Supervisor: Dr Yi Ge & Prof Joe Lunec
January 2015

This thesis is submitted in partial fulfilment of the requirements for the degree of PhD
(NB. This section can be removed if the award of the degree is based solely on examination of the thesis)

ABSTRACT

Carbon nanotubes (CNTs) are of special interest to industry and they have been increasingly utilised as advanced nanovectors in drug/gene delivery systems. They possess significant advantages including high surface area, well-defined morphologies, unique optical property, superior mechanical strength and thermal conductivity. However, despite their unique and advanced physico-chemical properties, the low compatibility of some of those materials [e.g. multi-walled CNTs (MWCNTs)] in most biological and chemical environments has also generated some serious health and environment concerns. Chemical functionalization broadens CNT applications, conferring new functions, and at the same time was found potentially altering toxicity. Although considerable experimental data related to functionalised CNT toxicity, at the molecular and cellular levels, have been reported, there is very limited information available for the corresponding mechanism involved (e.g. cell apoptosis, genotoxicity.

The toxicity of carbon nanotubes has been confirmed on many cell lines including A549 (lung cancer cell line) and MRC-5 (lung fibroblasts). However, the sensitivity of each cell line in terms of cellular morphology, apoptosis and DNA damage are still unknown. In this report the different levels of cellular response to oxidative stress and phagocytosis have been investigated in A549, MCF-7 and MRC-5 cell lines to better understand the mechanisms of the toxicity pathway.

siRNA as an ideal personalized therapeutics can specifically regulate gene expression, but efficient delivery of siRNA is difficult while it has been shown that MWCNTs protect siRNA, facilitate entry into cells.

In this study, we comprehensively evaluated the *in vitro* cytotoxicity of pristine and functionalized (-OH, -COOH) multi-wall carbon nanotubes (MWCNTs), via cell viability test, reactive oxygen species (ROS) generation test, cell apoptosis and DNA mutation detection, to investigate the non-toxic dose and influence of functional group in A549, MCF-7 and MRC-5 cells exposed to 1-1000 μg/mL

MWCNTs from 6 to 72 hours. In addition, 84 toxicity related genes have been detected to investigate the change of RNA regulation after treatment with MWCNTs. The research findings suggest that functionalized MWCNTs are more genotoxic compared to their pristine form, and the level of both dose and dispersion in the matrix used should be taken into consideration before applying further clinical applications of MWCNTs. Among all three cell lines, MCF-7 was the most sensitive to cell death and DNA damage induced by pristine carbon nanotubes. The majority of MCF-7 cell death was in necrotic. In A549 cells, apoptosis played a notable role in cytotoxicity. MRC-5 didn't show significant cell loss or membrane damage, which might be explained by its low cell growth rate, notably however, a great reduction of the F-actin and attachment points was observed after treatment which indicates that MRC-5 cells are under very unhealthy condition and less attached to the bottom of flasks. Despite their toxicity, which is still being researched, carbon nanotubes have a great potential in clinical medicine. Thus, understanding the sensitivity of different cell lines could offer a more individualized approach for future treatment regimes. In regards to gene delivery, MWCNTs were found to be less toxic than chemical agents (positive control) without weakening the delivery efficiency, which proves that MWCNTs have a good potential in medicine area.

Keywords: Multi-walled carbon nanotubes, characterization, aggregation, functionalization, cytotoxicity genotoxicity siRNA delivery, cell lines

ACKNOWLEDGEMENTS

I would firstly like to thank my mother and my father for their support and encouragement during the last 3 years, without their love and understanding this was not possible.

I also thank Professor Joe Lunec and Dr Yi Ge for their patience and guidance. I thank Dr Huijun Zhu for providing the A549 cell line as a gift, and Adeel Irfan and Dr Natalie Kenny and Dr Alex Charlton for their great help and advice in practice. I also thank Dr Xianwei Liu for his professional contribution in part of the project. Special thanks to Jake Chandler for his technical advice and long-term help in English improvement.

TABLE OF CONTENTS

LIST OF FIGURES

LIST OF TABLES

LIST OF ABBREVIATIONS

BSA	Bovine Serum Albumin
CAT	Catalase
CO_2	Carbon dioxide
CNT	Carbon nanotube
DCFH-DA	2′,7′-dichlorofluorescein diacetate (DCFH-DA)
DC	Dendritic cell
DMEM	Dulbecco's modified eagle medium
DNA	Deoxyribonucleic acid
DWCNT	Double wall carbon nanotube
EDS	Energy dispersive spectrometry
EGF	Epidermal growth factor
ELISA	Enzyme linked Immunosorbant assay
FT-IR	Fourier transform infrared
FITC	Fluorescein isothiocyanate
f-MWCNTs	Functionalized Multi-walled Carbon nanotube
FBS	Foetal bovine serum
GFP	Green fluorescent protein
GPx	Glutathione peroxidase
GR	Glutathione reductase
GSH	Glutathione
GST	Glutathione-s-transferase
H_2O_2	Hydrogen peroxide
IL-1	Interleulin-1
IL-6	Interleukin-6
IL-8	Interleukin-8
LDH	Lactate Dehydrogenase
LOP	lipid peroxidation
mM	Millimolar
mg	Milligram
M	Molar
MMT	Montmorillonite
MPS	Mononuclear phagocytic system
MTS	3-(4,5-dimethylthiazol-2-yl)-5-(3-carboxymethoxyphenyl)-2-(4-sulfophenyl)-2H-tetrazolium
MTT	3-(4,5-Dimethylthiazol-2-yl)-2,5-Diphenyltetrazolium Bromide
MWCNT	Multi-walled Carbon Nanotubes
Nm	Nano meter

NPs	Nanoparticles
8-oxo-dG	8-oxo-2'-deoxyguanosine
PI	Propidium iodide
PBS	Phosphate buffer saline
PCR	Polymerase chain reaction
PEG	Polyethylene glycol
RNA	Ribonucleic acid
ROS	Reactive oxygen species
RT	Reverse transcription
RT-PCR	Real-Time polymerase chain reaction
SD	Standard deviation
SEM	Scanning electron microscopy
SOD	Superoxide dismutase
siRNA	Small interference ribonucleic acid
SWCNTs	Single-walled Carbon Nanotubes
TE	Tris-EDTA
TEM	Transmission electron microscopy
TNF	Tumor necrosis factor
µg	Microgram
µg/mL	Microgram per millilitre
WST	Water soluble tetrazolium

Chapter 1

1 Introduction

Carbon nanotubes (CNTs) are a family of nanomaterials made up entirely of carbon. They have emerged as one of the most advanced nanovectors for highly efficient delivery of drugs and bio-molecules due to the several appealing features such as large surface areas with well-defined physico-chemical properties as well as unique optical, magnetic and electrical properties (Vashist et al., 2011). In the field of medicine, carbon nanotubes have already shown great potential for cancer therapy by gene/drug delivery (Safari and Zarnegar, 2014) and as immunologic adjuvants (Scheinberg et al., 2013).

Despite their industrial and clinic applications, some carbon nanotubes present low bio-compatibility in most biological and chemical environments, which has already generated some health concerns. It was found that some carbon nanotubes could cause the loss of cell viability (Uusitalo and Hempel, 2012), due to ROS production (Van Berlo et al., 2012) and DNA damage (Manke et al., 2013) both *in vitro* and *in vivo*. The toxicity issues of CNTs CNT-polymer nanomaterials against various cell lines have also been evaluated. It has suggested that the factors of CNTs such as fibre dose (He et al., 2011), length (Johnston et al., 2010), diameter (Nagai et al., 2011), surface area (Kim et al., 2011b), tendency to agglomerate (Kim et al., 2011b) and dispersibility in media (Kim et al., 2011b) could influence the toxicity and reactivity of CNTs *in vitro* and *in vivo*. For example, a recent study showed that the pathogenicity observed for asbestos-like long pristine MWCNTs could be obviated if their effective length is decreased (Ali-Boucetta et al., 2013). Elgrabli and his co-workers further reported that CNT dispersed in bovine serum albumin (BSA) could significantly reduce the resulting toxicity (Elgrabli et al., 2007). Vashist et al. (Vashist et al., 2011) reported that functionalized CNTs were able to exhibit very low toxicity and higher propensity to cross cell membranes, increasing their potential for drug and gene delivery. Some other researchers observed that agglomerates induced more pronounced cytotoxic effects than asbestos fibre at the same mass concentrations (Wick et al., 2007).

This thesis aims to establish how the structure, length, functionalization and dispersibility of carbon nanotubes could influence their toxicity (Figure 1-1). The mechanisms of toxicity of carbon nanotubes both *in vitro* and *in vivo*, which are still under investigation, as well as the roles of cell internalization in relation to cytotoxicity were also introduced and discussed.

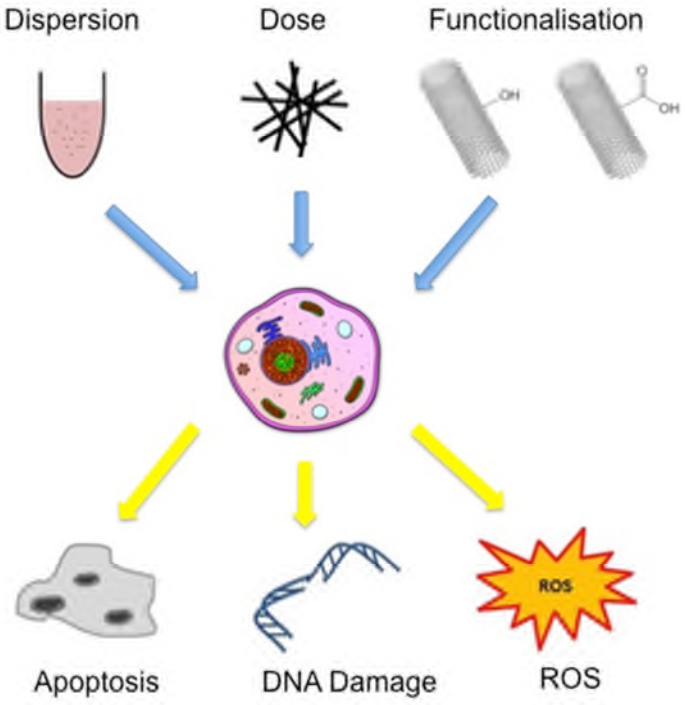

Figure 1-1 Factors (dispersion, dose and functionalization) which influence toxicity of CNTs and the endpoints (apoptosis, ROS and DNA damage) of cytotoxicity

1.1 .Carbon nanotubes

1.1.1 Structure and type of carbon nanotubes

Carbon nanotubes are allotropes of carbon with a cylindrical nanostructure. Nanotubes have been constructed with great length-to-diameter ratio (Avouris, 2002), significantly larger than any other material (Li and Chou, 2003) (Figure 1-2). These cylindrical carbon molecules have unusual properties such as aromatic and porous, which are valuable for nanotechnology, electronics, optics (Misewich et al., 2003) and other fields of materials science and technology. In particular, owing to their extraordinary thermal conductivity and mechanical

electrical properties, carbon nanotubes find applications as additives to various structural materials. Single-walled carbon nanotubes (SWCNTs) are composed of a rolled mono-layered graphene sheet and the diameter varies from 0.4 to 2nm (Klumpp et al., 2006a). SWCNT could be either semi-conducting or metallic (Popov, 2004). Multi-walled carbon nanotubes (MWCNTs) possess several concentric layers of graphite and the distance between each layer of a MWCNT is about 0.34nm. The diameter of MWCNTs varies from 1.4 to 100nm (Klumpp et al., 2006a). Unlike SWCNT, MWCNTs are only semiconducting (Popov, 2004). One of the most promising nanomaterial, the carbon nanotube, has attracted great attention in the field of molecular electronics (Avouris, 2002), sensoring (Qi et al., 2003) and cancer therapy (Qi et al., 2003) . However, the fact that CNTs are completely insoluble in all solvents has generated some health concerns. It was suggested that carbon nanotubes could accumulate in the human body, which then results in frustrated internalisation and inflammation, thereby potentially causing cancer (Donaldson et al., 2013). The similarity of the structure of CNTs to that of asbestos has prompted concern surrounding the exposure of humans, and so the applicability of the fibre paradigm to CNTs will be evaluated. (Johnston et al., 2010) Therefore, their biological properties are being studied for future applications (Colvin, 2003).

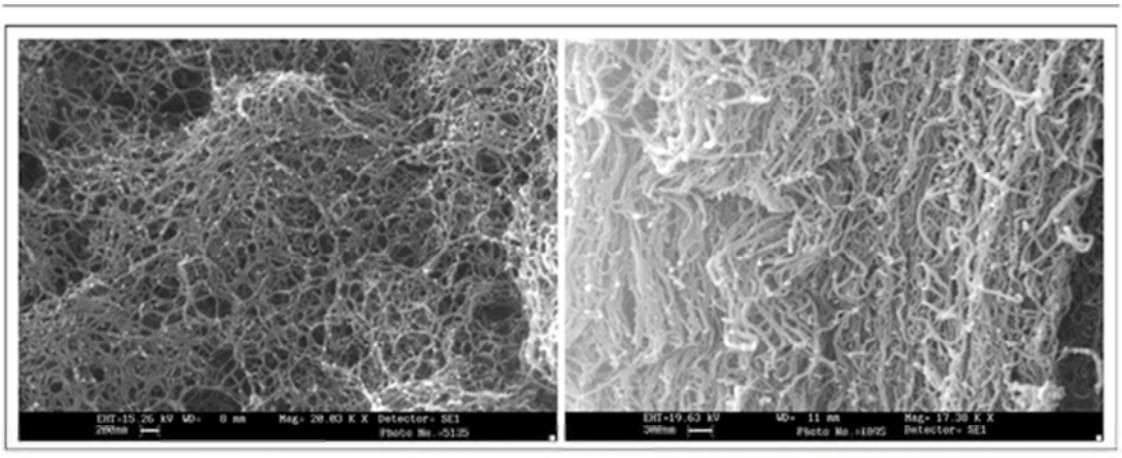

Scanning electron microscopy (SEM) images of pristine single- (left) and multi-walled (right) carbon nanotubes.

Figure 1-2 Carbon nanotubes. Left: SWCNT; Right: MWCNT (Bianco et al., 2005b).

1.1.2 Functionalization of Carbon nanotubes

It has been widely reported that structure functionalization of CNTs could optimise their solubility and dispersion, allowing innovative applications in materials and chemical processing (Martín et al., 2013a). Vashist et al. (Vashist et al., 2011) and Mali et al. (Mali et al., 2011) reported that functionalized CNTs were able to exhibit very low toxicity and higher propensity to cross cell membranes, increasing their potential for drug and gene delivery. The reduction of their length and addition of carboxylic groups increases their solubility (Liu et al., 1998) and dispersibility (Tasis et al., 2003) in aqueous solutions. Thus various methods of functionalization have been introduced to the production of more ‘useful’ carbon nanotubes with fewer side effects.

There are normally two functionalisation methods: covalent and non-covalent functionalization. In order to introduce the covalent bonds, two functionalisation approaches are widely employed for modification of CNT (Figure 1-3). CNT can be oxidised using strong acids, resulting in the reduction of their length while generating carboxylic groups, which increase their dispersion in aqueous solutions. Alternatively, it could also be reacted with amino acid derivatives and aldehydes to add solubilising moieties around the external surface. The non-covalent dispersion of CNTs in solution allows preservation of their aromatic structure and thus is able to retain their electronic characteristics (Figure 1-4). The dispersion procedures usually involve ultrasonication, centrifugation and filtration. Three classes of molecules were mainly used for CNT dispersion: surfactants, biopolymers (nucleic acids and peptides) and polymers (Klumpp et al., 2006b).

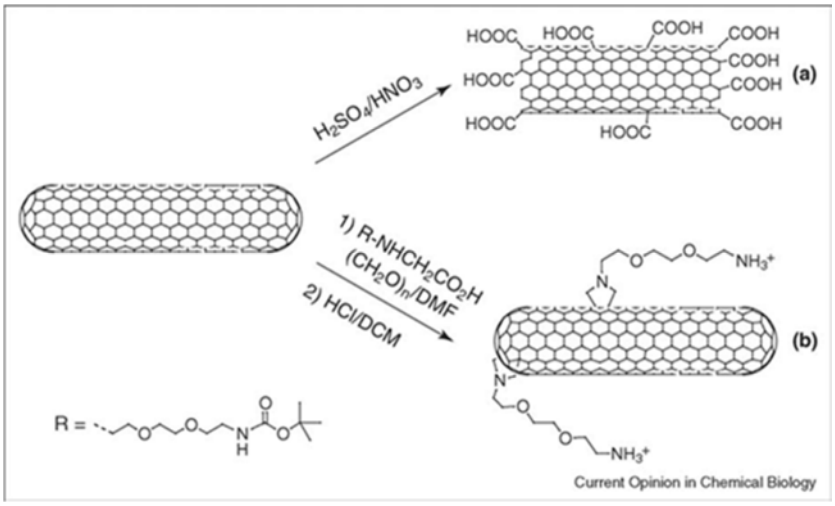

Figure 1-3 Example of a functionalization process of carbon nanotubes (Bianco et al., 2005b)

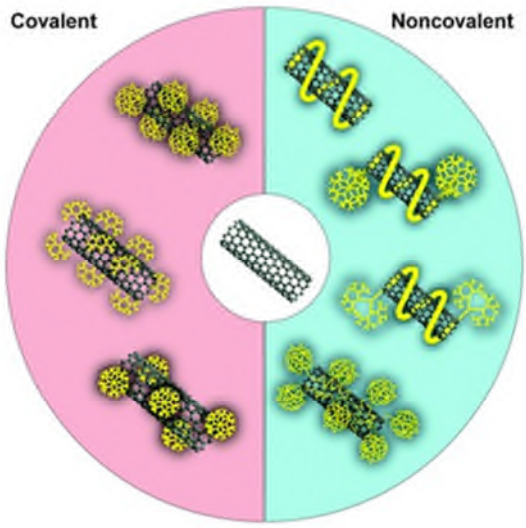

Figure 1-4 Covalent and noncovalent interactions between CNTs and linear, dendritic and hyperbranched polymers and also biomacromolecules for producing CNT-polymer hybrid nanomaterials as anticancer drug delivery system (Adeli et al., 2013)

1.1.3 Medical application of carbon nanotubes

1.1.3.1 Mechanism of internalization

These nanometer-sized materials offer distinct advantages for drug delivery. Because of their sub-cellular size, nanoparticles can penetrate deeply into tissues through fine capillaries, and are usually taken up efficiently by cells. This

property could result in increased efficiency for delivering therapeutic agents to target sites in the body (Panyam and Labhasetwar, 2003). M.P. Desai et al. reported that 100 nm size nanoparticles showed 2.5 fold greater uptake compared to 1μm, and 6 fold higher uptake compared to 10μm micro-particles in Caco-2 cell line (Desai et al., 1997).

Understanding of the mechanisms of cell entrance, intracellular translocation, subcellular locations, and excretions of CNTs is of great importance to understand the toxicity and potential applications of carbon nanotubes. On the basis of previous investigations, SWCNTs enter cells through direct penetration while MWCNT bundles enter through endocytosis (Mu et al., 2009). The nano-bundles then might transport through early endosomes to the sorting endosomes and are released afterwards (Figure 1-5).

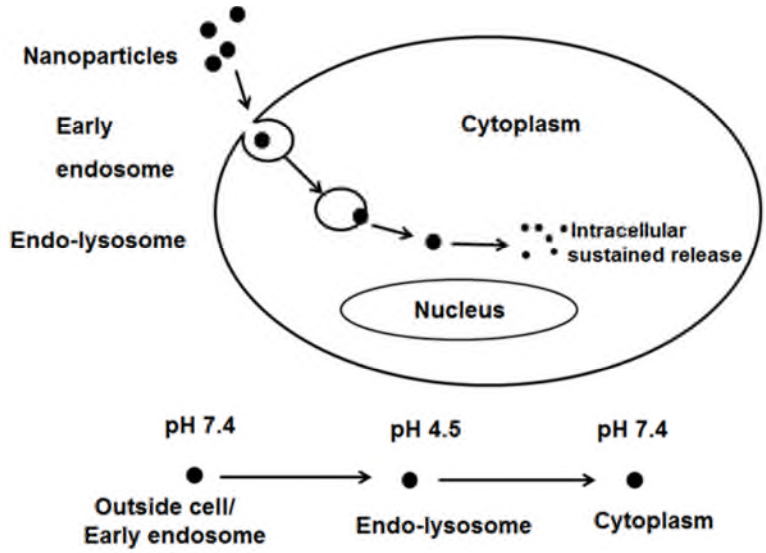

Figure 1-5 Process of nanoparticles internalization (Panyam and Labhasetwar, 2003).

1.1.3.2 Drug delivery

Cancer nanotechnology is a quickly evolving field of interdisciplinary research that involves the biomedical application of carbon nanotubes, which are nanoscale devices that are able to overcome biological barriers, specifically

recognize a single type of cancer cell, and accumulate preferentially in tumours (Hauser-Kawaguchi and Luyt, 2015).

Drug delivery can be simply described as the method, or process, of administering a pharmaceutical compound to achieve a therapeutic effect in humans or animals. Conventional drug delivery systems have some inherent limitations such as suboptimal bioavailability and limited effective targeting. Nanoparticles (NPs), comprised of nano-engineered complexes, are providing new opportunities and platforms for enabling targeted delivery of a range of therapeutic reagents such as drugs and molecules. Multifarious functionalities can be engineered within a nanoparticle complex. For instance, the surface attachment of cell-specific ligands would facilitate a targeted delivery, and the surface coating could increase circulation times for enhanced bioavailability. Specific materials on the surface, or in the nanoparticle core that enable the storage of therapeutic reagent, could result in a controlled release when the target site is reached. In addition, smart materials that are sensitive to stimuli such as specific enzyme, pH and local or remote actuation cues, could be conjugated to the nanoparticle complex, allowing smartly controlled delivery of therapeutic reagent to the target cells. In this context, Table 1-1 summarises and compares some recent examples of functionalized carbon nanotubes applied in drug and gene delivery.

Doxorubicin was frequently used in drug delivery research of carbon nanotubes. By varying the concentration of MWCNTs with the doxorubicin, it forms a conjugate. It shows high loading, prolonged release and improved cytotoxicity against cancer cells due to supra molecular interactions between the drug and MWCNTs. Some studies showed the phenomenal pH responsiveness and prolonged drug release to the cancerous microenvironment. SWCNT dispersions were stable in water for at least several weeks at room temperature, but SDC prepared dispersions were prone to agglomeration in the presence of salt and doxorubicin. The critical PL-PEG concentration for stability in physiologic conditions was about 5 times its critical micelle concentration.

Other anti-cancer drugs such as cisplatin and etoposide, and the pain killer ibuprofen were also applied in preclinical tests of carbon nanotubes for tumour treatment as listed in Table 1-1. Different methods of functionalisation of carbon nanotubes have been considered to increase their dispersibility and biocompartment delivery, efficiency. For example, sodium alginate was used to modify oxidized single-walled carbon nanotubes to improve their dispersibility. The humanized anti-vascular endothelial growth factor (anti-VEGF) monoclonal antibody was bound to the sodium alginate as targeting group to selectively kill the tumour cells (Ma et al., 2014). Successfully engineered poly (lactic-co-glycolic) (PLGA) functionalized CNTs to reduce toxicity concerns, provide attachment sites for pro-apoptotic protein caspase-3 (CP3), and tune the temporal release profile of CP3 within bone cancer cells.

Both SWCNTs and MWCNTs have a great potential as a drug carrier; however, the efficient formulation strategy requires further study (Anbarasan et al., 2015).

Table 1-1 Functionalised carbon nanotubes and their medical applications in drug and gene delivery

Type	Functional group	Delivered reagent	Target site	Reference
Oxidized multi-walled carbon nanotubes	PEGylated	Doxorubicin	Brain glioma	(Ren et al., 2012)
Multi-walled carbon nanotubes	Capping at the ends with functionalised gold nanoparticles to achieve a "carbon nanotube bottle" structure	Cisplatin	MCF-7 cells	(Li et al., 2012)
Single-walled carbon nanotubes	Chitosan-Ce6	Chlorine 6	HeLa cancer cells	(Xiao et al., 2012)
Single-walled carbon nanotubes	Epidermal growth factor (EGF)	Etoposide	A549	(Chen et al., 2012)

Type	Functional group	Delivered reagent	Target site	Reference
Single-walled carbon nanotubes	Dioleoylphosphatidyl ethanolamine-polyethylene glycol (PL-PEG) and sodium deoxycholate (SDC)	Doxorubicin	N/A	(Chen et al., 2012)
Multi-walled CNTs	Dendrimer-modified	Doxorubicin	high-affinity folic acid receptors (FAR)	(Wen et al., 2013)
Multi-walled CNTs	Carboxyl group	Ibuprofen	N/A	(Ali et al., 2013)
Single-walled CNTs	Polyethylene glycol (PEG)	Doxorubicin	Breast cancer cells	(Jeyamohan et al., 2013)
Oxidized carbon nanotubes	lactic-co-glycolic (PLGA)	Caspase-3	Osteosarcoma cells MG-63	(Cheng et al., 2013)

Single/Multi-walled CNTs	Polyethylenimine (PEI-NH)	Small interfering RNA (siRNA)	HeLa-S3 cells	(Huang et al., 2013)
Single-walled CNTs	Chit oligosaccharide	Gliotoxin	Human cervical cancer (HeLa) cells	(Bhatnagar et al., 2014)
Multi-walled CNTs	Amine-terminated TEG groups	Platinum(IV) prodrug, PtBz	Human breast cancer cells MCF-7	(Yoong et al., 2014)
Single-walled CNTs	Asparagine-glycine-arginine (NGR) peptide deoxycholate (SDC)	Tamoxifen	4T1cells/tumor-bearing mice	(Chen et al., 2013)
Single-wall carbon nanotube	cell penetrating peptide (CPP, including a positively charged segment, a linear segment, and a hydrophobic segment)	Small interfering RNA (siRNA)	Hela cells	(Jiang et al., 2013)

Single-walled carbon nanotubes	succinated polyethyleimine	Cy3-labeled siRNA specific to Braf (siBraf) and gene silencing in the tumor tissue	C57BL/6 mice melanoma model	(Siu et al., 2014)

1.1.3.3 siRNA delivery

Small interfering RNA (siRNA) is known to modulate enzymatic-induced cleavage of homologous mRNA and subsequently interrupt gene expression. siRNA gained its popularity in cancer therapy by its ability of inhibiting mRNA transcription and consequently the expression of the target gene would be silenced (Hutvágner and Zamore, 2002). However, some problems make the delivery of siRNA to specific tissue remain a great challenge. First of all, siRNA does not cross cellular membranes efficiently due to its relatively large size, low negative charge density and hydrophilicity. In addition, siRNA treatment gets hampered by its rapid degradation, poor cellular uptake, non-specific distribution and low endosomal escape efficiency. Several studies of functionalized CNTs have shown promising results. It has been reported that therapeutic silencing using ammonium, functionalized MWCNTs-mediated siRNA delivery can lead to tumour growth arrest (Al-Jamal et al., 2011). Ammonium-functionalized MWCNTs (MWNT-NH^{3+}) has been showed higher level of cellular internalization while exhibiting less toxicity compared to Pluronic F127 coated MWNTs (MWNT:F127) (Ali-Boucetta et al., 2011). However, the mechanisms and effects of different functionalization on cell internalization efficiency still remain unaddressed.

As listed in Table 1-1 all the functional group of carbon nanotubes for siRNA delivery were positive charged (succinated polyethyleimine, cell penetrating peptide and Polyethylenimine). SWCNTs were frequently used in those studies. More studies are needed to further compare the loading and delivery efficiency of SWCNTs and MWCNTs as well as the different functionalization.

1.2 Toxicity of carbon nanotubes

Recent experimental results have shown that carbon nanotubes could be toxic both *in vitro* and *in vivo* (Du et al., 2013). It has been suggested that MWCNTs caused the release of reactive oxygen species (ROS) and decreased the mitochondrial membrane potential in cells of the A549 line (Simon-Deckers et al., 2008). Similarly, *in vivo*, whilst the lungs of mice exposed to carbon black

were unaffected (Ma-Hock et al., 2013), those treated with carbon nanotubes exhibited an inflammatory response indicating greater toxicity of carbon nanotubes compared to carbon black (Lam et al., 2004).

In considering the need to exploit the full potential of medical applications of carbon nanotubes, it is imperative to systemically understand their bio-compatibility and comprehensively investigate their toxicity. The hazard assessment of exposure of CNTs to humans could be implemented via a variety of models.

1.2.1 Pulmonary toxicity

To understand the effects of carbon nanotubes on health, it is necessary to estimate their respiratory toxicity through inhalation (Figure 1-6). Existing data showed that CNTs could cause pulmonary inflammation as well as pulmonary fibrosis (Cui et al., 2005). Stoker (Stoker et al., 2008) assessed the health risk of carbon nanotubes on the human respiratory system by treating immortalised human fibroblasts with SWCNTs. The results showed an increased production of nitrous oxide and decreased cell viability after the exposure of immortalised human fibroblasts to different concentrations of SWCNTs. Similarly, the experiments conducted by Ursini (Ursini et al., 2012b) indicated a phenomenon of induction of apoptosis and DNA damage without cell membrane damage, suggesting a direct carbon-nucleus interaction. Li and his co-workers' *in vivo* study found that the aerosolized MWCNTs did not induce significant pulmonary toxicity in 30 days exposure. However, severe pulmonary toxicity was observed following 60 days of exposure (Li et al., 2009). In addition, it has been reported that carbon nanotubes might stimulate the production of TNF-α in the lungs of treated rats (Muller et al., 2005).

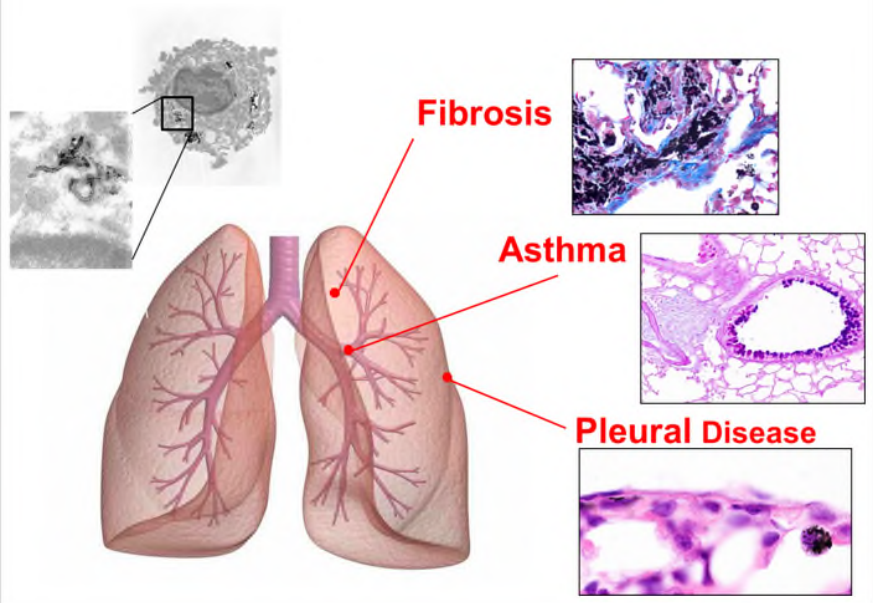

Figure 1-6 Effects of nanoparticles on pre-existing respiratory diseases, including fibrosis, asthma and pleural disease (http://bonnerlab.wordpress.ncsu.edu/research, 23/3/2015).

1.2.2 Neurotoxicity

Neurological diseases (e.g. Alzheimer's disease and Parkinson's disease) and stroke, including an extended range of disorders, have affected a large percentage of the world's population but the therapeutic efficacy is limited mainly due to the selectivity of the blood brain barrier (BBB) (Nunes et al., 2012). Despite the fact that there is a lack of study on intravenous administration for the treatment of brain tumours, therapeutic approaches based on the administration of CNTs via intracranial injection have shown some promising results. CNTs have been investigated as a candidate for the treatment of neurodegenerative diseases by enhancing the survival of neurons (Nunes et al., 2012). The effectiveness of amino-functionalised MWCNTs was successfully demonstrated by *in vivo* siRNA delivery to silence caspase 3 which promoted behavioural recovery in endothelin-1 stroke murine models (Nunes et al., 2012).

However, concerns regarding the neurotoxicity of metal nanoparticles have been raised due to their possible side effects on the brain. Silver nanoparticles

were found having an association with disturbance of the BBB (Win-Shwe and Fujimaki, 2011). *In vivo* experiments showed that silver nanoparticles induced more BBB disruption and caused more neuronal degeneration. However, another study suggested that similar nanoparticles were able to translocate through the BBB by endocytosis rather than by disruption of the barrier (Kreuter et al., 2003). Although the study of neurotoxicity of CNTs is still in its infancy, it is worth noting that Bardi et al. reported that pristine carbon nanotubes caused no adverse toxicological effect at the cellular level injected in the mouse cerebral cortex (Bardi et al., 2009).

1.2.3 Immune toxicity

The interaction of carbon nanotubes with the immune system plays a key role in their recognition and elimination. There have been many *in vitro* studies investigating the ability of MWCNTs to trigger an inflammatory response in immune cells such as macrophages, T cells and dendritic cells (DCs), or to modulate their function. MWCNTs have been found to activate the recruitment of macrophages and neutrophils and the secretion of cytokines such as IL-1β, TNF-αand IL-6 (Laverny et al., 2013). In the research work conducted by Kim et al. (Kim et al., 2013), macrophages treated with SWCNTs produced normal levels of nitric oxide but induced the expression of tumour necrosis factor. There also has been reported that the immune pathways activated by the carbon nanotubes are functionally relevant and important to the development of effective inflammatory response (Pescatori et al., 2013). MWCNTs were also found supressing systemic immune function, since T cell functions were inhibited in mice exposed to inhaled MWWCNTs for 2 weeks (Mitchell et al., 2009).

1.2.4 Genotoxicity

Genotoxicity can be defined as the damage to the genetic material encrypted within DNA. Well defined forms of DNA damage include strand breakage, oxidative DNA damage and accumulation of bulky adducts (Van Berlo et al., 2012). Genotoxicity could result from either physical interactions of particulate material with genomic DNA or from increased ROS generation on interactions

with other cellular components (Figure 1-7). The assessment of genotoxicity has shown that CNTs can damage DNA both *in vitro* and *in vivo* (Kato et al., 2013) In non-immortalised human dermal fibroblasts, both pristine and functionalized SWCNTs could elicit enhanced DNA strand breakage (Patlolla et al., 2010a). MWCNTs could also induce DNA strand breakage in A549 cells. Similarly, significant induction of DNA strand breakage was observed in murine bone-marrow cells after exposure to functionalised and pristine carbon nanotubes (Patlolla et al., 2010b).

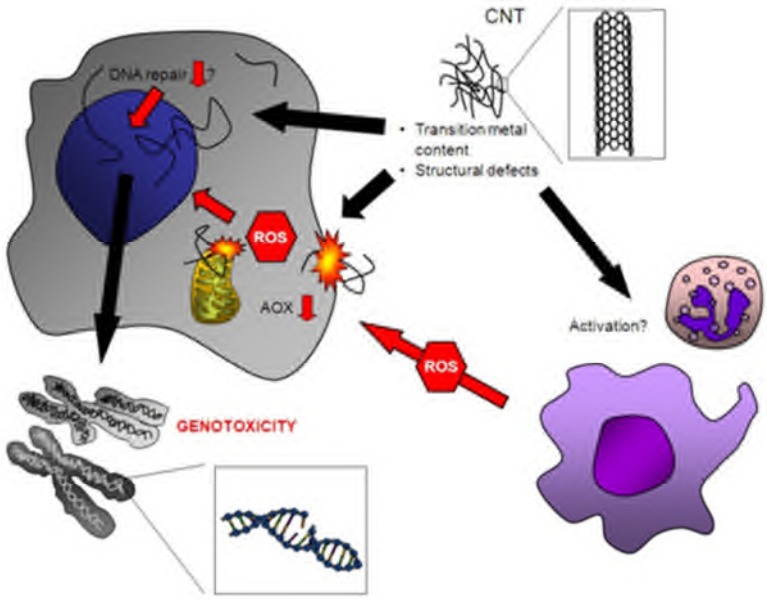

Figure 1-7 Proposed mechanisms of CNT genotoxicity (Van Berlo et al., 2012).

The induction of oxidative stress is considered a likely mechanism of carbon nanotubes exposure-associated genotoxicity. 8-hydroxy-2'-deoxyguanosine (8-OHdG) is one of the most frequently used index, which can be detected using liquid chromatography in the detection of DNA damage caused by oxidative stress. Other methods, such as the comet assay and micronuclei assay, could also be applied for the detection of DNA damage. It has been reported that SWCNTs could lead to augmented 8-OHdG in the lung and liver of rats after oral administration (Folkmann et al., 2009). In single and multi-walled carbon nanotubes treated RAW 246.7 cells, enhanced oxidation of purines was found by using comet assay (Van Berlo et al., 2012). Significant induction of micronuclei in A549 was also found in cells upon the treatment with SWCNTs

(Kato et al., 2013). In addition, apart from DNA damage, some CNTs could also inhibit DNA repair, which is regarded as one of the main mechanisms for the carcinogenicity (Beyersmann and Hartwig, 2008). Activation of p53, higher expression of 8-oxoguanine-DNA glycosylase (OGG1) and Rad 51 were detected in mouse embryonic cells treated with MW-CNTs, indicative of modulation of DNA repair (Zhu et al., 2007).

The carbon nanotubes treated DNA was transferred into bacteria Escherichia coli cells for mutation observation for mutation observation. Certain types and degrees of DNA damage were observed, such as single strand break and double strand break and bacterial mutation was confirmed. The DNA damage increased with contacting time in an exponential manner (Thongkumkoon et al., 2014).

1.2.5 Factors in relation to toxicity of carbon nanotubes

Carbon nanotubes are capable of exhibiting significantly different physical and chemical properties depending on their structure and other factors. As a result, their corresponding toxicity may be affected, determined and altered.

1.2.5.1 Length

CNT length is suggested to critically determine their toxicity. This stems from in vitro and in vivo rodent studies and in vitro human studies using cell lines (typically cancerous) (Sweeney et al., 2014) . It has been found that length could influence the clearance of carbon nanotubes, since it dictates the ability of phagocytic cells to completely internalize CNTs. Longer fibres promote the development of frustrated phagocytosis. They reduce the ability of clearance, thereby causing long-term damage (Johnston et al., 2010) (Figure 1-8).

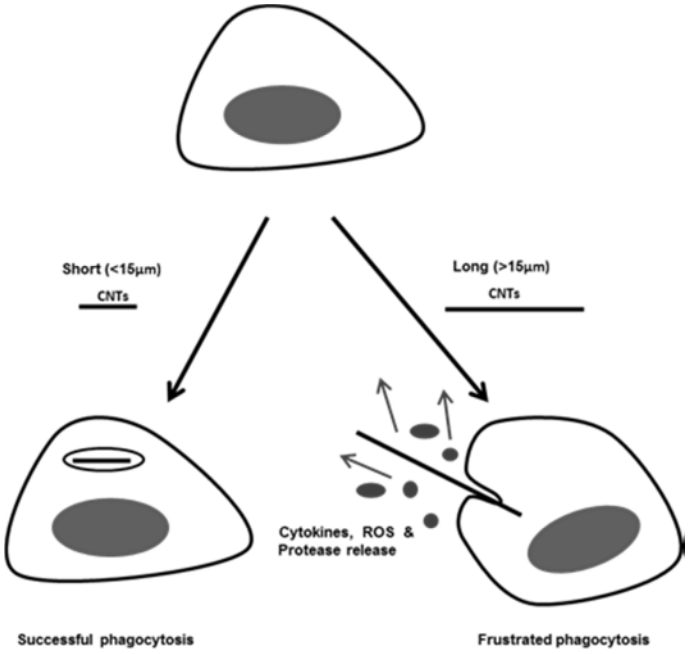

Figure 1-8 Importance of CNT length to their clearance by cells (Johnston et al., 2010).

Many studies have been published discussing the relation between the length of CNTs and their toxicity. It has been shown that longer carbon nanotubes are more toxic than the shorter ones. It is possible that short CNTs (<15μm) may be more readily taken up by cells but potentially enable the delivery of an enhanced dose to cells (Table 1-2). Most short CNTs were located in the cytosol of macrophages while longer CNTs remained free floating and stimulate frustrated phagocytosis with associated increases in ROS and TNF while short CNTs are easily internalized, with no ROS and TNF generated. According to most of the studies, long carbon nanotubes are more toxic compared with shorter ones, however, it was found that enhanced pro-inflammatory and pro-oxidative response was observed with short (oxidized) MWCNTs compared to long (pristine) MWCNTs (Bussy et al., 2012). These results could also been related to oxidation of carbon nanotubes rather than the length.

Table 1-2 Importance of length to toxicity of carbon nanotubes

Material	Length	Findings	Reference
Multi-walled CNTs	~0.22μm, >0.8μm	Most short CNTs were located in the cytosol of macrophages while longer CNTs remained free floating and caused inflammation	(Sato et al., 2005)
Single-walled CNTs	1 to 5μm	Functionalized and native SWCNTs of 1-5 mm in length had limited toxicity to endothelial cells *in vitro*.	(Albini et al., 2010
Multi-walled CNTs	220nm, 825nm	825 nm CNTs generate a stronger inflammatory response than 220 nm CNTs because cells are less able internalize them	(Sato et al., 2005)
Multi-walled CNTs	Long straight	Longer CNTs stimulate frustrated phagocytosis with associated increases in ROS and TNF while short CNTs are easily internalized, with no ROS and TNF generated.	(Brown et al., 2007)
Multi-walled CNTs	0.5-2μm/10–30μm	Increased length or diameter corresponded with increased bioactivity as measured by inflammasome activation.	(Hamilton Jr et al., 2013)

Material	Length	Findings	Reference
Multi-walled CNTs	Short: average length=0.94µm Long: average length=3.4µm	Inflammatory response in the lung was slightly higher for long MWCNTs than for short MWCNTs when compared at the same mass dose	(Lee et al., 2013)
Multi-walled CNTs	Short: 1.5 µm Long: 3-14µm	Longer (3 to 14 µm) MWCNTs exert high toxicity, especially to RAW264.7 cells, shorter (1.5 µm) MWCNTs are significantly less cytotoxic.	(Liu et al., 2012)
Multi-walled CNTs	Short: ~150nm Long: ~10 µm	The high aspect-ratio MWCNTs were found to be more toxic than the low-aspect-ratio MWCNTs.	(Kim et al., 2011a)
Multi-walled CNTs	Short: ~4.8 µm Long: ~9.5µm	Enhanced pro-inflammatory and pro-oxidative response was observed with short (oxidized) MWCNTs compared to long (pristine) MWCNTs.	(Bussy et al., 2012)

1.2.5.2 Functionalization

The fact that pristine CNTs are completely insoluble in all solvents has generated some health concerns. Consequently, their biological properties were studied in terms of toxicity (Tasis et al., 2003). The development of efficient methodologies for the chemical modification of CNTs has stimulated the preparation of soluble CNTs (Bianco et al., 2005b). Functionalized CNTs exhibit some promising characters: (1) high propensity to cross cell membranes (Mali et al., 2011); (2) increased efficiency of DNA transfer; (3) Improved immuno-stimulating activity.

Two functionalization approaches were widely employed for modification of CNTs. One was acid treatment resulting in COOH functionalized CNTs and OH functionalized CNTs, the other one was a basic treatment resulting in NH2 functionalized CNTs. It was demonstrated by Vashist et al that functionalized CNTs appeared to exhibit very low toxicity and were not immunogenic. Thus, they could be promising carriers with a great potential for the development of a new-generation delivery system for drugs and biomolecules (Vashist et al., 2011). Moreover, adequately functionalized CNTs could be rapidly eliminated from the body following systemic administration offering further encouragement for their development (Prato et al., 2008). However Liu et al (Liu et al., 2011) determined that COOH-CNT induced autophagic cell death in A549 cells through the AKT-TSC2-mTOR pathway and caused acute lung injury *in vivo*. Saxena et al also found that acid-functionalized SWCNT preparations exerted strong toxic effects *in vitro* and *in vivo* (Saxena et al., 2007).

Total gene expression analysis is a powerful approach to identify early biological responses *in vitro* and *in vivo* systems following exposure to carbon nanotubes (Sarigiannis et al., 2012). However, there is still limited information on how chemical functionalization may affect CNT toxicity. Literature data are controversial showing either increased or reduced toxicity associated with functionalization.

1.2.5.3 Aggregation

Endocytosis is an energy-using process by which cells absorb molecules by engulfing them. It is used by all cells of the body. Phagocytosis is the process by which cells bind and internalize particulate matter larger than around 0.75 µm in diameter, such as small-sized dust particles, cell debris, micro-organisms and even apoptotic cells, which only occurs in phagocytes such as macrophages.

Injected pharmaceutical nanoparticle products with a size in the range of about 50–100µm cannot be taken up by cells at all, because the particles are larger than the cells of the body (rather 6–10µm). Nanoparticles up to 1000 nm and particles with a size of a few micrometres can only be taken up by cells with phagocytic activity, e.g. the macrophages of the mononuclear phagocytic system (MPS). There are only a limited number of cells able to take up the particles. In addition, some of these cells are not easy to access; consequently, the toxic risk is limited. However, it is different for particles with a size below 100 nm as these particles could be taken up by all cells by endocytosis. Therefore, they can be considered as high risk nanoparticles (Müller et al., 2011) (Figure 1-9).

It has been reported that only non-aggregated CNTs that were free in the medium were able to reach the cytoplasm and subsequently the nucleus and then cause toxicity (Johnston et al., 2010). On the basis of experiments conducted by Song et al., the toxicity effects of SWCNTs on MCF-7 accompanied the increase of dispersibility stability in cell culture medium (Song et al., 2013). However, cellular uptake of well dispersed SWCNTs has been shown to result in higher delivery efficiency which will facilitate biomedical and biotechnological applications of SWCNTs (Mao et al., 2013).

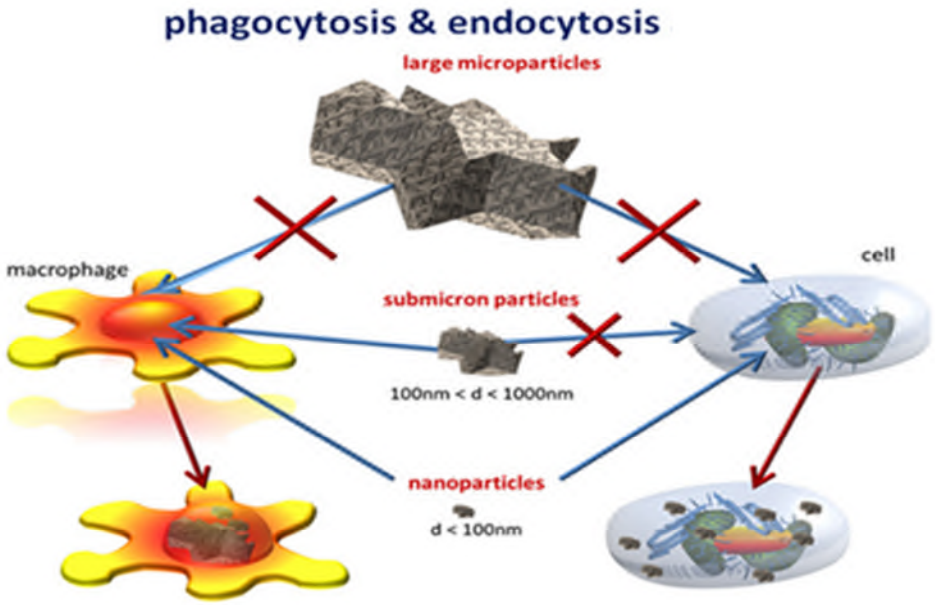

Figure 1-9 Mechanism of endocytosis and phagocytosis of nanoparticles in terms of particle size (Müller et al., 2011)

1.2.5.4 Layer thickness

The crystal structure of a nanotube depends on the axis along which the cylinder is formed from the graphene sheet. It is reported that thin (approximately 50nm diameter) multi-walled carbon nanotubes with a crystalline-like structure can pierce the membrane of mesothelial cells and can lead to inflammation and generation of mesotheliomas *in vivo* (Lin, 2007). Thicker carbon nanotubes caused less damage and were less carcinogenic (McCarthy, 2012).

1.2.5.5 Type

Comparison of cytotoxicity induced by different materials in alveolar macrophages showed that SWCNTs present more toxicity (Kang et al., 2008) compared to MWCNTs. The enhanced toxicity of SWCNTs may be attributed to: (1) A smaller nanotube diameter that facilitates internalization and partial penetration of nanotubes into the cell wall, (2) A larger surface area for contact and interaction with the cell surface, (3) Unique chemical and electronic properties generating greater chemical reactivity and metallic properties. For practical purposes, MWCNTs are more attractive than SWCNTs also because

of their relatively low production costs and availability in large quantities (Tahermansouri and Ghobadinejad, 2013). However, in comparison with SWCNTs, MWCNTs appear to receive more interests owning to their higher tensile strength, ease of mass production, low product cost per unit (Osswald et al., 2007), and enhanced thermal and chemical stability (Choi et al., 2014). In addition, unlike SWCNTs, MWCNTs could preserve their intrinsic properties of carbon nanotubes after the surface modification, where the outer wall of MWNTs is exposed to chemical modifiers.

1.2.5.6 Diameter

Higher aspect ratio nanotubes cause more health concern than lower aspect ratio nanotubes owing to their physical similarity with asbestos. Thinner carbon nanotubes generate more toxic effects both *in vitro* and *in vivo*. The cytotoxic activity, uptake, and ability to induce oxidative stress (ROS production and GSH depletion) were investigated by comparing Two samples of highly pure multi-walled carbon nanotubes with similar length (<5μm) but markedly different diameters (9.4 vs 70nm). The results indicated that thinner MWCNTs appeared significantly more toxic than the thicker ones, both *in vitro* and *in vivo* (Fenoglio et al., 2012). It has also been reported that thin multi-walled carbon nanotubes could lead to inflammation while the thicker version didn't (McCarthy, 2012).

1.2.5.7 Purity

Carbon nanotubes are primarily fabricated through catalytic methods and typically contain significant quantities of transition metal catalyst residues such as iron and nickel. Iron-catalysed generation has been hypothesized to contribute to oxidative stress and toxicity on exposure to carbon nanotubes *in vitro* (Kagan et al., 2006).

A number of studies have attempted to investigate the role of metals in CNT-induced toxicity. Early studies showed that SWCNTs containing a high (30%) iron content were able to elicit toxicity with cells (Shvedova et al., 2003). However further investigation by the same group also demonstrated that SWCNTs with low iron content were still toxic to mice, implying that iron may

not be the only reason for SWCNT toxicity (Shvedova et al., 2005). Lam et al. utilized a number of different CNTs samples that varied in purity. The result showed that there was no impact on SWCNT potential to produce granulomas, suggesting that granuloma formation was not simply related to iron content (Lam et al., 2004). However, in 2006, Kagan et al. utilized two types of SWCNT: iron-rich SWCNTs and iron-stripped (purified) SWCNTs to study their interaction with RAW 264.7 macrophages. The results showed that non-purified SWCNTs were more effective in generating hydroxyl radicals than purified SWCNTs and caused significant loss of intracellular low molecular weight Glutathione (GSH) and accumulation of lipid hydro peroxides in macrophages (Kagan et al., 2006).

1.2.5.8 Cell line

The type of cell lines could also determine the toxicity of CNTs. It has been reported that CNTs were toxic to all cells tested, but the H596 cells were most sensitive to the toxicity exerted by MWCNTs compared with H446 and Calu-1 (Magrez et al., 2006).Ye et al. (Ye et al., 2009) illustrated that MWCNTs were cytotoxic to A549 and BEAS-2A epithelial cells in a dose dependent manner (25-200 μg/mL). In addition, different mechanism of toxicity pathway could be presented on different cell lines. For example, MWCNTs were toxic to the RLE lung epithelial cell line via an apoptotic mechanism and introduction of gene mutation whilst were cytotoxic to A549 and BEAS by enhanced ROS production and the induction of an inflammatory response.

1.2.6 Toxicity Evaluation

1.2.6.1 Physicochemical characterisation

Characterization of carbon nanotube plays a vital role in toxicity evaluation as toxicity is related to their psychochemical character as mentioned earlier.

1. Scanning electron microscopy (SEM) and Transmission electron microscopy (TEM)

   TEM (Zhang et al., 2014b) and SEM (Abe et al., 2014) are frequently used to investigate length, shape, structure and aggregation of MWCNTs

SEM is an electron microscopy technique, which produces images by scanning samples with a focused beam of electrons. The interaction of the focused electrons with the electrons on the surface of the sample produces various signals enable visualising the length and diameter of carbon nanotubes. TEM are capable of imaging at a higher resolution than SEM and electrons could be transmitted through an ultra-thin specimen, interacting with the specimen as it passes through, thereby, giving better idea about the structure of MWCNT such as structure of side wall.

2. Energy dispersive spectroscopy (EDS)

   EDS is a technique for measuring the intensity of x-ray emission of energetic electrons, photons or ions. The method was applied in determination of trace metal ions in tap water and wastewater samples (Skorek et al., 2013). EDS could be applied for impurity detection of carbon nanotubes to provide idea about the recourse of toxicity derided from.

3. Fourier transform infrared spectroscopy (FTIR)

   FITC spectroscopy is used to assess the identity of molecular interactions and chemical bonds present in a sample. FT-IR is based on information gathered by infra-red examination of samples. Light is generated from a source, and passed through a monochromater (this may be a salt prism). This separates the source wavelengths. The selected wavelengths are then passed through the sample, according to the chemical properties some light is absorbed and this is recorded by the detector. The collected radiation is presented in a spectrum of absorbance or transmittance (Gable, 2000). It is applied to provide information about functional group on the surface of carbon nanotubes, although it’s not a quantitative method.

1.2.6.2 Cell counting

Cell counting is a very important step in conducting any in vitro experiment. Invitrogen countess was used in all the experiments to ensure high cell viability and cell number in plates seeding. The countess uses trypan-blue staining to differentiate between live and dead cells. Dead cells can easily be stained in blue while the live cells could exclude the dye from getting in inner cells as their membrane is intact. In Figure 1-10, the transparent cells are live cells.

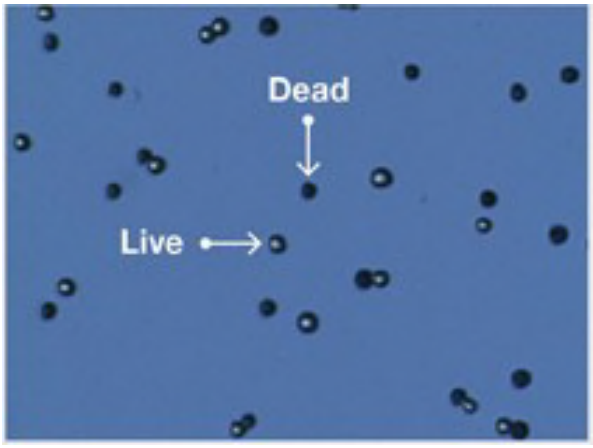

Figure 1-10 Cells stain with trypan blue under countess.

1.2.6.3 Morphology observation

Nanoparticles were found to lead to alterations in cell skeleton structure (Soenen et al., 2009) and could be evaluated by F-actin formation as determined by phalloidin staining. Phalloidin is a bicyclic peptide that belongs to a family of toxins and is commonly used in imaging applications to selectively label F-actin in fixed cells. Phalloidin could deliver significant advantages over antibodies for actin labelling. The binding properties of phalloidin conjugates do not change appreciably with actin from different species, including plants and animals. In addition, they exhibit negligible nonspecific staining, so the contrast between stained and unstained areas is high. It was suggested that nanoparticles diminished the efficiency of protein expression and hindered the mature actin fibres, and thus could have detrimental effects on cell migration and differentiation. It was also found that intracellular nanoparticle only transiently affect actin cytoskeleton architecture, formation of focal adhesion

complexes and cell proliferation: traits which return to control levels after approximately 7 days post incubation with magnetoliposomes in both 3T3 and C17.2 cell lines (Soenen et al., 2009). These studies pointed out the great need for thorough characterization of cell-nanoparticle interactions as subtle time-dependent effects are hard to monitor. Commonly used viability and functionality assays were not sufficient to address the broad spectrum of possible interferences of the nanoparticles with normal cell functioning in long term.

The effects on cells exposed to carbon nanotubes have been summarized in a working model (Figure 1-11). The non-aggregated CNT in suspension adsorbed to the substrate and affected cell spreading, development of focal adhesion points, development of the actin cytoskeleton and cell adhesion without seriously affecting other important parameters such as cell viability, apoptosis, and cellular signalling and cell-cell communication. These important cell functions were unaffected despite adhering to carbon nanotubes instead of the underlying surface, as long as the cells were exposed to a relatively low concentration of CNT. It seems that for the cells it makes no difference, if a part of the integrin is bound to CNTs, as long as a substantial amount of integrin is able to bind to substrate.

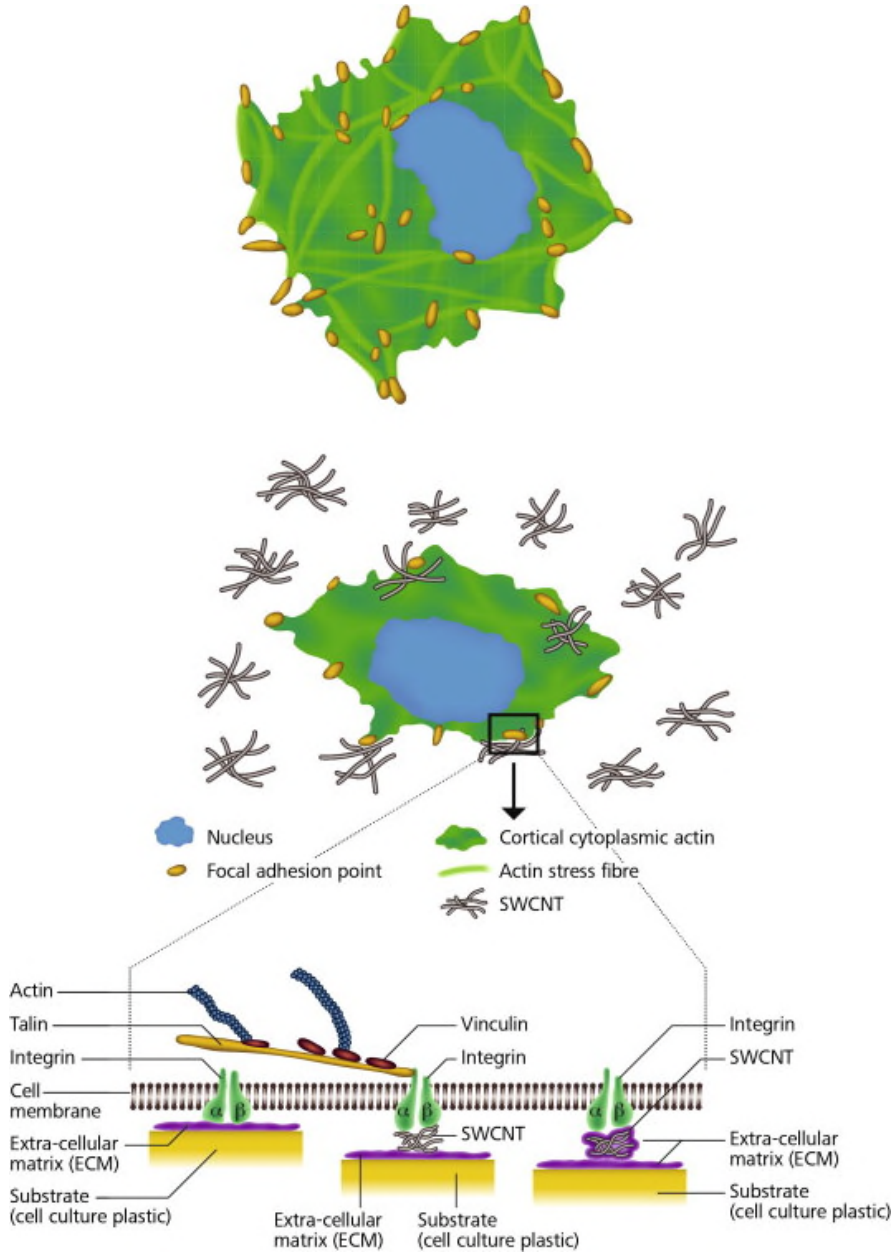

Figure 1-11 A working model for the adhesion of CNTs to cell integrins (Kaiser et al., 2013).

1.2.6.4 Viability assay

Cell viability assays include those dependent on mitochondrial activity, (Kaneko et al., 2014), DNA amount (nucleus stain), and cell membrane integrity (LDH, trypan blue).

1. Mitochondrial activity dependent assays

   All the MTT (Tan et al., 2015), CCK-8 (Li et al., 2014) and WST-1 (Cho et al., 2011) assays are mitochondrial activity-dependent assays. For MTT assay, enzymes are capable of reducing the tetrazolium dye MTT 3-(4,5-dimethylthiazol-2-yl)-2,5-diphenyltetrazolium bromide to its insoluble formazan, which has a purple colour. Other closely related tetrazolium dyes including WSTs, are used in conjunction with the intermediate electron acceptor (3-(4,5-dimethylthiazol-2-yl)-5-(3-carboxymethoxyphenyl)-2-(4-sulfophenyl)-2H-tetrazolium), in the presence of phenazine methosulfate (PMS), which produces a formazan product that has an absorbance maximum at 490-500 nm in phosphate-buffered saline. The WSTs assay are often described as a 'one-step' MTT assay, which offers the convenience of adding the reagent straight to the cell culture without the intermittent steps required in the MTT assay. WST-1 and WST-8 (CCK-8) based assays are reported to possess higher sensitivity than MTT based assays due to the formation of soluble formazan. CCK-8 is not toxic to cells and exhibits highest detection sensitivity (Figure 1-12).

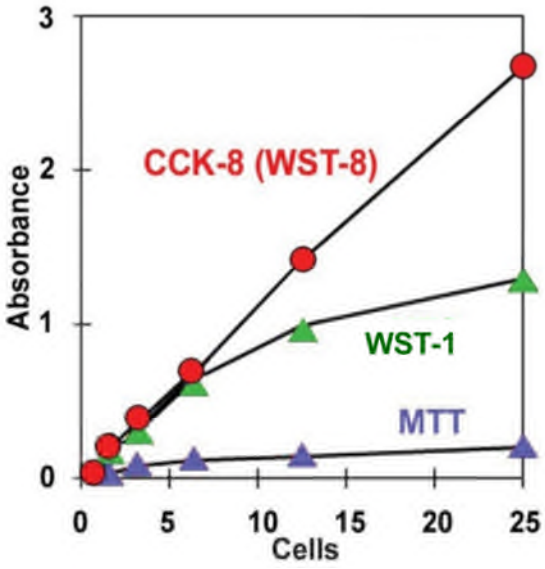

Figure 1-12 Sensitivity comparison of cell viability among MTT, WST-1 and CCK-8 assay (http://www.dojindo.com/Shared/Flyer/CK04_MTT_MTS_WST1.pdf, accessed on 01/04/2014)

2. Membrane integrity dependent assays

   Assessing cell membrane integrity is also one of the most common ways to measure cell viability. Compounds that have cytotoxic effects often compromise cell membrane integrity. Vital dyes, such as trypan blue (Sheng et al., 2012) or propidium iodide (PI) (Overchuk et al., 2013) are normally excluded from the inside of healthy cells; however, if the cell membrane has been compromised, they freely cross the membrane and stain intracellular components. Alternatively, membrane integrity can also be assessed by monitoring the passage of substances that are normally sequestered inside cells to the outside.

3. DNA amount dependent assays

   The direct way to measure DNA amount is to dye cell DNA using fluorescent assays and followed by fluorescence intensity detection. The frequently used DNA dyes are PI, DAPI, 7-AAD and Hoechst.

1.2.6.5 Apoptosis analysis

Apoptotic DNA fragmentation is a key feature of apoptosis, a type of programmed cell death. Apoptosis is characterized by the activation of endogenous endonucleases with subsequent cleavage of chromatin DNA into internucleosomal fragments of roughly 180 base pairs (bp) and multiples thereof (360, 540 etc.) (Walker et al., 1993). Carbon nanotubes were reported to cause apoptosis in certain cell lines such as A549 (Ursini et al., 2012a) (Fujita et al., 2013) and MCF-7 et al.(Song et al., 2013). Many techniques have been developed for apoptosis detection. For early apoptosis detection, AnnexinV and PI double staining could be applied. Both DNA laddering and apoptotic body observation identify late apoptosis. (Herrmann et al., 1994).

Apoptotic bodies have been found in both A549 and HEK293 cell lines (Cui et al., 2005) (Srivastava et al., 2011). In the experiment conducted by Srivastava, the apoptotic cells were observed to exhibit typical apoptosis features such as membrane vesicles, nucleus condensation, fragmentation and apoptotic bodies (Srivastava et al., 2011).

1.2.6.6 Assessment of inflammatory factors

MWCNTs could induce cells to release inflammatory cytokines such as IL-6, TNF-α, and IL-1β *in vitro* (Hamilton Jr et al., 2013). Similarly, *in vivo*, the single walled carbon nanotubes significantly induced greater levels of IL-6 and IL-8 in rats exposed to SWCNTs than those exposed to the control treatment (Tian et al., 2013). Cytokines are a broad and loose category of small proteins (~5–20 kDa) that are important in cell signalling. They are released by cells and affect the behaviour of other cells, and sometimes the releasing cell itself. Leukocytes and vascular cells are both sources of cytokines and targets for them (Dosquet et al., 1995). The release of pro-thrombotic and inflammatory cytokines such as IL-1, IL-2 and IL-6 et al. (Wada et al., 1992) could imply oxidative stress and inflammation (Tian et al., 2013). They act through receptors, and are especially important in the immune system; cytokines modulate the balance between humoral and cell-based immune responses, and they regulate the maturation, growth, and responsiveness of particular cell populations. Some cytokines

enhance or inhibit the action of other cytokines in complex ways. Thus, the assessment of inflammatory factors would facilitate understanding the mechanism of toxicity induced by CNTs. Inflammatory factor could be detected by ELISA, Weston Blot and RT-PCR.

1.2.6.7 Assessment of Antioxidants

Oxidative stress has been shown to play a pivotal role in the progression of disease pathogenesis and tissue damage by induction of inflammatory responses (Roberts et al., 2009). The latter one is caused by an imbalance between damaging oxidants and protective antioxidants (Pichardo et al., 2012). These effects are believed to be due to nanoparticles' large surface area to volume ratio, on which reactions producing ROS species can occur (Karakoti et al., 2006; Wallace et al., 2007).

Cells have built-in defences for neutralising oxidative stress by removing ROS by producing enzymes and using compounds like vitamins, such as vitamin C and E. Superoxide dismutase (SOD) is an enzyme that functions to counteract over production of ROS.

Biomarkers assayed include lipid peroxidation (LPO), total superoxide dismutase (SOD), catalase (CAT) activity (Beers Jr and Sizer, 1952), Glutathione reductase (GR), (Carlberg and Mannervik, 1975) glutathione peroxidase (GPx) and Glutathione-s-transferase (GST) (Habig et al., 1974). It has been reported that SWCNT could induce oxidative damage on cultured PC12 cells by formation of SOD, CAT and GSH (Wang et al., 2012). The change in vitamin E levels also resulted in alterations in antioxidant status, which increased susceptibility to oxidative stress (Shvedova et al., 2007).

To measure total amount of reactive oxygen species, 5-(and 6) - carboxy-2',7'-dichlorodihydrofluorescein diacetate (DCFDA) is very commonly used. When in contact with ROS, it is converted to fluorescent 5-(and-6)-carboxy-2',7'-dichlorofluorescein by oxidative cleaving of one acetate group (Herzog et al., 2009). Antioxidant can be measured by ELISA (Hussain et al., 2014), flow cytometer (Ye et al., 2010) or western blot (Ahamed et al., 2010).

1.2.6.8 Assessment of Gene mutation

As shown in Figure 1-13, through the period of exposure DNA could be damaged in the form of single and double strand breaks, loss of excision repair, abasic site formation and chromosomal aberrations. The compromised integrity of the genome can lead to cancer. Many sophisticated techniques including the comet assay (Kisin et al., 2007), the mouse lymphoma assay (Sofuni et al., 1996), the Ames test (Di Sotto et al., 2009) and the micronucleus assay (Lindberg et al., 2009) have been developed to assess CNT's potential to cause DNA damage. Fluorescent in situ hybridization and Giemsa staining was developed to look at chromosomal translocations and rearrangements. High throughput gene expression assays, such as RNA arrays (Hitoshi et al., 2012) could offer information clues as to which toxicity pathways are involved, which will facilitate further understanding of the mechanisms of toxicity.

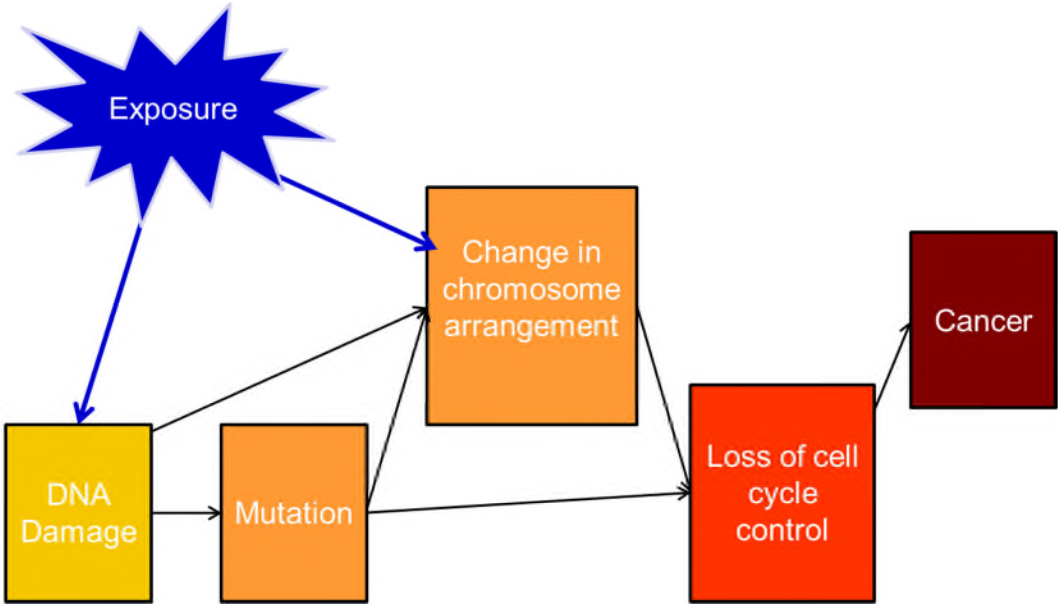

Figure 1-13 Schematic diagram of mechanism of genotoxicity induced by exposure to carbon nanotubes.

Numerous studies have been conducted in the last years on toxicological effects of CNTs. However, existing data are controversial and findings have been difficult to interpret in some cases. Gene expression profiling offers considerable potential for identifying chemical causation of effects induced in

exposures to complex mixtures and for understanding the mechanistic basis for their phenotypic effects.

Tanscriptomics analysis of the whole genome in the keratinocytes selected as *in vitro* models in this study showed that gene expression significantly differs according to the duration of exposure. A large number of genes (between 1200 and 2200) of A549 cell line changed their expression level when the cells were exposed for 6 hours to the different types of CNTs analysed, namely SWCNT, MWCNT, MW-NH_2 and MW-COOH. Only in case of SWCNT and MWCNT, long-lasting exposure (48 hours) resulted in a significant reduction in the number of genes expression differentially compared to the control. On the contrary, both types of functionalised CNTs showed practically no difference in the number of genes with modulated expression when comparing short and long term exposure. The mechanisms of time dependent pattern of pristine and functionalised CNT were not explained in this cited study. The results are summarized in the following tables (Table 1-3).

Table 1-3: Differential gene expression in the oxidative stress pathway and in the chemokine/cytokine signalling-mediated inflammation pathway in HaCaT cell line (Sarigiannis et al., 2012)

Duration (h)	SWCNT		MWCNT		MW-NH_2		MW-COOH	
	a	**b**	**a**	**b**	**a**	**b**	**a**	**b**
6	6	9	7	17	2	4	7	7
48	2	5	2	3	1	4	2	6

a, Differential gene expression in oxidative stress pathway; b, Differential gene expression in the chemokine/cytokine signalling-mediated inflammation pathway

Table 1-3 described analysis of the whole genome in HaCaT selected as in vitro model. A large number of genes changed their expression level when the cells were exposed for 6 hours to the different types of CNTs analysed.

The data of chemokine/cytokine signalling-mediated inflammation pathway showed a reduction in the number of genes that had modulated their expression level after long-term exposure (48 hours); on the contrary both types of functionalized CNTs showed practically no difference in the number of genes with modulated expression when comparing short and long-term exposure data.

In addition, functionalization contributes to the different degree of gene mutations. Through the in vitro observations, similar numbers of genes modulate their expression level after exposure to pristine SWCNTs and MWCNTs, whereas significant differences exist between the two functional CNTs: NH_2-MWCNTs exerted a less effect than the non-functionalized MWCNTs while COOH-MWCNTs affect a much higher number of genes.

Table 1-4 Comparison of modulated gene expression in the chemokine/cytokine signalling-mediated inflammation pathway between HaCaT and A549 cells (Sarigiannis et al., 2012)

Cell model	SWCNT	MWCNT	MW-NH_2	MW-COOH
HaCaT	9	17	4	7
A549	21	22	20	14

The same experiments (chemokine/cytokine signalling-mediated inflammation pathway) have been done on both A549 and HaCaT cell lines. A549 cells were much more sensitive than HaCaT cells in respect to genotoxicity (Table 1-4).

In summary, the mechanisms of carbon nanotube toxicity are not yet fully understood. It is evident from the literature that many variables influence both the nature and extent of carbon nanotube toxicity; both the physical properties of the nanotube and the affected tissue are important factors. However the existing studies strongly suggest that carbon nanotube toxicity cannot be neglected if the development of clinical applications is to progress and a better understanding of the toxicity mechanisms will help to minimise the risk of adverse side-effects. As well as the observed effects of carbon nanotubes on cell viability, morphology and behaviour it is also apparent that exposure to

carbon nanotubes influences gene expression. Thorough investigation of the effects of different types of carbon nanotubes on gene expression, in conjunction with the aforementioned traits, in a variety of systems may help to elucidate the important mechanisms of toxicity in each case. This in turn will provide valuable data for the customisation of clinical carbon nanotube applications.

In this thesis, the physical characterisation of MWCNTs such as diameter, aggregation and purity has been confirmed and investigated through SEM, TEM and EDS in the first part (Chapter 3). Then functionalisation (pristine, -OH and –COOH functionalised) dependent toxicity and cell line dependent toxicological mechanism of MWCNTs has been studied in the following sections. Multiple assays have been applied for geno- and cyto-toxicity evaluation including WST-1, LDH, AnnexinV-FITC, 8-oxodG, fluorescent stain and RNA array. In the last section, NH_2-MWCNTs has been used as siRNA delivery agent to inhibit certain gene expression and compared with chemical agent.

1.3 Aims and objectives

The specific aim of this project is to test the hypothesis that the functional group of MWCNTs has a critical role in toxicity mechanisms including oxidative stress, apoptosis, DNA damage and gene expression. Several specific objectives have been set to structure work progression throughout the project, as shown below:

1. To characterize of MWCNTs.

   The physical properties could play a key role in toxicity of carbon nanotubes. It was found that functionalization of carbon nanotubes could broaden their applications but would also modify toxicity by changing their dispersibility, degree of aggregation and the interaction with cells. This section aims to confirm the functional groups, purity, diameter and length of pristine, -OH functionalized and –COOH functionalized MWNCTs) which will be used for toxicity study and medical application.
2. To investigate the link of aggregation and toxicity
   BSA could allow a more uniform dispersion of MWCNTs in cell culture medium. MWCNTs dispersion with BSA and without BSA is compared.

3. To investigate the cytotoxic effects of the MWCNTs (pristine and functionalised), such as effects on cell morphology, the loss of cell viability, oxidative stress, apoptosis and DNA damage in lung cancer cell line A549.

   MWCNTs are suspended in cell culture media and incubated with A549 cells for 24, 48 and 72 hours. Wst-1, LDH, Annexin-V, ELISA, and DNA detection assays are applied to evaluate the toxicity of carbon nanotubes.
4. To investigate the cell line dependent toxicological mechanism
   Toxicity experiments are applied in three different cell lines (A549, MRC-5 and MCF-7) in order to find out the different sensitivity of cells to MWCNTs. Cell morphology, the loss of cell viability, oxidative stress, apoptosis and DNA damage are evaluated.

5. To study the relationship between toxicity effects and dose of MWCNTs.
   Dose dependence is a vital toxicological characteristic and it will also suggest the appropriate dose for medical application. IC-50, top effect and bottom effect will be evaluated from concentration 1 to 1000µg/mL.

6. To study toxicity related gene expression regulation after exposure to MWCNT *in vitro*.
   Expression of 84 toxicity related genes (oxidative stress, hypoxia, osmotic stress, cell death, inflammatory response, DNA damage signalling and heat shock protein related genes) are quantified to investigate gene regulation at transcriptional level which can help to understand the mechanism of toxicity.

7. To synthesize siRNA and NH_2-MWCNT delivery system and evaluate the delivery efficiency on GFP expressing MCF-7 cells.
   Concentration will be chosen according to literature review then the cell viability could be detected after the incubation with delivery system after 72 hours. The intensity of green fluorescent will be detected by both plate reader and confocal microscopy.

1.4 Rationale of the project

The toxicity potential and mode of action of multi-walled carbon nanotubes has been assessed using *in vitro* models. Based on the evidence that the characteristics including size, shape, aspect ratio and surface chemistry determines the toxicity properties of MWCNTs, the following hypothesis forms the basis of my research.

1. Toxicity of MWCNTs is related to functional groups and aggregation.
2. Metal content is not the most important factor in MWCNT toxicity
3. MWCNTs could induce cytotoxicity through mechanisms including apoptosis, oxidative stress and cell death
4. Toxicity mechanisms are cell line dependent and different cell lines would exhibit different levels of sensitivity.
5. DNA damage and the alteration of gene expression will be induced by MWCNTs
6. MWCNTs have a great potential in gene/drug delivery which will benefit drug development and gene therapy in the future.

To our best knowledge, this is the first investigation of the cell dependent mechanisms of toxicity induced by MWCNTs. In addition, the sensitivity of different cell lines to different types of MWCNTs was also never conducted by any other groups. The alteration of gene expression induced by MWCNTs (pristine and COOH functionalised is investigated to find the difference of genotoxicity in order to better understand the toxicity pathway for the first time.

The function of functional groups and aggregation in toxicity evaluation was very controversial according to the reported literatures. In this project, both cytotoxicity and genotoxicity of different functionalized MWCNTs are compared. Bovine serum albumin is added to find out if aggregation will increase the cytotoxicity or not.

Chapter 2

2 Materials and Methods

2.1 Materials

Table 2-1 Materials used in this study and suppliers

Material	Supplier	Cat no
Penicillin-Streptomycin (5,000 U/mL)	invitrogen	15070063
0.5% Trypsin-EDTA (10x)	Invitrogen	15400054
***In Vitro* Toxicology Assay Kit, MTT based**	Sigma-Aldrich	TOX1
Cell proliferation reagent WST-1	Roche	11644807001
2′,7′-Dichlorofluorescin diacetate	Sigma-Aldrich	D6883
Cell counting chamber slides	Invitrogen	C10312
Lactate dehydrogenase kit	Sigma Aldrich	TOX7
Dulbecco's modified eagle medium F-12	Invitrogen	31330038
Fluorescein isothiocyanate	Sigma Aldrich	F7250
Human foetal lung fibroblast cell line MRC-5 cells	Sigma Aldrich	84101801
Human breast cancer cell line	CELL BIOLABS.INC	AKR-211
Human lung carcinoma A549 cells	Sigma Aldrich	86012804
Hydrogen peroxide	Sigma Aldrich	216763
Annexin V-FITC Apoptosis Detection Kit	Sigma-Aldrich	APOAF
Annexin V-PE Apoptosis Detection Kit	eBioscience	88810272
Isopropanol	Sigma Aldrich	4028932L
RNeasy Mini kit	Sabioscience	217004
RNase-Free DNase Set	Qiagen	74104
Experion RNA stdsens reagents and supplies	Bio-Rad	7007154
Experion Electrode Cleaner	Bio-Rad	700-7252
High Capacity cDNA Reverse Transcription kit	Applied Biosystems	4368814
Safeview Nucleic Acid Stain	NBS Biological Ltd	NBS-SV1
GeneRuler Low Range DNA ladder	Thermo	SM1191

	Scientific	
2-Mercaptoethanol (100mL)	Sigma	M6250-100
QIAshredder (50 reactions)	Qiagen	79654
Bovine Serum Albumin	Sigma-Aldrich	A2153
Phosphate buffer saline tablets	Sigma-Aldrich	18912014
Albumin from Bovine Serum (BSA), Alexa Fluor® 488 conjugate	Invitrogen	A136100
Alexa Fluor® 633 Phalloidin	Invitrogen	A22284
Trypan blue stain 0.4%	Invitrogen	15250061
EGFP-siRNA	Invitrogen	AM4626
Lipofectamine RNAiMAX	Invitrogen	13778150
Virkon®	Anachem	330002
FlexiGene DNA Kit	Qiagen	51204
HT 8-oxo-dG ELISA KIT II	Trevigen	4380-096-K
Stress & Toxicity PathwayFinder	SABiosciences	PAHS-003Z
A549 cell line	Health Protection Agency Culture Collections	N/A
MCF-7 cell line	Cell Bio-Labs	AKR-211
MRC-5 cell line	Sigma-Aldrich	N/A

Pristine Multiwalled carbon nanotubes, carboxylic acid, hydroxy functionalized Multiwalled carbon nanotubes (COOH-MWCNT, OH-MWCNT and NH_2-MWCNT) were purchased at Cheap Tubes.Inc (United States, Sku-030111, 030112, 030113). Outside diameter: 13-18nm; functional group content: 7.0%+/-1.5%; length: 1-12µm; purity: >99wt%. Water used in all the experiment was deionized reverse osmosis water.

2.2 Main Instruments

2.2.1 Fourier Transform Infra-Red (FTIR-IR)

FTIR is a technique which is used to obtain an infrared spectrum of absorption, emission, photoconductivity or Raman scattering of a solid, liquid or gas.

2.2.2 Scanning electric microscope

SEM is a type of electron microscope that produces images of a sample by scanning it with a focused beam of electrons. The electrons interact with atoms in the sample, producing various signals that can be detected and that contain information about the sample's surface topography and composition. SEM produces various signals including secondary electrons (SE), back-scattered electrons (BSE), characteristic X-rays.

2.2.3 Transmission electric microscope

Transmission electron microscopy (TEM) is a microscopy technique in which a beam of electrons is transmitted through an ultra-thin specimen, interacting with the specimen as it passes through. An image is formed from the interaction of the electrons transmitted through the specimen.

2.2.4 Energy dispersive spectroscope

EDS is an analytical technique used for the elemental analysis or chemical characterization of a sample. It relies on an interaction of some source of X-ray excitation and a sample. It’s capabilities of characterization depends on the fundamental principle that each element has a unique atomic structure allpwing unique set of peaks on its X-ray emission spectrum.

2.2.5 Plate reader

Plate reader is an instrument which is used to detect biological, chemical or physical events of samples in microtiter plates. Common detection modes for microplate assays are absorbance, fluorescence intensity, luminescence, time-resolved fluorescence, and fluorescence polarization.

2.2.6 Flow cytometer

Flow cytometry is a laser-based, biophysical technology employed in cell counting, cell sorting, biomarker detection and protein engineering, by suspending cells in a stream of fluid and passing them by an electronic detection apparatus. It allows simultaneous multiparametric analysis of the physical and chemical characteristics of up to thousands of particles per

second. In this project, flow cytometer has been applied for apoptosis detection and cell internalization investigation.

2.2.7 RT-PCR

A real-time polymerase chain reaction is a laboratory technique of molecular biology based on the polymerase chain reaction (PCR), which is used to amplify and simultaneously detect or quantify a targeted DNA molecule and the amplified DNA is detected as the reaction progresses in real time using fluorescence.

2.2.8 Picodrop

Picodrop is used to measure the purity of DNA and RNA. Light travels from the light source onto a convex air/plastic interface and then onto a convex plastic/liquid interface. Next the light goes through the liquid sample and onto a concave liquid/plastic interface and then through a concave plastic air interface and onto the detector.

2.2.9 Experion™ Automated Electrophoresis Station (RNA Integrity detection)

The Experion automated electrophoresis station performs all of the steps of gel-based electrophoresis in one compact, durable unit. It automates analysis the integrity of RNA by combining electrophoresis, staining, de-staining, band detection, and imaging.

2.2.10 Confocal microscope

Confocal microscopy is an optical imaging technique for increasing optical resolution and contrast of a micrograph by means of adding a spatial pinhole placed at the confocal plane of the lens to eliminate out-of-focus light. It enables the reconstruction of three-dimensional structures from the obtained images which will provide information about nanoparticles-cell interaction and cell morphology. In this project, it has been applied for cell morphology and cell-CNT interaction observation.

2.3 Methods

2.3.1 Physical and Chemical Characterization of multi-walled carbon nanotubes

The practical work of SEM, TEM and EDS were operated by Dr. Xianwei Wang of School of Applied Science.

2.3.1.1 Fourier Transform Infra-Red (FTIR-IR)

The samples were mixed with potassium bromide (KBr) by grinding them in to powder, and then compressed into a disc. FTIR spectra of the samples were recorded in the spectral range of 4000 cm-1 to 400 cm-1 using a Nicolet FTIR (Thermo Ncolet).

2.3.1.2 Preparation of MWCNTs solutions

Weight 5mg pristine MWCNT/OH-MWCNT/COOH-MWCNT into 50mL tubes respectively. The material was suspended in FBS free medium (DMEM/F12, Invitrogen) medium at the concentration of 1000μg/mL (stock) followed by sonication (Hilsonic) for 20min. Then suspensions were prepared by dispersing and diluting the initial concentration of 1000μg/mL to yield 5, 20, 50 and 200μg/mL COOH-MWCNT.

2.3.1.3 Aggregation observation

1. Three types of MWCNTs were suspended at 200μg/ml in the serum free F12/DMEM cell culture medium with and without BSA. They were then place at room temperature on bench still for 5min.
2. A549 cells were seeded in 24 well plate 24 hours in advance. Pristine, -OH and –COOH functionalised MWCNTs were suspended in serum free cell culture medium at concentration 20, 50 and 200μg/ml in 24 well plate. The plate then was placed in incubator for 24 hours.
3. Pictures were taken by Canon and microscope.

2.3.1.4 Transmission electron microscopy (TEM)

Tested MWCNTs were suspended in water at 1 μg/mL and sonicated for 1 hour to minimise the aggregation. A droplet of this solution was allowed to dry on the

disc, and then allowed to dry by using hair dryer. The TEM used was Philips CM20.

2.3.1.5 Scanning Electron Microscopy (SEM)

Pristine and functionalised MWCNTs were dispersed in water at concentrations of 1 µg/mL and then followed by sonication for one hour to minimise the aggregation. A droplet of this solution was allowed to dry on the microscope stub and dried by hair dryer. These were imaged with High Resolution SEM (FEI XL30 SFEG analytical SEM).

2.3.1.6 Energy dispersive spectrometry (EDS)

Tested MWCNTs were suspended in water and sonicated for 30 mins to minimise the aggregation. The following steps were completed by Dr. Xianwei Wang of School of Applied Science.

2.3.1.7 MWCNTs treatment with ethylene-diamine-tetra-acetic acid (EDTA)

10mg pristine MWNCTs, OH-MWCNTs and COOH-MWCNTs were dispersed in PBS which contains 0.5M EDTA at 1000µg/ml respectively in 15ml centrifuge tubes. Then they were washed three times and re-suspended in cell F12/DMEM cell culture medium at concentration 200, 50 and 20µg/mL.

2.3.1.8 Carbon dots collection and dispersion

Carbon dot was a gift from Yanliang Gu in the same group. Basically, paraffin wax candles were lit and soot deposition was allowed on the bottom of the flask. Paraffin wax candle soot was then transferred into a round bottom flask with solution of nitric acid was made and mixed with deionised water in accordance to the molar calculation totalling up to 40ml solution. The ratio of carbon soot to nitric acid was stated to be 100mg: 40ml. Then the solution was then poured and mixed with the candle soot and set to reflux overnight followed with centrifugation. In the end, the washed sample was mixed with water to make a solution and frozen with help of liquid nitrogen before freeze drying. The samples were freeze dried at below -40°C overnight and even longer if needed.

Before using, C-dots were dispersed in DMEM/F12 cell culture medium to make the concentration of 200, 50 and 20µg/mL.

2.3.2 Toxicity study in relation to surface functionalisation in vitro

2.3.2.1 Cell culture

The passage numbers of A549, MRC-5 and MCF-7 used are 76-79, 3 and 9, respectively. Before using, bacterial, yeast and fungal contamination were checked under a microscope, and mycoplasma was tested using the Gibco's Mycotect kit (Cat.No. 15672017). All three cell lines were cultured in F12/DMEM (Dulbecco's Modified Eagle Medium) (Invitrogen, United Kingdom) supplemented with 10% fetal calf serum (Sigma-Aldrich, United Kingdom). All experiments were conducted using the identical passage number for each cell line. Six T-75 flasks of cells were collected and re-suspended in freezing media (90% serum+10% dimethylsulfoxide), and then they were aliquoted into 1mL vial. The cells were frozen at -20°C for 2 hours and then -80°C overnight. They were later moved to the -150°C freezer on the next day. The same protocol was repeated for more passages.

For culturing, cells were defrosted in water bath at 37 °C suspended in DMEM supplemented with 10% FBS and 1% antibiotics. The cells were seeded at a density of 1 x 10^5 cells/cm^2 in flasks and incubated at 37 °C under a humidified atmosphere with 5% CO_2 and 95% air. The cells were sub-cultured every 3-4 days. To subculture these cells firstly they must be detached, as they are all adherent cells, with trypsin-EDTA (0.25%), followed by centrifugation at 1200 RPM in Thermo-Scientific (UK) centrifuges. The cell pellets were collected and resuspended for further culture.

2.3.2.2 Cell counting

Cells were detached from the growth surface area with trypsin. Once detached the cells were centrifuged and resuspended in fresh media. A small volume was removed from this suspension and placed into Eppendorf tube and mixed with equal amount of trypan blue. 10µl of mixture is pipetted into a Countess Chamber slide® and analysed in the Countess®.

For MWCNT treatment, cells were stained with trypan blue for determining number and viability using a cell counter (Countess Automated Cell Counter, Invitrogen). Cells were seeded at a density of 1 x 10^4 cells per cm^2 of growth surface area in 96 well plates and left to attach over night at 37°C with 5% CO_2. The wells containing cells were filled with 200 µl of DMEM containing 25-100µg/ml of different dust NP or 'raw' NP samples. Cells without carbon nanotubes treatment were used as negative control. These were then examined at different time intervals (6-72 hours) for assessing different toxicity endpoints

2.3.2.3 Cell viability

200µl A549, MCF-7 and MRC-5 cells, were seeded in 96-well plates at 3×10^4 cells/mL each well and treated by carbon nanotube the following day for 24 hours. The tetrazolium salt WST-1 cell proliferation reagent was added to cells at the recommended concentration (5µl/well) and incubated at 37°C in a humidified atmosphere of 5% CO_2. Plates were shaken (3µM for 1 min) and absorbance was measured after 2 hours 405nM with a Varioskan Flash Multimode plate reader (Thermo Scientific). Unexposed cells were used as negative control.

2.3.2.4 IC50 curve

A549 cells were seeded in 96-well plates at 3×10^4 cells/mL each well and treated by carbon nanotube at concentration 1, 3.16, 10, 31.6, 100, 316 and 1000 µg/ml the following day for 24 hours. Then WST-1 was applied for proliferation test of cell viability of each treatment.

2.3.2.5 Cell growth curve

Cell growth curves were established for A549, MRC-5 and MCF-7 cell lines in 96-well plates. Cell number is confirmed at seeding by countess cell counter (Invitrogen, UK). For A549 cells and MCF-7 cells, the seeding density is 1×10^4, and for MRC-5 the cell density at seeding is 4×10^4. Then cells were placed in incubation and were subsequently counted at 24, 48 and 72 hours respectively using WST-1reagent. Then the data of these numbers were uploaded in excel

table format to *http://www.doubling-time.com/compute.php* (Roth, 2006). The cell doubling time were calculated based on the cell growth rate.

2.3.2.6 Cell membrane integrity

Lactate dehydrogenase activity release, used as indicator of cell membrane damage was measured by LDH assay kit (Cytotoxicity Detection Kit, sigma, United Kingdom) on the culture medium of cells exposed to MWCNTs for 24 hours. Unexposed cells were used as negative control. This colorimetric assay is based on the cleavage of a tetrazolium salt when LDH activity is present in the cell culture supernatant. Briefly, aliquots (50 µl) of supernatant and reaction mixture were transferred into corresponding wells of an optically clear 96-well plate and incubated for 30 min at 25 °C, protecting the plate from the light. The increase in enzyme activity directly correlates to the amount of formazan produced by reduction of the tetrazolium salt. The absorbance was measured at 490 nm using Varioskan Flash Multimode plate reader. A background and negative controls were obtained by LDH measurement of assay medium and unexposed cell medium, respectively. Data from control and MWCNT exposed cells were calculated as percentage of control and represent the mean of three independent experiments, each using triplicate wells per concentration.

2.3.2.7 ROS generation

The production of ROS was assessed on intact cells in 96 wells microplates using the dichlorofluorescein (DCF) assay after 6 hours treatment. 2′,7′-dichlorofluorescein diacetate (DCFH-DA) (Sigma, United Kingdom) was dissolved in culture medium to give a final concentration of 20 µM. Cells at 2×10^4/mL were incubated with the DCFH-DA solution (200 µl) at 37 °C for 30 min, and then washed with PBS (phosphate buffered saline) and re-suspended in 100 µl of PBS. The formation of the fluorescence oxidized derivative of DCF was monitored at an emission wavelength of 520 nm and excitation wavelength of 485 nm with Varioskan Flash Multimode plate reader. ROS production was expressed as fluorescence arbitrary units.

2.3.2.8 Cell uptake of pristine MWCNTs monitored by flow cytometry

1. Labelling of MWCNT with BSA-Alex488

MWCNT (2.0 mg) was dissolved into 2 mL deionized water by sonication for 20 minutes. BSA-Alex488 (2.0 mg) was dissolved in 2 mL PBS. MWCNT and Alex488-BSA were mixed with gently pipetting. MWCNT/Alex488-BSA mixture was incubated at 4°C overnight. Free BSA-Alex488 was removed through centrifuge (16,000g, 30 min) and washing. MWCNT/ BSA-Alex488 was re-suspended in cell culture medium (DMEM/F12).

2. Cell uptake detection

1mL cells were seeded in 6-well plate at 1×10^5/mL and then incubated with 50μg/mL MWCNT/Alex488-BSA for 12 hours the following day. Then the cell culture medium was removed and the cells were washed with 4ºC PBS to move any excess MWCNTs and debris which may interfere with the results. Cells were then loaded into flow cytometer for analysis (Accuri C6).

2.3.2.9 Cell uptake detection of pristine MWCNTs using confocal microscope

1. Labelling of MWCNT with BSA-Alex488 could refer to 2.2.2.7.
2. Cell treatment

   A549 cells were plated on chamber slides (Ibidi, Cermany) at 3×10^4/mL and allowed to attach overnight. Then they were incubated with or without MWCNT/Alex488-BSA for 12 hours. After incubation, A549 cells were washed three times with PBS. Chamber slides were then incubated at room temperature with Propidium iodide (PI) at 1mg/ml. Cells were directly visualized by confocal microscopy (LSM 510 META) and representative photographs were obtained.

2.3.2.10 Apoptosis detection

A549 cell apoptosis was evaluated by AnnexinV–FITC, PI apoptosis detection kit (Ebioscience, United Kingdom) binding to phosphoatidylserine in presence of calcium in the membrane of cells which are beginning the of DNA condensates indicative of apoptosis.

Cells were cultured in 48 well plate at 1×10^4/mL each well and then exposed for 48 hours to MWCNTs culture medium the following day; control cells were

incubated without MWCNTs. Before detection, the cell culture medium were removed and washed by cold PBS. Then the detached cells were centrifuged at 1200RPM and placed on ice. After a 10 minute incubation period with 2µl Annexin-V and 4µl PI, the cells were analysed by flow cytometer (Accuri C6).

2.3.2.11 Cell skeleton formation

Confocal microscopy allows the visualisation of morphology of cell skeleton by using a focused beam and excites only specific areas of interest in a sample through a pinhole which allows higher resolution.

A549, MRC-5 and MCF-7 cells were plated on chamber slides (Ibidi, Cermany) at 3×10^4/mL and allowed to attach overnight. Then they were incubated with or without MWCNTs at a concentration of 50µg/mL for 24 h. After incubation, the cells were fixed with 3.7% formaldehyde and permeabilised with 0.1% Triton X-100 in 2% BSA solution. Chamber slides were then incubated at room temperature with Alex 633-phalloidin. A549 cells were washed three times with PBS. Cells were directly visualized by confocal microscopy (LSM 510 META) and representative photographs were obtained.

2.3.2.12 Oxidative DNA damage

A549, MCF-7 and MRC-5 cells were seeded in 6-well plates exposed to pristine and functionalized MWCNTs at 50µg/mL for 72 hours. Control cells were incubated without MWCNTs. The concentration of 8-oxodeoxyguanosine (8-OHdG) in DNA, indicating oxidative DNA damage, was quantified by colorimetric antibody ELISA assay which has been widely used for the 8-OHdG detection.

a. DNA extraction

DNA isolation from cells treated with three types of MWCNTs was carried out by DNA extraction kit from QIAGEN (United Kingdom). The assay was performed according to manufacturer's instruction. After exposure to MWCNTs, cells were treated with cell lysis buffer and then centrifuged at 300×g for 3min. The supernatant was discarded and the tube was inverted on a clean piece of absorbent paper. The DNA pellets were cleaned using 600µg 70% ethanol and

then centrifuged at 10000×g for 3mins. Discard the supernatant and Air-dry the DNA pellets until all the liquid has evaporated. Then DNA was dissolved in Tris-EDTA buffer for 30min at 65°C. All the DNA samples were stored at -20°C for later use.

b. ELISA

The concentration of 8-OHdG was measured by HT 8-oxo-dG kit (TREVIGEN, United Kingdom) based on ELISA. The assay was performed according to manufacturer's instruction. Briefly, the DNA samples were diluted to 50µg/mL (Picodrop) and then further diluted 2:3 in Assay Diluent. 25µg 8-OHdG standards and DNA samples were added to each well, followed by adding 25µg monoclonal antibody. Then the plate was covered with film sealer and incubated at 25°C for 1 hour. After washing the plate 4 times with PBST, add 50µl HRP conjugate to each well, followed by 1 hour incubation. After aspirating and washing with washing solution, the plate was inverted and blotted against clear paper towels and this process was repeated four times. Each well was added 50µl of TACS-Sapphire^{TM} gently mixed and incubated at 37 °C for 15 min, then stopped with 50µl of 1M hydrochloric acid. Assay plates were read at 450nm with a plate reader.

2.3.3 Toxicity pathway finder-RNA array

RNA expression was analysed for genotoxicity at transcriptional level. A549.The PCR array is a set of optimized real-time PCR primer assays on 100-well ring for pathway or disease focused genes and includes blank control, positive control, housekeeping gene control and cDNA control. The PCR array performs gene expression analysis with real-time PCR sensitivity and the multi-gene profiling capability of a microarray. Simply mix cDNA template with the appropriate ready-to-use PCR master mix, aliquot equal volumes to each well of the same plate, and then run the real-time PCR cycling program.

The human RNA array was used (PAHS-003ZR-12, Qiagen). This array contains a total of 84 RNAs in 100 well disc formats. Each ring contained 84

sequence targets with 4 internal controls. Housekeeping genes were also present within each ring to allow normalisation of the results in post processing. The PCR was performed in the Qiagen rotor gene PCR machine.

The process of this experiment is showed as Figure 2-1: 1, RNA extraction; 2, RNA was reversed to cDNA; 3, real time PCR.

2.3.3.1 Cell treatment

A549 Cells were seeded in 6 well plates over night at 1×10^5/well over night. Then A549 cells were treated with pristine MWCNTs and COOH-MWCNTs MWCNT respectively for 48 hours at 50μg/mL. Cells with blank treatment were used as negative control

2.3.3.2 RNA extraction

RNA was isolated using RNeasy mini Kit (Qiagen, UK) according to the manufacturer's protocol. Briefly, cell lysate was homogenised using Qiashredder (Qiagen, UK) and followed by being mixed with ethanol. Then DNase set was used to remove genomic DNA. RNA was washed then dissolved using RNase-free water. The RNA samples were diluted to 200ng/mL after assessment of purity (A260/A280>1, A260/A230>1.8). The concentration was measure by picodrop (Picodrop) and the quality was confirmed by Bio-Rad Experion according to manufacturer's instructions.

2.3.3.3 Reverse transcription

1. The same amount of total RNA for reverse transcription of each sample was used (0.8 μg total RNA for Rotor-Disc 100 formats).
2. The genomic DNA elimination mix for each RNA sample was prepared according to Table 2-2.

Table 2-2 Genomic DNA elimination mix

Component	Amount
RNA	**800ng (4µl)**
Buffer GE	**2µl**
RNase-free water	**4µl**
Total Volume	**10µl**

3. The genomic DNA elimination mix was incubated for 5min at 42ºC, and then placed immediately on ice for at least 1min.
4. Reverse-transcription mix was prepared according to Table 2-3

Table 2-3 Reverse-transcription mix

Component	Volume for 1 reaction
5×Buffer BC3	**4µl**
Control P2	**1µl**
RE3 Reverse Transcription Mix	**2 µl**
RNase-free water	**3µl**
Total volume	**10µl**

5. 10µl reverse-transcription mix was added to each tube containing 10µl genomic DNA elimination mix.
6. Incubate at 42ºC for exactly 15min. then immediately stop the reaction by incubating at 95ºC for 5 min.

2.3.3.4 RT-PCR

1. PCR components mix was prepared in a 5mL tube, as described in Table 2-4

Table 2-4 PCR component mix

Array format	Rotor-Disc 100
2×RT^2 SYBR Green ROX FAST Mastermix	**1200µl**
cDNA synthesis reaction	**100µl**
RNase-free water	**1100µl**
Total Volume	**2400µl**

2. Program the real-time cycle according to Table 2-5

Table 2-5 Cycling conditions for Rotor-Gene cyclers

Cycles	Duration	Temperature	Comments
1	**10min**	**95ºC**	**HotStart DNA Taq Polymerase is activated by this heating step**
40	**15s**	**95ºC**	
	30s	**60ºC**	**Perform fluorescence data collection**

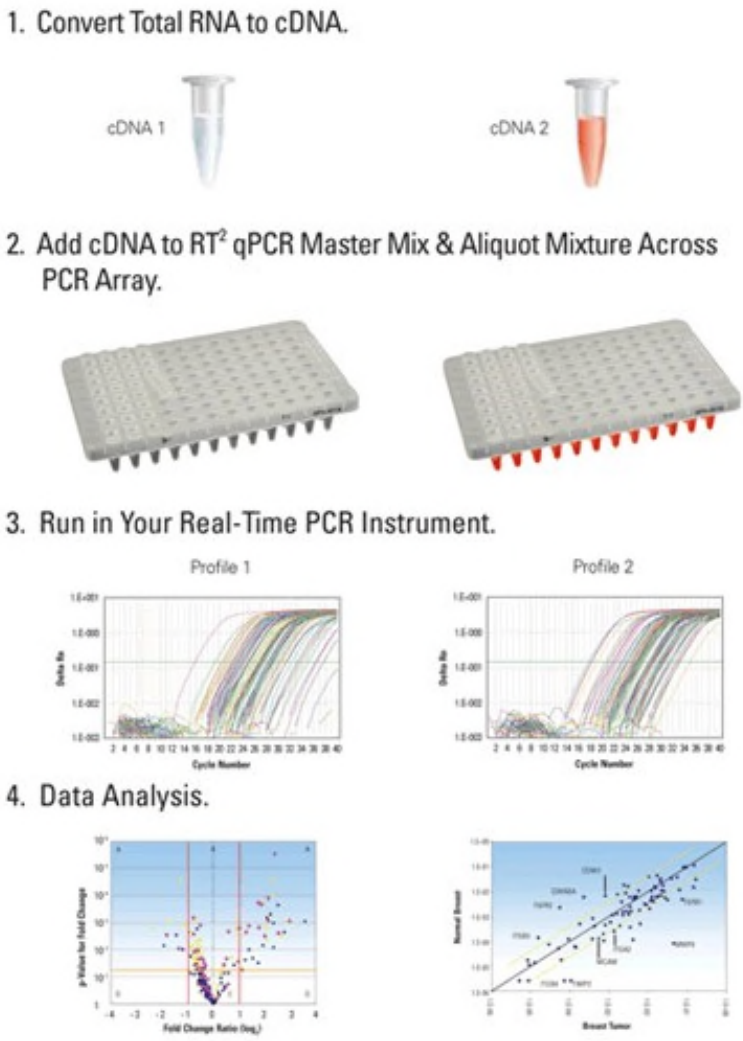

Figure 2-1 Schematic representation of RNA toxicity array.

2.3.3.5 Data interpretation

The formula used to calculate the relative gene expression level (2 ^ (-Δ Ct)) in the "Results" worksheet is: Δ Ct = Ct (GOI) – avg. (Ct (HKG)), where GOI is each gene of interest, and HKG are the housekeeping genes.

The Ct (cycle threshold) is defined as the number of cycles required for the fluorescent signal to cross the threshold. Ct levels are inversely proportional to the amount of target nucleic acid in the sample (the lower the Ct level the greater the amount of target nucleic acid in the sample).

During the exponential amplification phase, the quantity of the target DNA template (amplicon) doubles every cycle. For example, a DNA sample who's Ct

precedes that of another sample by 3 cycles contained 2^3 = 8 times more template. To quantify gene expression, the Ct for an RNA or DNA from the gene of interest is subtracted from the Ct of RNA/DNA from a housekeeping gene in the same sample to normalize for variation in the amount and quality of RNA between different samples. This normalization procedure is commonly called the ΔCt-method and permits comparison of expression of a gene of interest among different samples.

2.3.4 Enhanced green fluorescent protein (eGFP) inhibited siRNA delivery using NH_2-MWCNTs

2.3.4.1 siRNA delivery

1. Lipofectamine mediated cell transfection (positive control)

   Cells were seeded in a six-well plate at a density of 10^5/well. After 24 hours when they were 60-80% confluent, they were transfected with 10pmol eGFP siRNA using Lipofectamine RNAiMAX reagent according to the manufacturer's protocol. As shown in Table 2-6, firstly, 9μL Lipofectamine RNAiMAX reagent was diluted in 150μL Opti-MEM medium. Secondly, 3μL (30pmol) siRNA was diluted into 150μL Opti-MEM medium. Then they were left at room temperature for 5 min. final siRNA-lipid complex per well is 250μL.

Table 2-6 System of siRNA solution in siRNA delivery

Component	6-well
siRNA-lipid complex per well	**250μl**
Final siRNA used per well	**50 pmol (5μl)**
Final Lipofectamine® RNAiMAX used per well	**2.5 μl**

2. siRNA and NH_2-MWCNTs synthesis

9 µL aqueous solution of siRNA was added to a 2mL centrifuge tube with 250mL 1 µg/mL NH_2-MWCNTs. The mixture was thoroughly dispersed by vortexing for 30s and then was continuously sonicated for 5min.

3. Cell treatment

   MCF-7 cells were treated with 250µL NH_2-MWCNTs, Lipofectamine RNAiMAX and siRNA- NH_2-MWCNTs. Each treatment was repeated three times. Fluorescence was detected at 24, 48 and 72 hours respectively using plate reader. The excitation wavelength was at 488nm and emission wave length was at 509nm.

2.3.5 Statistical method

For cell viability, LDH, ROS, apoptosis, DNA damage, cell uptake, apoptosis detection and siRNA delivery assays, three independent experiments were performed. Each concentration was assayed in triplicate, in each independent experiment. The data were expressed as mean values of three replicates with standard deviation (mean ± SD). The results were represented as a percentage of the negative control (cells without treatment). Statistical analysis was carried out using analysis of variance (ANOVA), followed by Tukey's multiple comparison tests. Differences were considered significant from $P < 0.05$. *p<0.05, **p<0.01, ***p<0.001.

Three independent experiments of RNA array assay were ran with one replicate. All the date were uploaded to the template download from Qiagen website (http://www.sabiosciences.com/rt_pcr_product/HTML/PAHS-003Z.htmL) which automatically displays the replicate Ct values for the chosen housekeeping genes in samples and the then run the statistical tests.

Chapter 3

3 Physical and chemical characterisation of multi-walled carbon nanotubes

The characteristics of carbon nanotubes can determine the nature of their interaction with biomolecules and cells, and therefore their potential toxicity. It has been reported that the functionalization/modification of the structure of MWCNTs could optimise their solubility and dispersion, allowing innovative applications in materials (Martín et al., 2013b), electronics (Castranova et al., 2013), chemical processing (Martín et al., 2013a) and energy management (Mauter and Elimelech, 2008). However, the functionalization of MWCNTs raises more uncertainties about the toxicity. For example, Vashist et al and Mali et al. (Mali et al., 2011) reported that functionalized CNTs were able to exhibit very low toxicity and higher propensity to cross cell membranes (Vashist et al., 2011), increasing their potential for drug and gene delivery. On the contrary, Magrez et al. showed that the toxicity of MWCNT, in human lung-tumor cell lines, was increased when carboxyl and hydroxyl groups were present on their surface (Magrez et al., 2006).

Because of their geometry and hydrophobic surface, CNTs have a tendency to form agglomerates with a bundle-like form (Wick et al., 2007). Additionally, CNTs are bundled with an especially high van der Waals interaction energy which makes CNT dispersion one of the most important challenges for the application of CNTs (Girifalco et al., 2000). It has been reported that MWCNTs showed a very good dispersion in 0.5% bovine serum albumin (Elgrabli et al., 2007). Mercer et al.(2008) found that acetone treated CNTs tended to induce a fibrotic response whilst untreated CNTs were more likely to form granulomatous inflammation using mice as model.

The aim of this project is to confirm the functional group on the surface and aggregation tendency in cell culture medium of four MWCNTs (pristine, -OH and -COOH functionalised). Secondly, purity needs to be confirmed and how

the degree of dispersion and agglomeration affects MWCNTs cytotoxicity needs to be found out. EDS was applied to determine the impurity elements. The materials used in the project have purities above 99% according to the manufacturer's information. Both SEM and TEM figures were taken to characterize their diameter and surface shape. In addition, a comparison experiment of cell viability test (WST-1) of cells treated with MWCNT and BSA-contained MWCNT suspension, from 0 to 200μg/mL, has been conducted in order to evaluate toxicity of more thoroughly dispersed CNTs.

3.1 Results

The data of SEM, TEM and EDS were generated by Dr. Xianwei Wang of School of Applied Science.

3.1.1 SEM

SEM (Figure 3-1) showed the diameter range of Multi-walled carbon nanotube, which is 13-30nm. The graphs indicated that all three kinds of carbon nanotubes purchased are within the same diameter range, which in agreement with the information offered by datasheet.

The length of MWCNT could be many micrometres for all the types; however, it's difficult to find out by either TEM or SEM as the tubes are coiled. It is known that MWCNTs have a tendency to clump together to form bundles and entangled structures which are longer and wider than single tube (Donaldson et al., 2006).

Pristine MWCNT

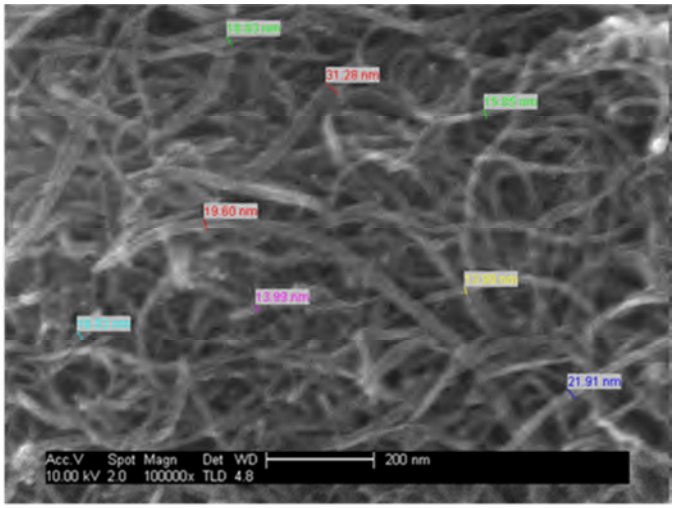

OH-MWCNT

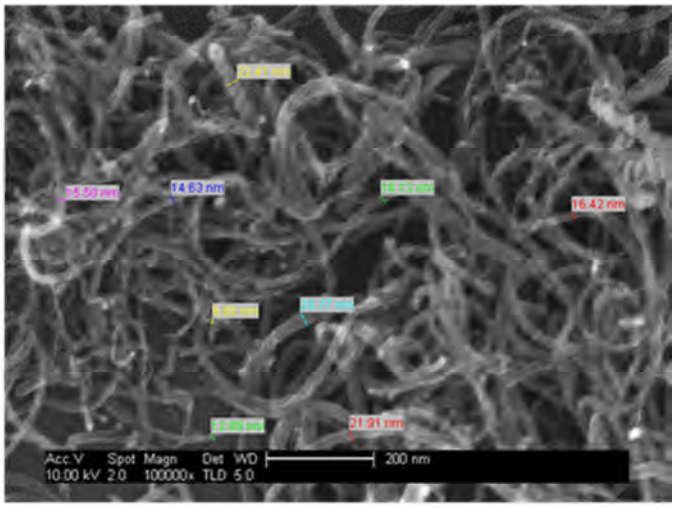

COOH-MWCNT

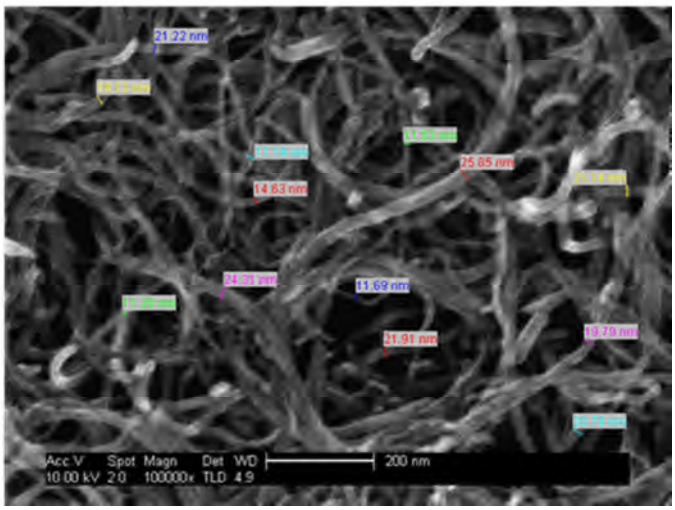

Figure 3-1 SEM images of pristine and functionalized MWCNTs. The MWCNTs were distributed in water. The diameter of them was marked on the pictures. The scale bar corresponds to 200nm.

3.1.2 TEM

The TEM image indicates all three types of MWCNTs are mainly mono-dispersed. Pristine carbon nanotubes have smoother surface compared with the functionalized ones (Figure 3-2). As all the samples have been put under sonication for 30 min, no aggregation is found according to the figure. Same as SEM figures, all the MWCNTs are tangled, so it's difficult to measure their length. The picture on the right had higher resolution than the pictures on the left and through them, the structure and the surface of carbon nanotubes could be observed. Pristine MWCNTs have smoother surface than the functionalised MWCNTs.

TEM is better for this application as the transmission of electrons through the material will allow the visualisation of particles deep below the surface film. The high electron density created by their aromatic structure makes them easily observable by transmission electron microscopy. Unlike SEM which could only provide information about materials' surface, TEM showed the multi-walled structure through the high resolution photos.

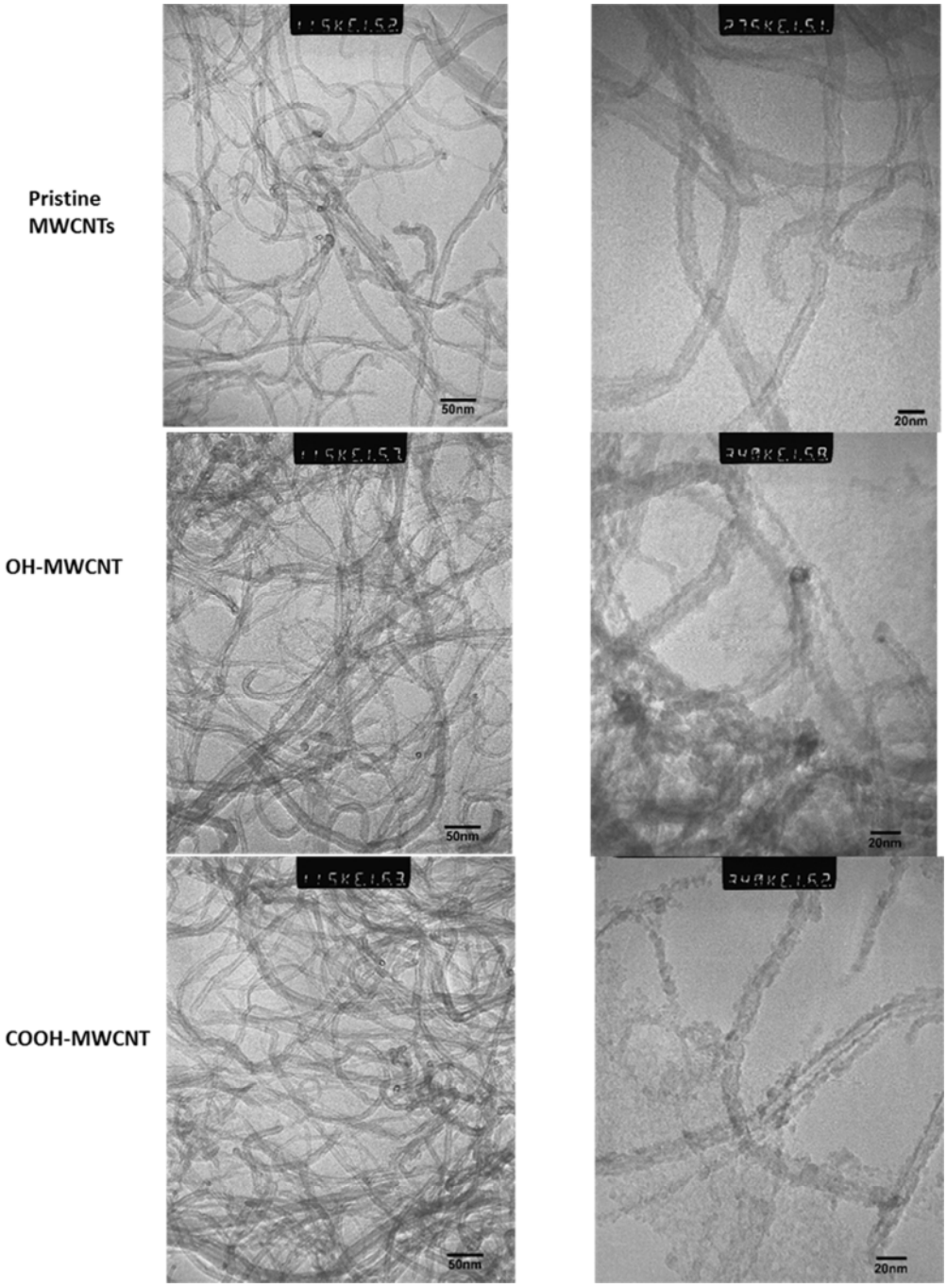

Figure 3-2 TEM images of pristine and functionalised MWCNTs. The particles were dried after suspension in water. The scale bars correspond to 50nm and 20nm respectively.

3.1.3 Fourier transform infrared (FT-IR)

Fourier transform infrared (FT-IR) spectra of pristine MWCNT, OH-MWCNT and COOH-MWCNT were measured to investigate chemical structure (Figure 3-4).

The peak of –OH fluctuating from 3400-3600cm^{-1} was observed in the spectrum of all the three kinds of MWCNTs. The carboxylic group O=C peak at 1634cm-1 was clearly detected in the spectrum of CNT–COOH due to a high degree of carboxylation (Figure 3-4). The peak of C-O at around 1100 cm-1 was showed in spectrum of pristine and –COOH functionalized carbon nanotubes.

The FT-IR analysis suggests that all three types of MWCNTs contain –OH group which is consistent with FTIR results in literature (Tehrani et al., 2013, Cunha et al., 2012) (Figure 3-3). –OH group of pristine MWCNTs on the surface might result from exposure to air. H_2O in atmosphere could be quickly absorbed by the samples.

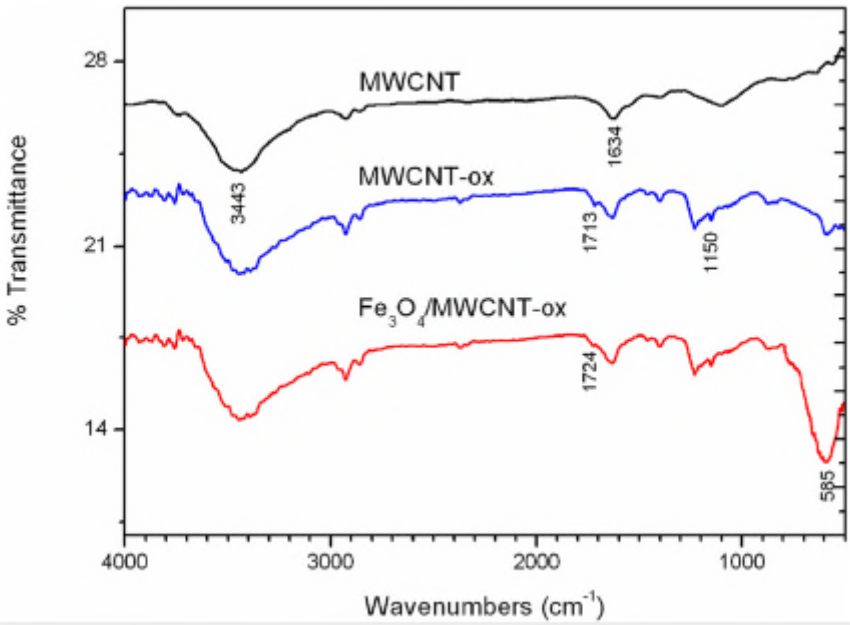

Figure 3-3 FITR figure of oxidised and pristine MWCNTS in literature review (Cunha et al., 2012).

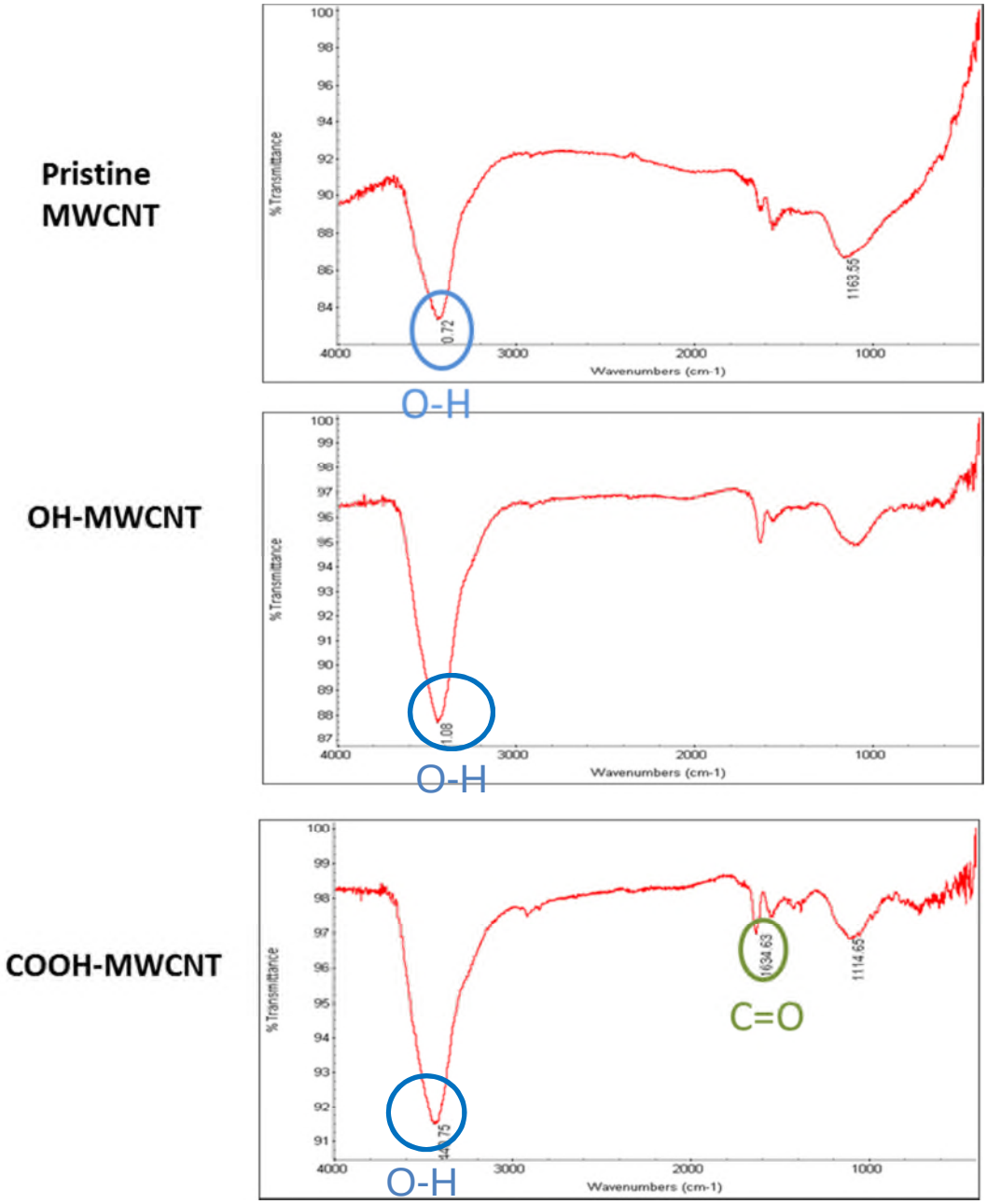

Figure 3-4 FT-IR of MWCNTs. a, pristine MWCNTs; b, OH-MWCNTs; c, COOH-MWCNTs.

3.1.4 Energy Dispersive spectrometry (EDS)

EDS is an analytical technique used for the elemental analysis of samples. It relies on an interaction of X-ray excitation and the sample. Its characterization capabilities are due in large part to the fundamental principle that each element has a unique atomic structure allowing unique set of peaks on its X-ray spectrum.

EDS was applied here to look at the purity of carbon nanotube samples. Background elemental composition analysis showed extremely high Cu content which could explain the high amount of Cu in pristine, -OH and -COOH functionalised MWCNT samples (Figure 3-5).

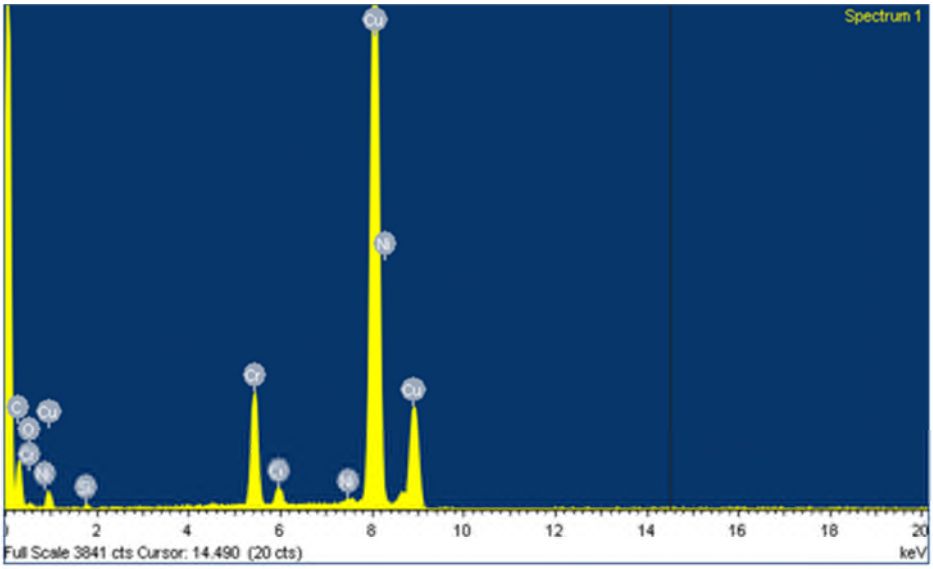

Element	Weight%	Atomic%
C K	3.99	17.53
O K	0.23	0.75
Si K	0.22	0.41
Cr K	10.04	10.20
Ni K	0.47	0.42
Cu K	85.06	70.70
Totals	100.00	

Figure 3-5 Energy dispersive spectrometry for elemental composition analysis (background)

Figure 3-5 described the element composition of background. Most of the elements of background were Cu which could be induced by the method of sample preparation. The second greatest amount of element is C which is followed by Cr. Background also contains some elements O, Si and Ni but with only tiny amount.

Figure 3-6, Figure 3-7 and Figure 3-8 showed the elements detected in pristine, -OH functionalized and -COOH carbon nanotube samples separately.

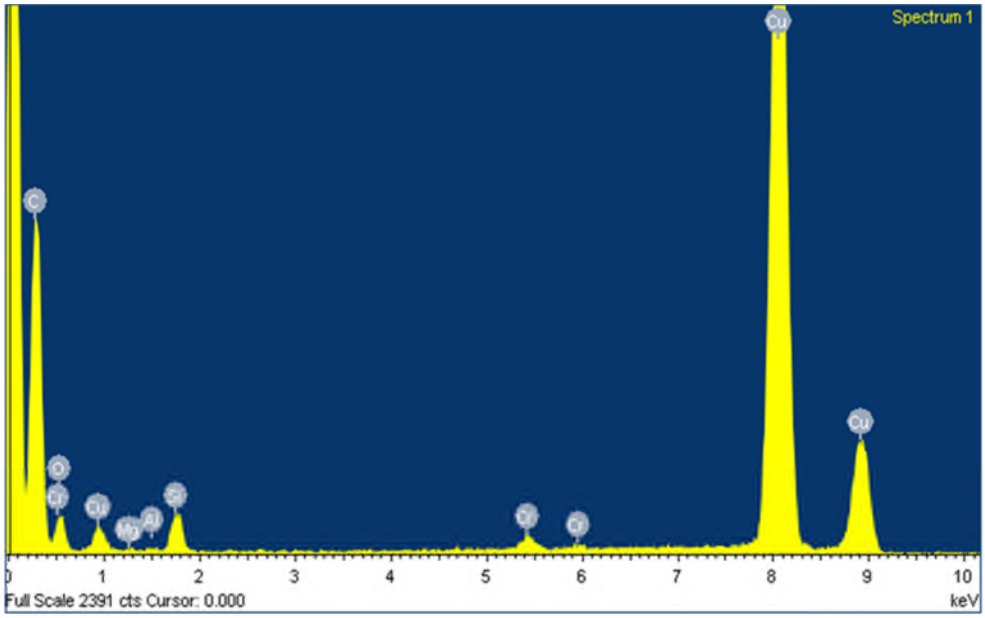

Element	Weight%	Atomic%
C K	14.51	45.03
O K	1.83	4.26
Al K	0.12	0.16
Si K	1.42	1.89
Cr K	3.55	2.54
Mn K	0.23	0.16
Cu K	78.34	45.96
Totals	100.00	

Figure 3-6 Energy dispersive spectrometry for elemental composition analysis of pristine MWCNTs

EDS analysis of pristine MWCNT showed the appearance of minor amount of Al and Mn in addition to elements on background. According to some literature, although all the amount of impurities is very minute, any impurity of carbon nanotubes might contribute to their toxicity (He et al., 2013). The high amount of Cu of background indicated that the measurement artefact and therefore, cooper content will not be discussed here (Figure 3-6).

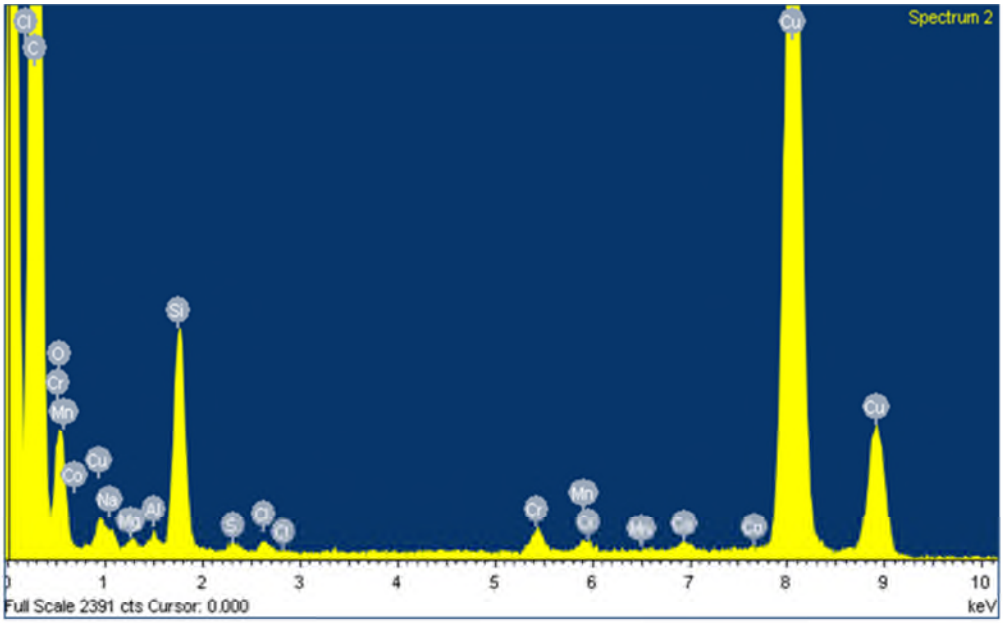

Element	Weight%	Atomic%
C K	22.85	58.87
O K	1.65	3.19
Mg K	0.11	0.14
Al K	0.11	0.13
Si K	1.52	1.68
Cr K	0.75	0.45
Cu K	73.00	35.55
Totals	100.00	

Figure 3-7 Energy dispersive spectrometry for elemental composition analysis of OH-MWCNTs

-OH functionalized MWCNTs didn't contain higher level of metal than pristine. The atomic percentage of all the elements except for Cu and C are very small. Other than the elements detected in pristine MWCNTs, it was also found small amount of Mg (Figure 3-7).

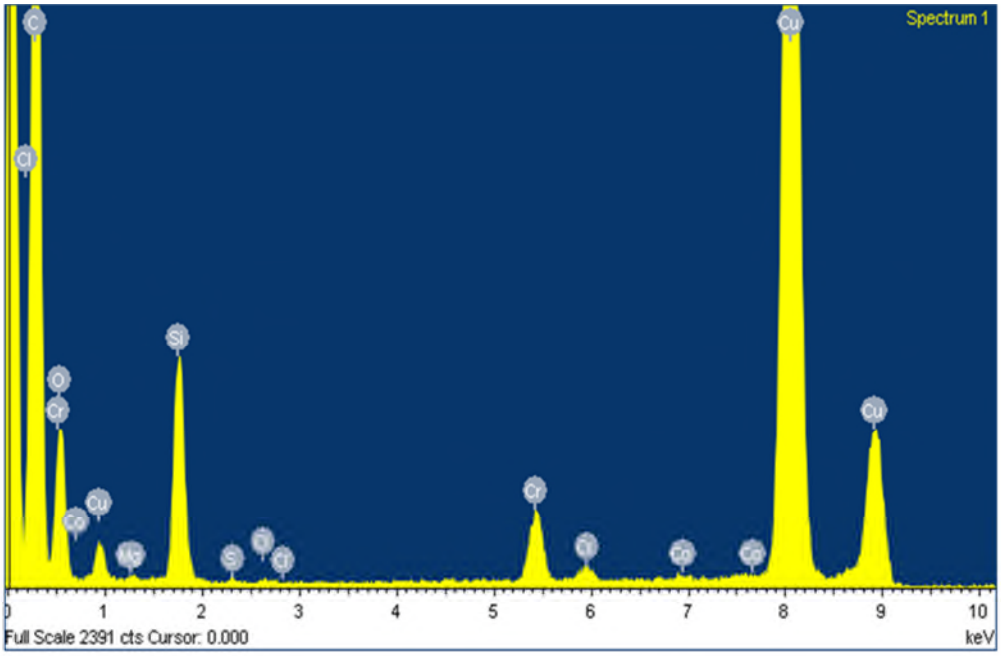

Element	Weight%	Atomic%
C K	30.59	64.16
O K	4.70	7.40
Mg K	0.11	0.12
Si K	4.83	4.33
S K	0.10	0.08
Cl K	0.08	0.06
Cr K	2.53	1.22
Co K	0.16	0.07
Cu K	56.90	22.56
Totals	100.00	

Figure 3-8 Energy dispersive spectrometry for elemental composition analysis of COOH-MWCNTs

As for COOH functionalised MWCNTs, the variety of the metal elements has increased compared to both pristine and OH functionalised MWCNTs. Elements Cl, Co and S could be detected as well as O, Cl, Si, Mg and Cr, however, they were all at minute amount (Figure 3-8).

However, accuracy of EDS spectrum can be affected by various factors. Many elements will have overlapping peaks. The accuracy of the spectrum can also be affected by the nature of the sample. X-rays can be generated by any atom in the sample that is sufficiently excited by the incoming beam. These X-rays are emitted in any direction, and so they may not escape the sample. The

likelihood of an X-ray escaping the specimen, and thus being available to detect and measure depends on the energy of the X-ray and the amount and density of material it has to pass through. This can result in reduced accuracy in non-homogeneous and impure samples.

3.1.5 Comparison of cell viability treated with MWCNTs with and without EDTA.

EDTA It is widely used to chelate metal ion. Its usefulness arises because of its role as a hexadentate ligand and chelating agent, after being bound by EDTA, metal ions remain in solution but exhibit diminished reactivity. This experiment is to find out the function of metal in toxicity of carbon nanotubes.

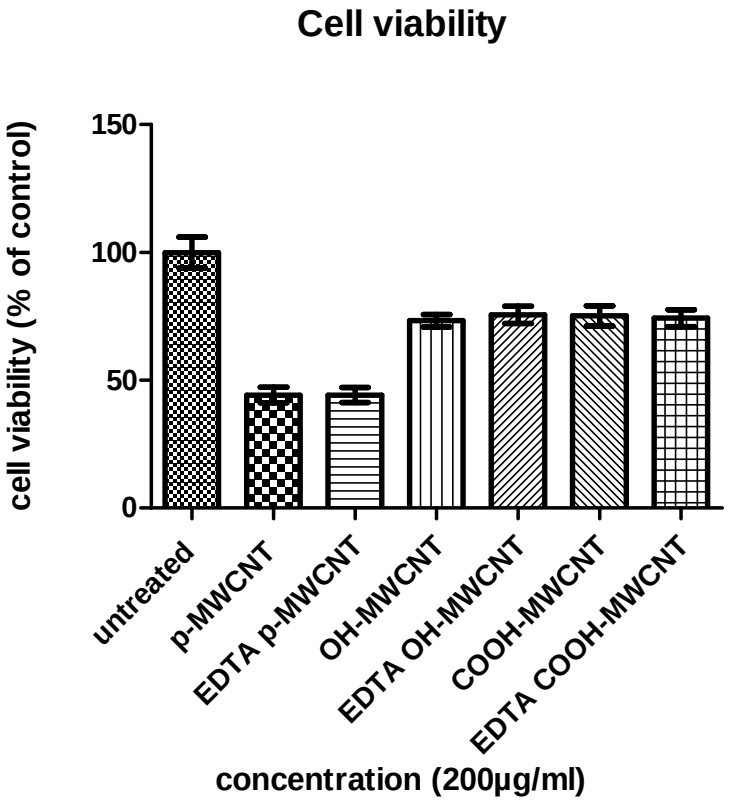

Figure 3-9 cell viability of pristine, -OH functionalised and –COOH functionalised MWCNTs treated A549 cells with and without EDTA at 200 µg/mL.

The experiment was conducted at 200µg/ml of carbon nanotubes. The concentration of EDTA was 0.5M. A549 cells were treated with three different types of carbon nanotubes and EDTA treated carbon nanotubes respectively.

Figure 3-9 exhibited the cell viability results of cells after 24 hours treatment by WST-1. The result didn't show any difference between cells treated with EDTA and without EDTA, which suggested that metal content didn't contribute to the toxicity of MWCNTs in this project.

3.1.6 Aggregation of MWCNTs

Figure 3-10 shows the pictures of pristine MWCNTs, OH-MWCNTs and COOH-MWCNTs dispersed in cell culture medium, which suggested different extent of aggregation. The samples were suspended at 200μg/mL and were left still for 5 min in order to allow them to settle and form the aggregates. From observation, pristine carbon nanotubes formed a more homogeneous suspension when compared to functionalized carbon nanotubes especially OH-MWCNTs.

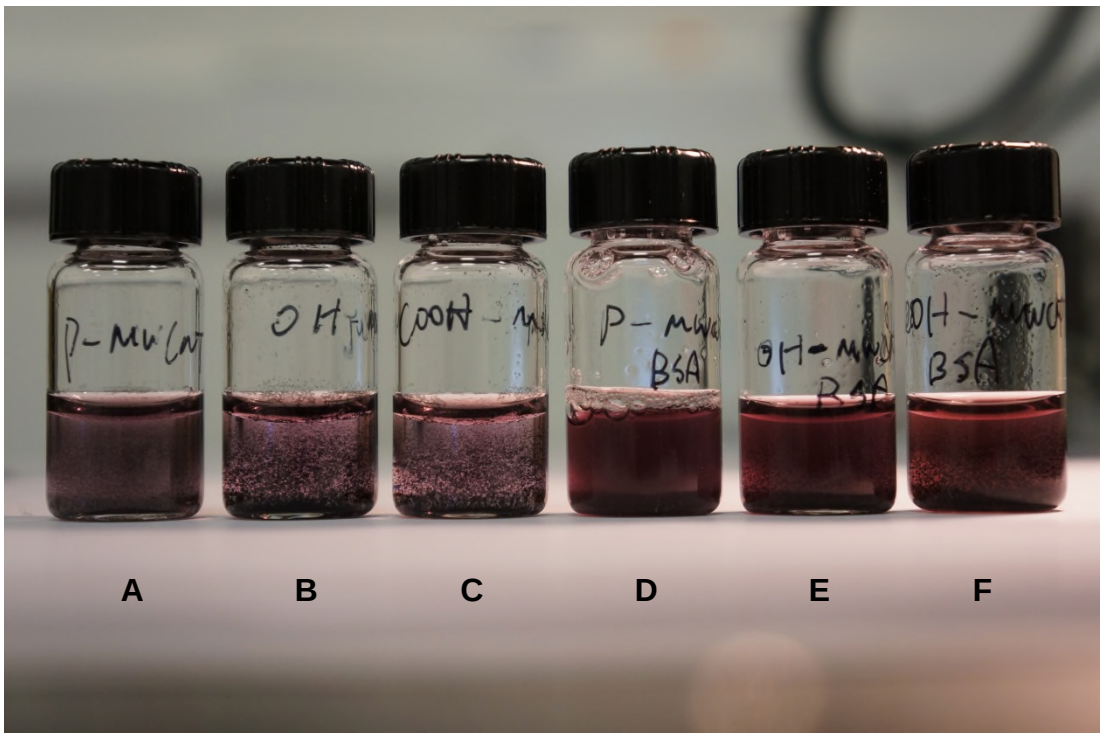

Figure 3-10 Photograph of MWCNTs in the F12/DMEM medium. A-C: pristine MWNCT, OH-MWCNT, COOH-MWCNT in the BSA- medium at 200μg/mL; D-F: MWNCT, OH-MWCNT, COOH-MWCNT in the BSA+ medium at 200μg/mL.

Figure 3-11 describes that in the cell culture plate, A549 Cells were treated with pristine, -OH and –COOH functionalised MWCNTs at 20, 50 and 200 μg/mL. After 24 hours incubation at 37 °C the aggregates in the supernatant of pristine

MWCNT could barely be observed at 20 and 50μg/ml whilst at 200 μg/ml, they aggregated in the medium. The functionalised MWCNTs obviously aggregated at both 50 and 200 μg/mL (Figure 3-11a). From the microscopic picture, it clearly showed that both single carbon nanotube and aggregates were likely to adhere to cells (Figure 3-11b).

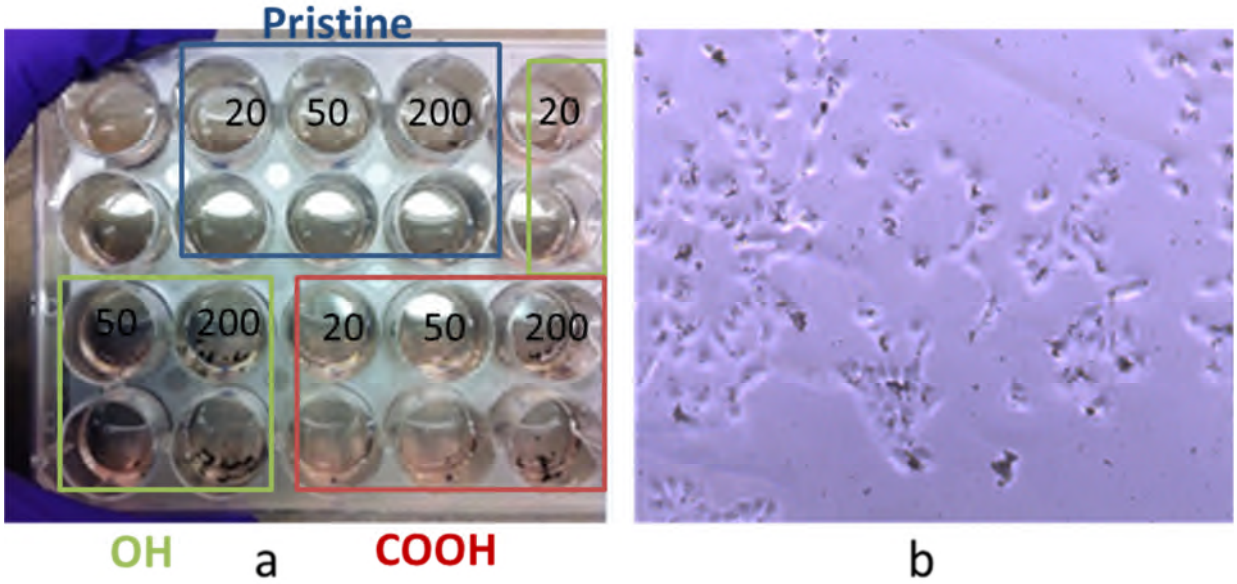

Figure 3-11 a, MWCNTs in 24-wells plate at 50μg/mL; b, Microscopic picture of cells incubated with pristine MWCNTs at 20μg/mL.

3.1.7 Toxicity comparison between BSA treated MWCNTs and untreated MWCNTs

To understand how aggregates contribute to toxicity of carbon nanotubes, an experiment was conducted to investigate MWCNTs' effect on cell viability. Different dispersing methods have been used in published studies, including saline, surfactant, Tween 80 and serum; however the use of a dispersing agent may modify the MWCNTs' behaviour in suspension and thus their toxicity (Elgrabli et al., 2007). In this study albumin was considered the most physiologically relevant dispersion medium due to its ubiquitous presence in the human body.

A comparison of cell viability test of cells treated with MWCNT and BSA-contained MWCNT suspension, at 0, 50 and 200μg/mL, was conducted in order to evaluate the alteration of cell viability of more thoroughly dispersed CNTs. The results of MWCNT effects on cell viability with and without 0.5% BSA (Figure 3-12) showed that the dispersion of carbon nanotubes was of great importance and significantly increased cell viability. At 50μg/mL, none of the three types of MWCNTs showed significant alterations to cell viability with or without BSA. However, at 200μg/mL, viability of functionalized carbon nanotubes (OH-MWCNTs & COOH-MWCNTs) treated cells was significantly decreased by adding BSA (the P values of slope difference are 0.01745 and 0.007834 respectively). But with respect to pristine MWCNTs, BSA didn't increase cell viability at the same concentration. It indicates that the toxicity of pristine MWCNTs is not change by adding BSA. These results could be explained by the fact that pristine MWCNTs were well dispersed, so additional BSA didn't change the dispersion significantly. In respect to graph b and c, although at 200μg/mL, the absorbance value didn't show significant difference with and without BSA, the p value of slope difference indicates that the adding BSA made functionalized MWCNTs more toxic. However, the absorbance values corresponding to pristine MWCNTs at both 50 and 200μg/mL are significantly higher in the presence than in the absence of BSA. In addition, the slopes of two curves are shown no significantly difference.

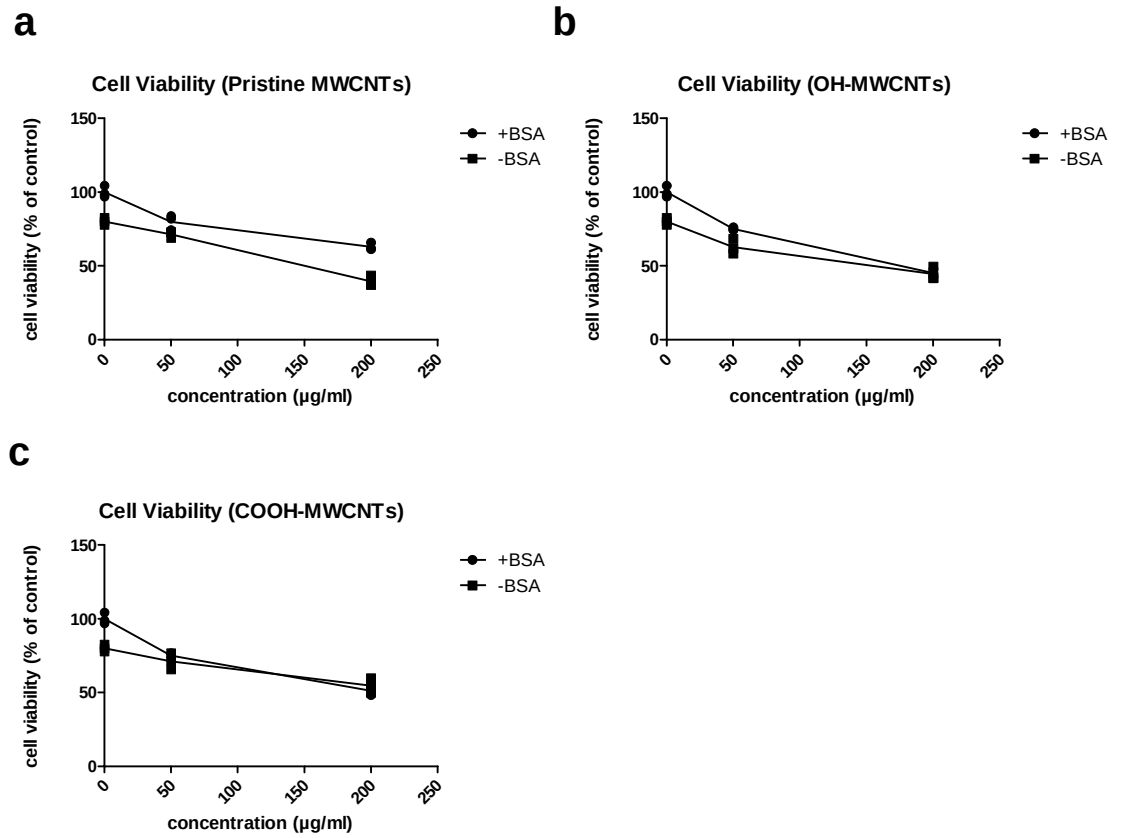

Figure 3-12 Comparison of cell viability with and without 0.5% BSA in FBS-free medium. The viability of A549 cell was detected by using WST-1 assay following 24 hours incubation with all three types of MWCNTs at concentrations of 0, 50 and 200 µg/mL. a, MWCNTs; b, OH-MWCNTs; c, COOH-MWCNTs. Data are represented as percentage of control of triplicate.

3.1.8 Comparison experiments between Carbon nanotubes and Carbon dots.

Carbon dots are a new class of carbon nanomaterials with sizes below 10nm. They were first derived from an electrophoretic purification experiment of single-walled carbon nanotubes obtained from arc discharge soot during the year of 2004 at South Carolina. Carbon dots also contain many carboxylic acid moieties at their surface which helps them have excellent water solubility and suitable for

successive functionalization with various organic, polymeric, inorganic or biological species.

3.1.8.1 Image of carbon dots

The sample was weighed 1mg and mixed with 10mL deionised water, making it the concentration of 1mg/mL (Figure 3-13). In observation, carbon dots exhibited better dispersibility than carbon nanotubes

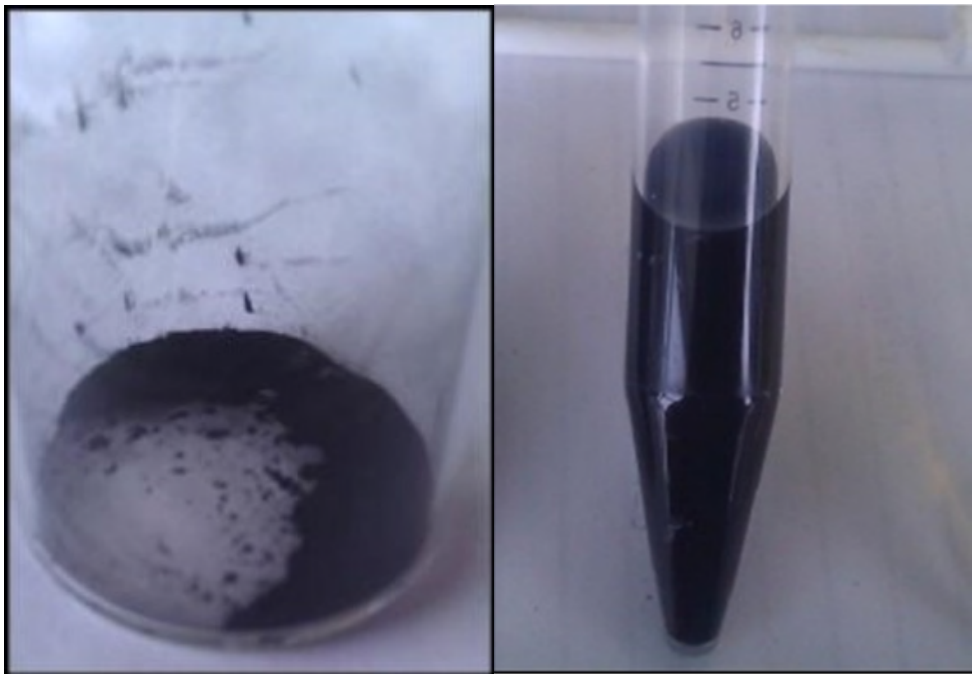

Figure 3-13 Pictures of carbon dots without and with solution (DMEM/F12)

3.1.8.2 Comparison of cell viability

In order to compare the toxicity of carbon nanotubes and carbon dots, A549 cells were treated with 20, 50 and 200μg/mL pristine MWCNT and C-dots respectively. Then WST-1 was applied for cell proliferation evaluation. Figure 3-14 described that cells treated with pristine MWCNTs exhibited significant higher cell viability at all the concentration than cells treated with carbon dots.

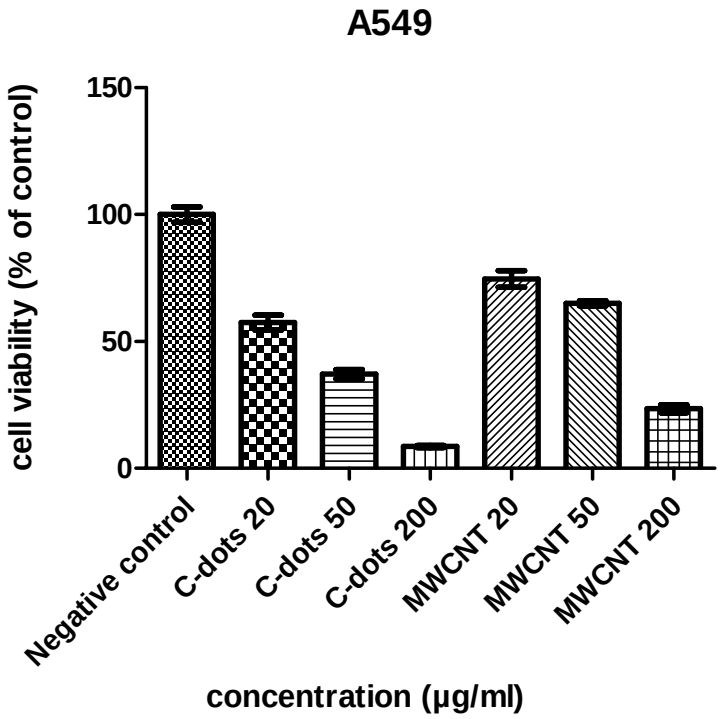

Figure 3-14 Comparison of cell viability of A549 treated with pristine MWCNTs and C-dots after 24 hours at 20, 50 200 µg/mL. Viability was detected by using WST-1 assay. Data are represented as percentage of control ± SD of triplicate. $p<0.05$

3.1.8.3 Comparison of LDH release

Membrane integrity detection experiment also showed that carbon dots induced more cell death with the same concentrations as pristine MWCNT (Figure 3-15). The results supported cell proliferation experiment using wst-1.

At 20µg/mL, no difference has been shown between MWCNT and C-dots. However, the difference became significant when the concentration increased to 50 and 200µg/mL.

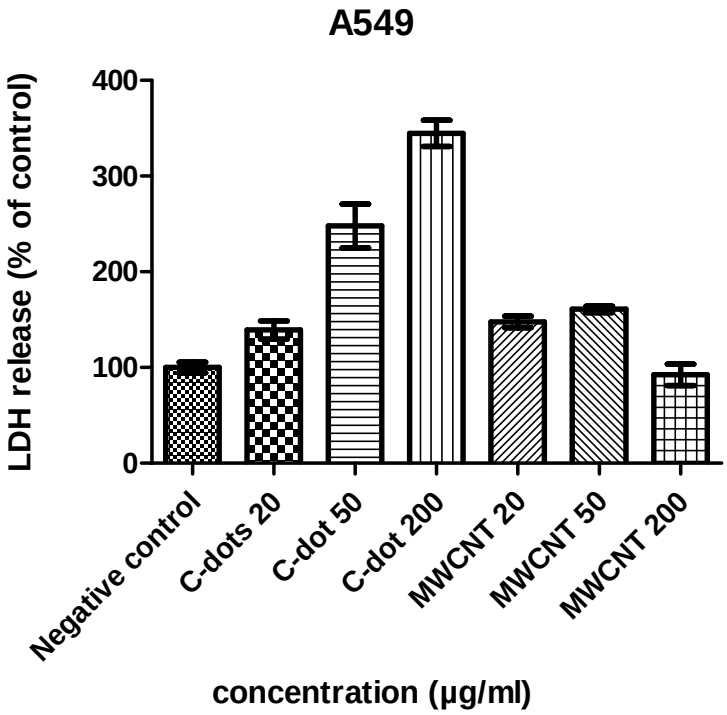

Figure 3-15 Cell viability of A549 cell line after 24 hours exposure to pristine MWCNTs and C-dot respectively with concentrations from 20 to 200 µg/mL. Viability was detected by using LDH assay. Data are represented as percentage of control±SD of triplicate. * p<0.05, **p<0.01, ***p<0.001.

Carbon dots exhibited better dispersibility in DMEM/F12 than carbon nanotubes at same concentration. However, at the same time, they exerted more cell death than carbon nanotube. This phenomenon also suggested that aggregation could decrease toxicity.

3.2 Discussion

Characterization of the carbon nanotubes used in these experiments has given insight into the nature of size distribution, dispersion pattern and purity of the experimental materials. Although all the carbon nanotubes used in this research were commercially available and supplied with the size in the range of 12-18nm, the size distribution measured by SEM suggested that the diameter of all the carbon nanotubes were within 12-32nm (Figure 3-1) and all the MWCNTs formed aggregates. They are evenly dispersed after sonication according to TEM figures. In our research of characterization of carbon nanotube, it was found similar fibre diameter of all the three types of carbon nanotubes and functional groups (-OH and –COOH) have been confirmed on the surface through FT-IR (Figure 3-4).

It was also detected that the different surface feature and impurity content (Figure 3-8) among pristine and functionalized carbon nanotubes which might contribute to the toxicity of carbon nanotubes *in vitro*. As the fact that CNTs can be made by different methods, by different manufacturers, who use different catalytic metals, carbon sources and processing conditions (such as temperature and/or pressure), the produced CNT might contain various metal elements. But in this study no alteration in toxicity profile was observed after chelation with ethylene diamine tetra acetic acid (EDTA), indicating that metal ions do not contribute significantly to MWCNT toxicity (Figure 3-9). According to the study conducted by Wick, critical features that determine CNT toxicity are the degree of CNT dispersion but not the content of entrapped metals (Wick et al., 2007).

Surface functionalization broadens carbon nanotube applications, conferring new functions, but at the same time potentially altering toxicity. The functional group percentage according to data sheet from manufacture is 7%, which could explain why there was no big C=O absorbance peak through FT-IR. In addition, surface Functionalization is also related to aggregation and zeta potential through the interaction with molecules in the medium and thus contributes toxicity of carbon nanotubes.

Due to van der Waals and electrostatic forces, CNT agglomerates causes problems in the investigation of CNT toxicity (Tagmatarchis and Prato, 2004). There are some methods to disperse CNT which were reviewed (Smart et al., 2006). The most commonly used method needs the utilization of organic solvents. However organic solvents are not suitable for biological studies as they are also highly toxic themselves (Kim et al., 2011b). Another method commonly employed is utilization of a surfactant such as albumin, which is a ubiquitous biomolecule within the human body. A possible explanation of these results was given in a study by (Casey et al., 2007) , in which, a better dispersion has been made in the presence of foetal calf serum and DMEM/F12 cell culture medium. This improved dispersion is explained by physical interaction between CNT and FCS-medium protein. The adsorption of CNT on the FCS-medium protein is possible because of the presence of van der Waals forces and induces no modification of CNT and protein identity (Elgrabli et al., 2007). Figure 3-10 indicates that at the same concentration, -COOH and –OH functionalized MWCNTs showed higher level of aggregation than pristine MWCNTs in the medium (F12/DMEM).

CNT agglomerates could cause problems in the investigation of CNT toxicity (Tagmatarchis and Prato, 2004). Methods to disperse CNT were reviewed by Smart et al. (Smart et al., 2006). The most commonly used method uses organic solvents such as DMSO, aqueous pluronic F127 and Tween 80 (Ciofani et al., 2009, Rastogi et al., 2008) However organic solvents are not suitable for biological studies as they are toxic (Kim et al., 2011b). Another method commonly employed is utilization of surfactant such as BSA which is a biomolecule representative of those present in the body. A possible explanation of these results was given by a study by (Casey et al., 2007), in which, a better dispersion has been made in the presence of FCS and medium. This improved dispersion could be explained by physical interaction between CNT and FCS-medium protein. In order to investigate the link between dispersibility and cytotoxicity, the cell viability of cell exposed to MWCNTs with and without BSA has been compared. A previous study conducted by Li et al. suggested that lowest suspension stability is more likely to settle at the bottom of the wells,

where they make more cellular contact (Li et al., 2013). However, in our experiments, results of functionalized MWCNTs showed that the differences between slopes are significant demonstrating carbon nanotubes with better dispersibility actually intensify the interactions with cells, thereby decreasing the cell viability (Figure 3-12). These results were also supported by Johnston et al. who suggested that only those carbon nanotubes which are not aggregated and free in the medium are able to reach the cytoplasm and subsequently the nucleus (Johnston et al., 2010).

To further compare the toxicity of aggregates and better dispersed sample, C-dots were introduced to this experiment. C-dot showed better dispersibility in DMEM/F12 cell culture medium as a member of carbon family. Similarly, it was found that C-dots exhibited more cell death and cell membrane damage compared with pristine MWCNTs at the same concentration. These results further confirmed aggregates could decrease the toxicity in terms of cell viability.

.

3.3 Conclusions

Characterization of MWCNTs has provided insight into the physical properties of MWCNTs, which will help us better understand the mechanism behind toxicity. It was also evidenced that these characteristic of MWCNTs can be altered when dispersed in the biological solution, due to their interaction with molecules present in the system.

The materials used in this project have similar diameter which is within 10-30nm by SEM. It was also confirmed that –OH functional group on –OH MWCNTs and C=O functional group on COOH-MWCNTs through FT-IR.

Metal content (Cr, Co Si and Mg) were also found through energy dispersive spectrometry, however, the amount of impurity is minute and didn't cause additional toxicity. The difference of impurity amount among three forms of MWCNTs couldn't be detected which indicates that impurities didn't contribute to the different degree of toxicity of them.

MWCNTs aggregates could be observed both microscopic and through SEM as well as macroscopic observation. The addition of 0.5% BSA made MWCNTs better dispersed in aqueous solution and through this mechanism increased their toxicity. The toxicity of pristine MWCNTs is not changed by BSA, which may indicate that pristine MWCNTs were already well dispersed in solution. In respect to OH-MWCNTs and COOH-MWCNTs, the significant slope difference indicates that the adding BSA made functionalised MWCNTs more toxic.

The study underlines the need for thorough material characterisation prior to toxicological studies.

Chapter 4

4 Toxicity study in relation to surface functionalization *in vitro*

4.1 Introduction

Carbon nanotubes (CNTs) are a family of nanomaterials made up predominantly of carbon. In this family, structurally multi-walled carbon nanotubes MWCNTs consist of multiple layers of graphite superimposed and rolled in on themselves to form a tubular shape. MWCNTs are of special interest for the industry and they have been increasingly utilised as advanced nano-vectors in drug/gene delivery systems (Vashist et al., 2011). They possess significant advantages including high surface area, well-defined morphologies and unique optical as well as electrical properties, in addition to their super mechanical strength and thermal conductivity.

It is worth noting that it has been reported that the functionalisation/modification of the structure of MWCNTs could optimise their solubility and dispersion, allowing innovative applications in materials (Martín et al., 2013b), electronics (Castranova et al., 2013), chemical processing (Martín et al., 2013a) and energy management (Mauter and Elimelech, 2008). However, the functionalisation of MWCNTs could raise more uncertainties about the toxicity. For example, Vashist et al (Vashist et al., 2011) and Mali et al. (Mali et al., 2011) reported that functionalised CNTs were able to exhibit very low toxicity and higher propensity to cross cell membranes, increasing their potential for drug and gene delivery. On the contrary, Magrez et al. showed that the toxicity of MWCNT, in human lung-tumor cell lines, was increased when carboxyl and hydroxyl groups were present on their surface (Magrez et al., 2006). A study conducted by Patlolla et al. performed on bone marrow cells of mice exposed to –COOH functionalized and pristine MWCNTS, found that functionalized MWCNTs had a higher clastogenic and genotoxic potential than non-functionalised CNTs (Patlolla et al., 2010b).

In addition, data on genontoxicity caused by pristine and functionalized MWCNTs are still very limited. Their ability to cause oxidative DNA damage has been investigated but the accumulation of 8-OHdG in DNA, a sensitive marker of oxidative damage to DNA, was not detected (Ogasawara et al., 2012). The overall information about apoptosis induced by MWCNT seems also inadequate, though pristine MWCNTs has been shown not to cause any apoptosis stimulation in lung cells by the research conducted by Ursini (Ursini et al., 2012a).The change of RNA regulation after treatment with MWCNTs were not detailed either, therefore, further investigation of the mechanism of toxicity of MWCNTs triggered cell death is warranted.

Hence, in this study, to the best of our knowledge, we are the first group to investigate the effect of dispersion of two most frequently used functionalized multi-walled carbon nanotubes (i.e. OH-MWCNTs and COOH-MWCNTs) on the A549 cell line, in terms of apoptosis and DNA damage. The primary route of human exposure to MWCNTs is likely to be via inhalation. The A549 cell line, which is a cancer lung cell line, was therefore believed to be the most appropriate selection for this study. Their proliferation and ability to undergo oxidative stress were investigated in order to provide a more comprehensive understanding of the potential mechanism of toxicity, as well as establishing the threshold of a safe dose for their medical applications. More importantly 84 toxicity related genes were analysed to detect possible modification after treatment. This would provide more information about the mechanism of the M WCNTs ability to trigger cell death.

4.2 Results

4.2.1 Cell proliferation

4.2.1.1 MTT

MTT has been used for cell viability test in the beginning. However, we realised that carbon nanotube left on the cell surface was interfering with the absorbance of purple formazan formed during the experiment. The data of MTT could be found in Appendix A

4.2.1.2 WST-1

To replace MTT, cell proliferation reagent WST-1 was used to evaluate cell viability in response to pristine and functionalized MWCNTs. As discussed in literature, WST-1 can form soluble yellow formazan which avoided an extra step to dissolve the crystal, and thus decrease the chance of making error. In addition, the yellow formazan successfully avoid the interference with the colour of carbon nanotubes during absorbance reading.

The results showed a dose dependent cell death after 24 hours exposure. Figure 4-1 describes the cell viability in relation to concentrations. The MWCNT treated cells' viability is not significantly changed at 20 and 50 µg/mL compared with negative control. However, at 200µg/mL, the pristine MWCNT induced a significant amount of cell death and the cell viability is less than 50% of negative control. Cells treated with 200µg/ml functionalised MWNCTs exhibited higher cell viability (about 75% of negative control) compared with those treated with pristine MWCNTs. There's no significant difference between the cell viability of two functionalized MWCNT at concentration 20 and 50µg/ml.

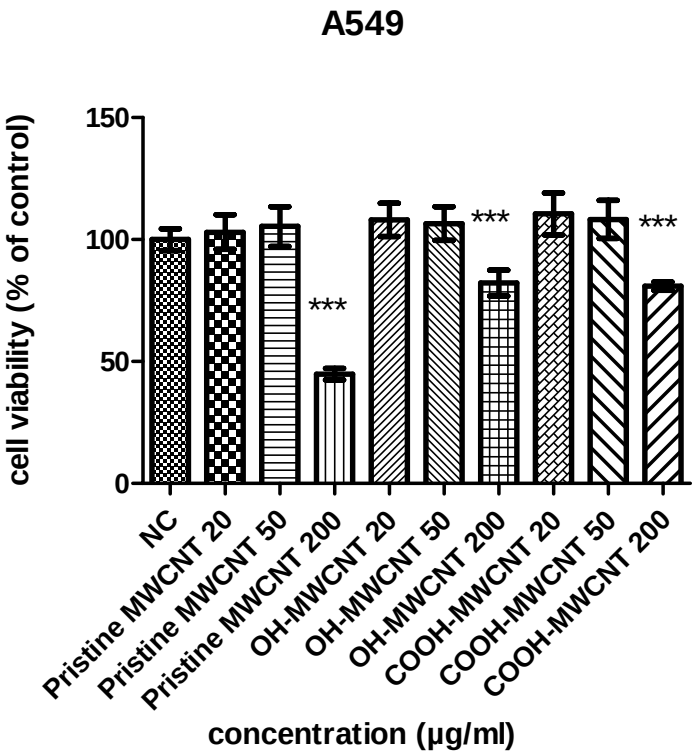

Figure 4-1 Cytotoxicity of A549 cells was evaluated after 24 hours exposure to pristine MWCNTs, OH-MWCNTs and COOH-MWCNTs with concentrations from 20 to 200 µg/mL. Viability was detected by using WST-1 assay. Data are represented as percentage of negative control of triplicate. ***p<0.001

Figure 4-2 describes the comparison of the concentration-response curves obtained for each MWCNT [Bottom (minimum effect), IC50 (concentration required for 50% of cell viability inhibition), Top (maximum effect)]. IC50 of pristine MWCNTs (255.2µg/ml) were significant different from IC50 of –OH and –COOH functionalized MWCNTs (2198, 2456 µg/ml). P<0.0001. The figure also suggested that concentration under 10µg/mL could be applied in vivo application. The concentration under 10 µg/mL didn't induce any significant cell death.

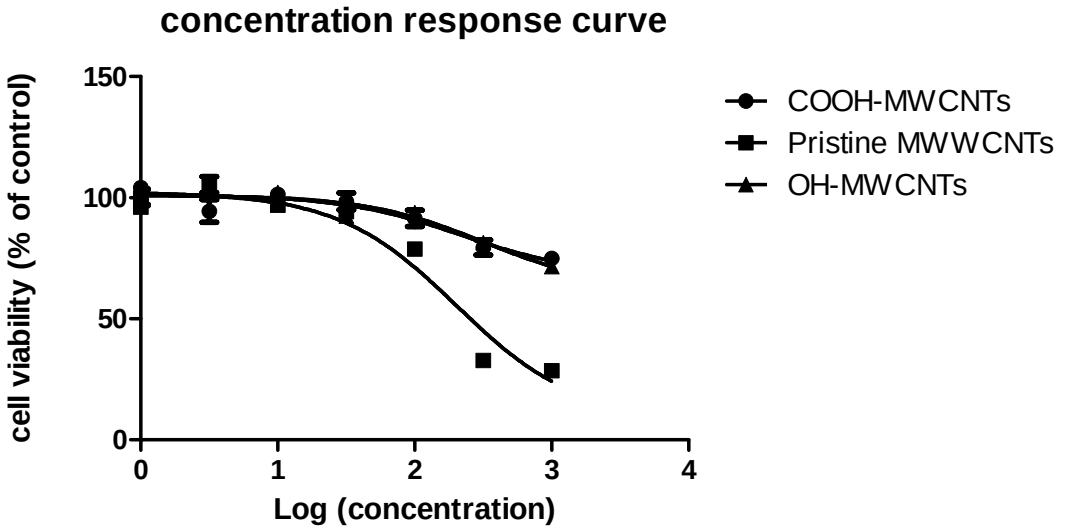

Figure 4-2 Cell viability curve of A549 cells was evaluated after 24 hours exposure to pristine MWCNTs, OH-MWCNTs and COOH-MWCNTs with concentrations from 1 to 1000μg/ml. Viability was detected by using WST-1 assay. Data are represented as percentage of negative control of triplicate. * p<0.05, **p<0.01

4.2.2 Cell membrane integrity

LDH release was also assessed on cells treated with MWCNTs. The increase of LDH in cell culture medium, indicative of cell membrane damage was detectable as early as 6 hours after treatment (data are not shown) and Figure 4-3 is obtained at 24 hour. The effect on LDH leakage was not significant at 20 and 50μg/ml upon all three treatments. However, at 200μg/ml, functionalized carbon nanotubes exhibited significant membrane damage while the pristine form showed no significant membrane damage compared with untreated cells.

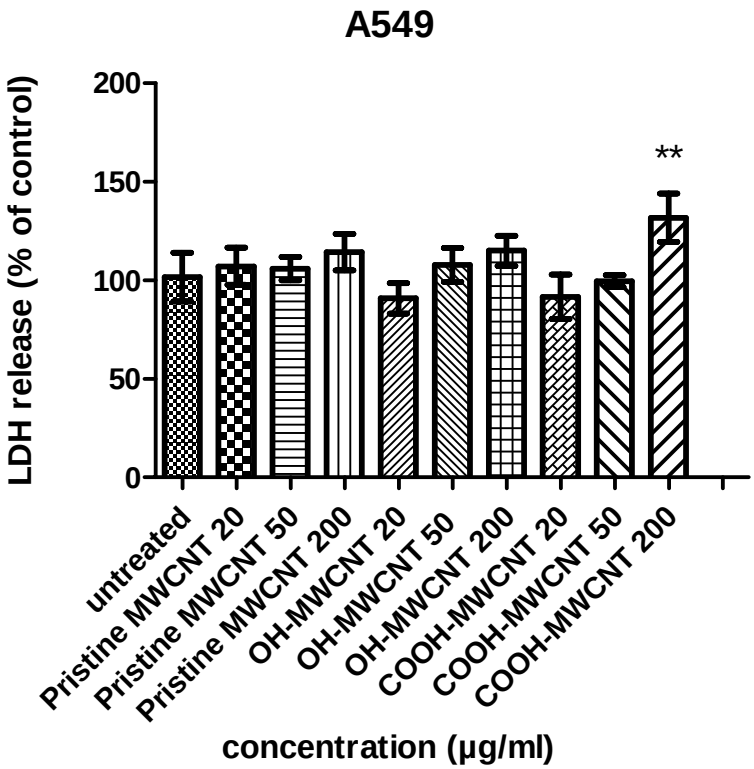

Figure 4-3 LDH release assay. Cytotoxicity of all the cell lines was evaluated after 24 hours exposure to pristine MWCNTs, OH-MWCNTs and COOH-MWCNTs with concentrations from 20 to 200 µg/mL. Viability was detected by using LDH assay. Data are represented as percentage of negative control of triplicate. * p<0.05, **p<0.01, ***p<0.001.

4.2.3 ROS generation

Oxidative stress plays a role in toxicity induced by carbon nanotubes (Pichardo et al., 2012). In this report, DCFDA, a fluorescent dye was used to measures hydroxyl, peroxyl and other reactive oxygen species (ROS) activity within cells.

The results of MWCNTs-induced ROS generation are summarized in Figure 4-4. A549 cells showed responsiveness following 6 hours exposure of MWCNTs at each concentration. At 20 µg/mL concentration, cells treated with 20µg/mL MWCNTs (pristine, -OH, -COOH) induced 5.35, 4.84 and 5.36 fold greater ROS levels than cells treated with H_2O_2. The Amount of ROS kept increasing when the concentration of MWCNTs has been increased to

50µg/mL. No significant difference in ROS generation among three types of MWCNTs has been detected here.

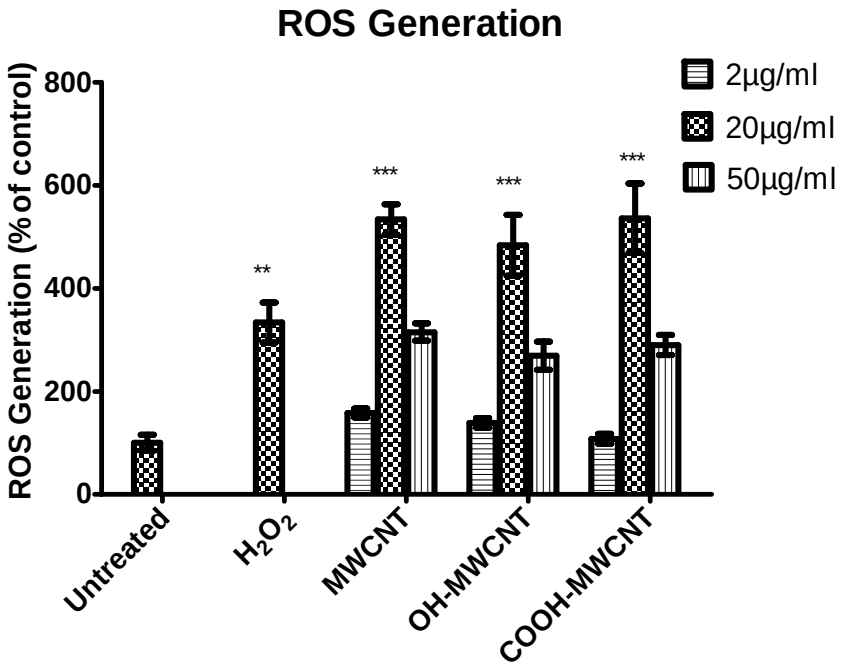

Figure 4-4 Reactive oxygen species (ROS) generation following 6 h exposure to various concentrations of MWCNTs in A549 cells. ROS generation was studied using dichlorofluorescin diacetate (DCFH-DA) dye assay. Positive control: 200 µM H_2O_2. Data are represented a as percentage of negative control of triplicate analysis.

4.2.4 Apoptosis

Flow cytometry is a laser-based, biophysical technology employed in cell counting, cell sorting, biomarker detection and protein engineering, by suspending cells in a stream of fluid and passing them by an electronic detection apparatus. It allows simultaneous multi-parametric analysis of the granularity and size as well as fluorescence intensity.

In this experiment, X line represent green fluorescent intensity induced by Annexin V and Y line represent red fluorescent intensity induced by PI stain. In early-stage apoptosis, the plasma membrane excludes viability dyes such as

propidium iodide (PI). These cells will stain with Annexin V but not a viability dye, thus distinguishing cells in early apoptosis.

The black dots showed in each picture are cells. The more they moved toward X direction, the big percentage of apoptotic cells. The more they moved toward Y line, the more they die through necrosis Figure 4-5.

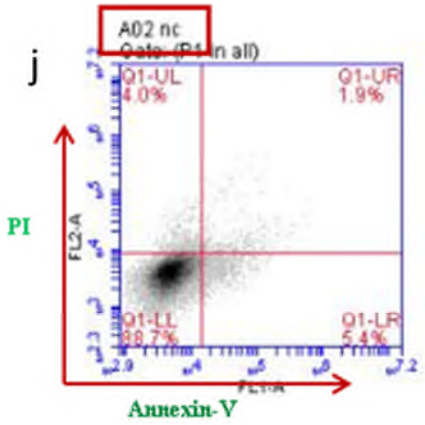

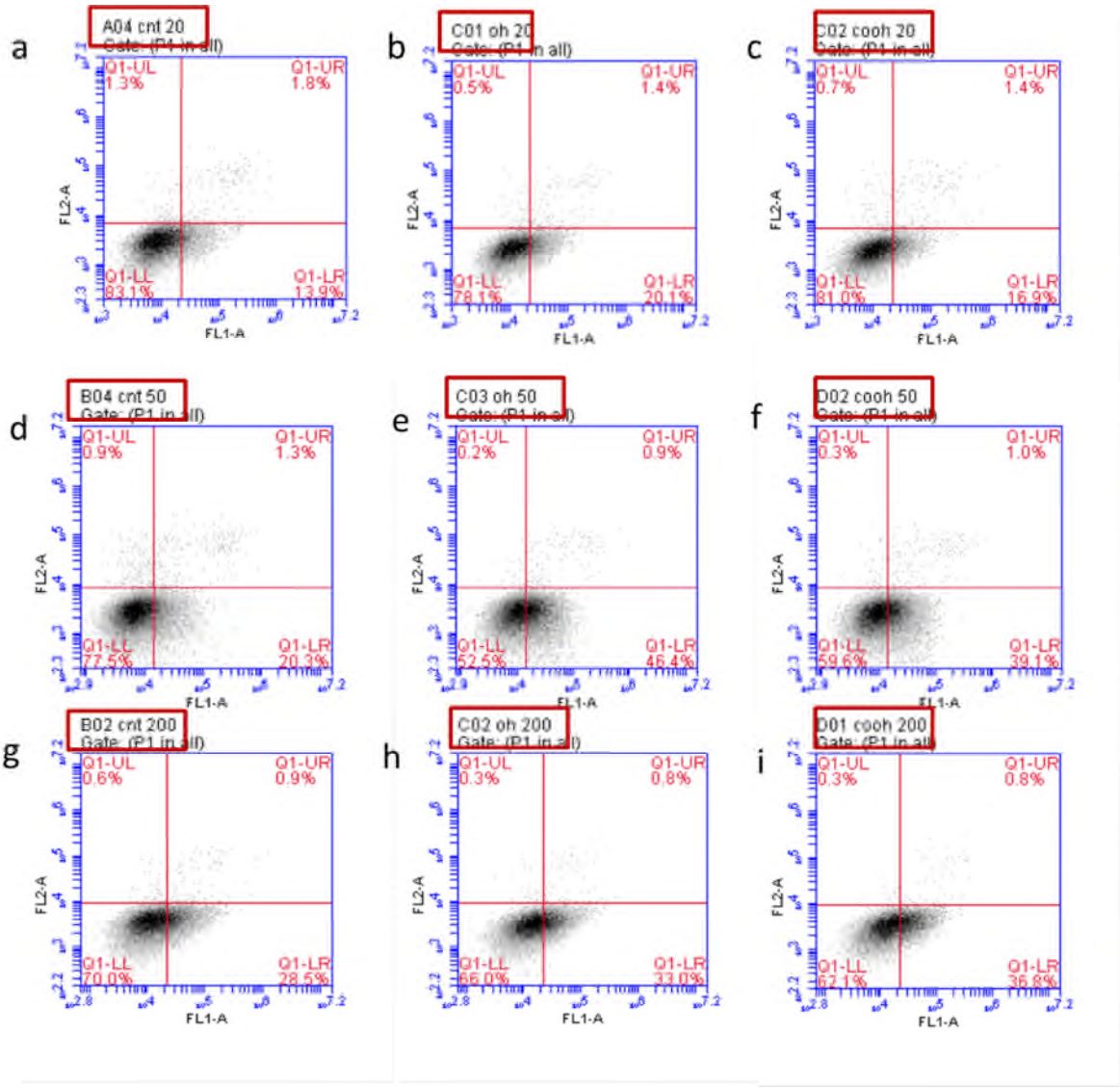

Figure 4-5 Flow cytometry Annexin V-PI apoptosis detection after 48 hours exposure to 20, 50, 200μg/mL MWCNTs in A549. a, MWCNT 20μg/mL; b, MWCNT 50μg/mL; c, MWCNT 200μg/mL; d, OH-MWCNT 20μg/mL; e, OH-MWCNT 50μg/mL; f, OH-MWCNT 200μg/mL; g, COOH-MWCNT 20μg/mL; h, COOH-MWCNT 50μg/mL; i, COOH-MWCNT 200μg/mL; j, non-treated cells

Table 4-1 Cell apoptosis induced by three types of MWCNTs in A549

Non-treated		P-MWCNT	OH-MWCNT	COOH-MWCNT
		Mean % apoptotic cells ±SD		
	20μg/mL	8.5%±2.09%	21.90%±3.80%	13.50%±1.58%
5.63%±0.66%	50μg/mL	18.8%±4.31%	42.7%±4.84%	36.8%±3.79%
	200μg/mL	25.0%±1.45%	29.7%±3.40%	33.9%±2.13%

Cell apoptosis detection on A549 cells. Cells were treated with three MWCNTs at 20, 50 and 200μg/mL for 48 hours. Untreated cells were used as negative control. Apoptosis was detected using Annexin v-FITC and PI.

Flow cytometer analysis of A549 cells treated for 24 hours with three types of MWCNTs respectively revealed an apoptosis induction from 20μg/mL to 200μg/mL (Figure 4-5). Functionalized carbon nanotubes elicited dose respondent and bigger apoptotic cell percentage compared with unexposed cells and pristine MWCNTs beginning from 20μg/mL, statistically significant starting from 20μg/mL and with a concentration-dependent trend. At 20μg/mL, pristine MWCNT induced 8.5 percent of apoptosis and –OH and –COOH functionalized MWCNT caused 2.58 and 1.59 times of pristine one respectively. At 50μg/mL, the percentage of apoptosis was increased in respect to three different MWCNTs. similarly, apoptosis induction was more pronounced which is 2.28 and 1.95 times of apoptosis induced by pristine one. However, at 200μg/mL, apoptosis induced by both functionalised MWCNTs have decreased whilst the percentage of apoptosis induced by pristine MWCNTs continued increase.

4.2.5 DNA damage

In order to measure DNA damage caused by oxidative stress and cell internalization of carbon nanotubes, 8-oxo-2'-deoxyguanosine (8-oxo-dG), a frequently used and sensitive biomarker of oxidative DNA damage was measured and quantified.

Figure 4-6a is a standard curve describing the link between fluorescence intensity and oxo-dG amount. The equation was generated by GraphPad Prism.

By 72h of exposure, all three kinds of MWCNTS induced 8-OHdG at 50µg/mL, which becomes statistically significant for pristine MWCNTs (0.745±0.0167ng/mL) compared to negative control (0.651±0.0139 ng/mL). OH-MWCNTs (0.998±0.0083 ng/mL) and COOH-MWCNTs (0.975±0.0336 ng/mL) were 1.40 and 1.31 fold more toxic than pristine MWCNTs respectively (Figure 4-6b).

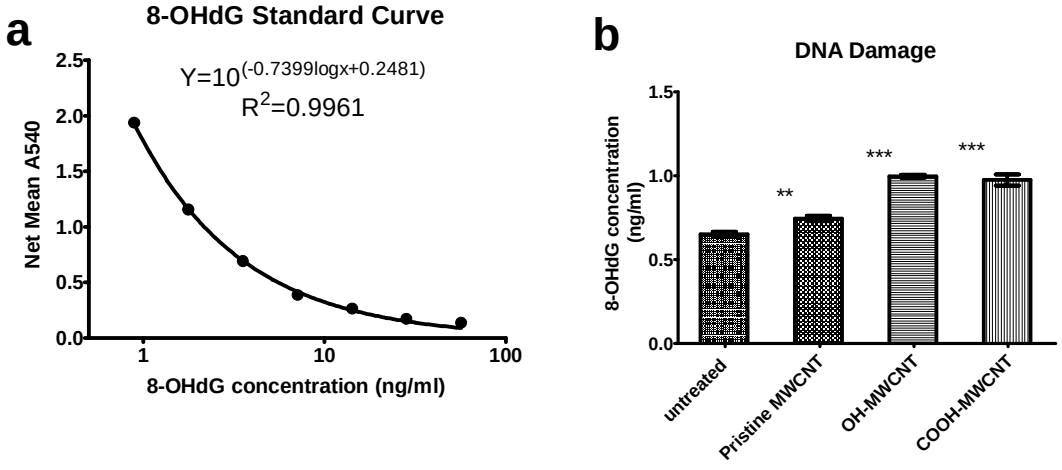

Figure 4-6 DNA damage induced by MWCNTs following 72 hours exposure at a concentration of 50 µg/mL. DNA damage was studied using DNA samples of untreated and MWCNTs treated A549 cells. 8-OHdG (ng/mL) was quantified by colorimetric antibody ELISA assay. Data are represented as mean±SD of triplicate. **p<0.01, ***p<0.001

4.2.6 Cell uptake detection

Flow cytometer offers a very effective method to test for cellular uptake of CNTs. This allows a fluorescent particle to be detected if it associated or has been taken up into the cell by assessing fluorescence present in a cell. The flow cytometry data can also be displayed as FL1 vs. forward scatter, which gives indication of cell size changes and therefore the status of cell health. Based on

the fluorescence level of control cells, a threshold level of fluorescence could be set.

All the MWCNTs are tagged with Alexa 488-BSA by Van der Waals for 24hours. The control cells show lower fluorescent intensity than those treated with MWCNTs. A dose-dependent increase in florescence intensity was evident for cells treated with all the three MWNCTs. It appeared that the uptake was more favoured for the pristine MWCNTs than the functionalized MWCNTs. In addition, the treated cells had wider range of green fluorescent values while the FSC range didn't show significant change, which means the cell size didn't change after the take up of MWCNTs.

Since the nanoparticles tended to adhere to the surface of the cells as well as be taken up, the range of fluorescent values came from the intensity of MWCNTs inside or on the surface of the cells.

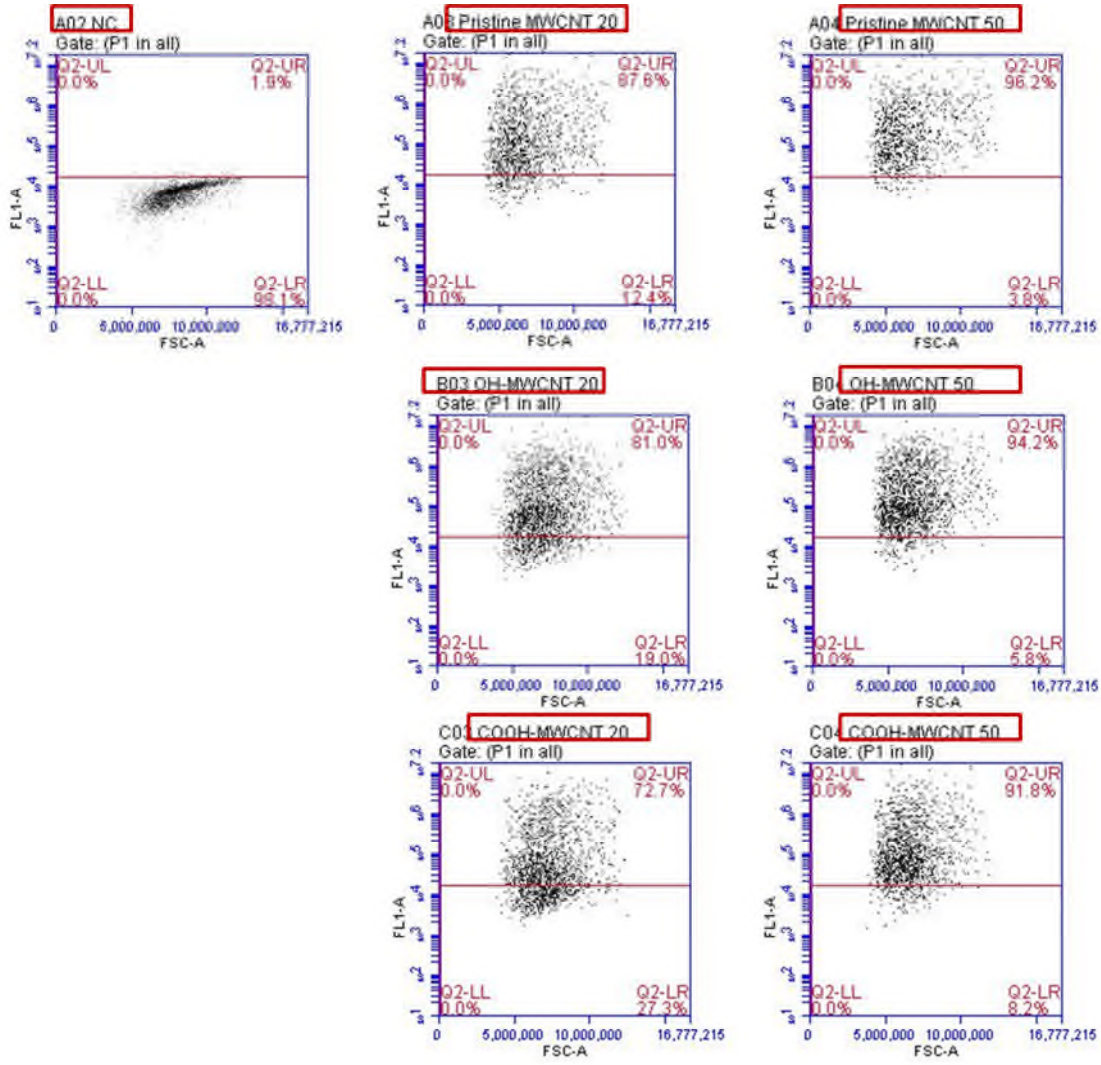

Figure 4-7 Flow cytometry MWCNTs uptake analysis in A549 cells after 24h treatment with MWCNT (20µg/mL). Results were displayed as cell count vs fluorescence intensity. FL1 represents the fluorescent channel for Alex488; any increase in Alex488 will lead to increased FL1 reading.

The detection of cells in samples treated with MWCNTs by flow cytometry suggests that cell uptake of MWCNTs occurred in a concentration dependent manner. Further to this, the degree of MWCNTs uptake in the A549 cells was in the order of pristine MWCNTs>OH-MWCNTs>COOH-MWCNTs, which was particularly evident at the lowest concentration (20µg/mL). (Figure 4-7)

4.2.7 Confocal images of cell uptake

Confocal imaging studies were conducted in conjunction with the flow cytometry to support the findings and to define the cellular location of the carbon nanotubes. It can be seen that the uptake of MWCNTs occurred in A549 cells at 2µg/mL. This was in agreement with the results from the flow cytometry assay.

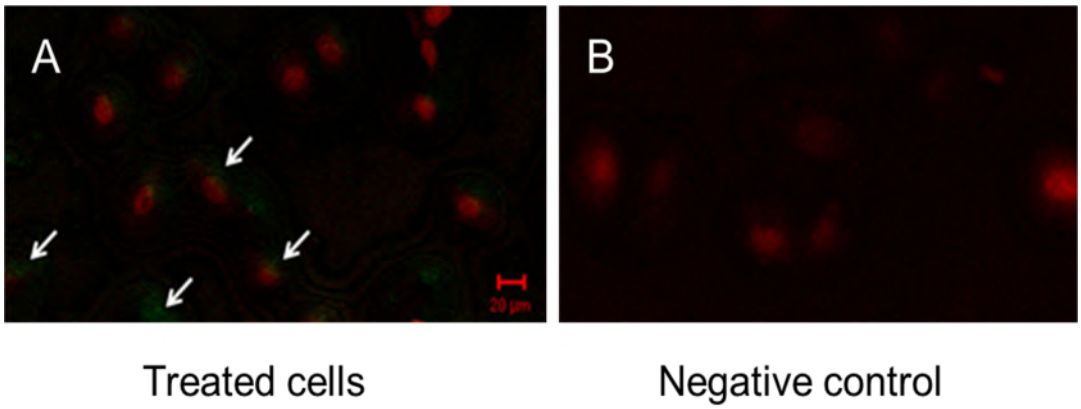

Figure 4-8 A549 cells under confocal microscope. A: untreated cells. B A549 cells treated with 2µg/mL pristine MWCNT for 24hours. Cell nucleus dye was PI (5µg/mL) and Pristine MWCNTs were stained with Alexa488-BSA.

The negative control showed that after 24 hours treatment, most of the A549 cells were unaffected after incubation with pristine carbon nanotubes. The control cells showed a clear fluorescence staining (PI) of the nucleus. After treatment with MWNCT for 24 hours, Figure 4-8 B showed the green fluorescent carbon nanotubes surround the cell nucleus instead of inside the nucleus (white arrow). This pattern of staining suggested that most of MWCNTs were internalised into cytoplasm after 24 hours.

4.2.8 RNA regulation

The Human Stress and Toxicity PathwayFinder™ RT²Profiler™ PCR Array profiles the expression of 84 genes whose expression level is indicative of stress and toxicity. The array includes genes that are directly up-regulated by

oxidative or metabolic stress and by heat shock. The array also includes genes representative of pathways activated by prolonged stress, which range from cell death by apoptosis or necrosis to growth arrest and senescence to proliferation and carcinogenesis.

The expression levels of genes associated with cell cycle, cell apoptosis, osmotic stress, hypoxia, inflammatory response, DNA damage signalling and heat shock protein in A549 cells cultured with 50μg/mL of or without MWCNTs (pristine and COOH functionalised) for two days were analyzed by microarrays. The analysis showed that oxidative response-associated genes such as PRDX1 and heat shock protein exhibited up-regulation expressions; further supporting those p-MWCNTs may induce oxidative stress of A549 cells. The heat shock proteins are also referred to as stress proteins and their up-regulation is sometimes described more generally as part of the stress response.

4.2.8.1 RNA integrity

For RNA assay, A549 cells were treated with p-MWCNTs and COOH-MWCNTs. Before assessing the RNA gene expression by RT-PCR, it is important to assess the quality of the RNA and the presence of any contaminations, which may alter or have major effects on any outcomes. For this bio-rad experion was used. As shown in Figure 4-9, each sample produced a thick and a thin band with size ~1600 and ~4000 respectively. Intact total RNA will have two sharp and clear bands which are 28s rRNA band (~4000) and 18s rRNA (~1600), thereby the consistency of these bands showed in Figure 4-9 suggested a high integrity of these RNA samples.

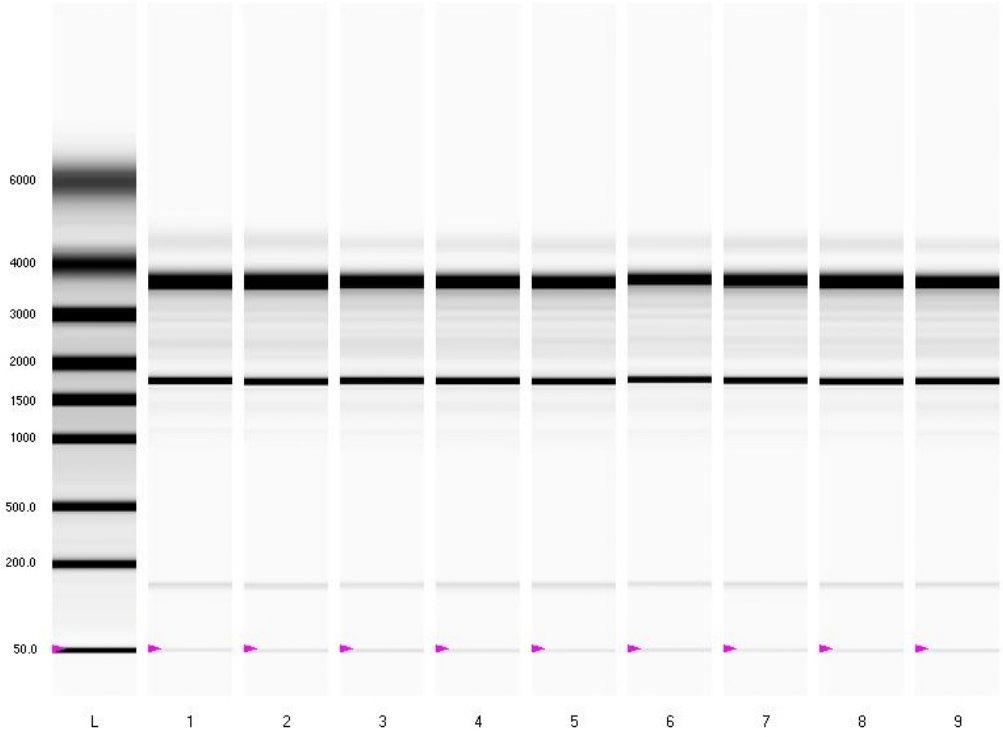

Figure 4-9 RNA integrity assay. The RNA ladder and RNA from controls and cells treated with p-MWCNTs and COOH-MWCNTs were separated by electrophoresis in Bio-Rad experion chambers.

4.2.8.2 Gene change induced by pristine MWCNTs

In order to look at the change of gene transcription, three independent experiments have been conducted for cell treatment, RNA extraction and RT-PCR.

According to Table 4-2, gene HSPA4, IL-8, LDHA and PRDX1 were more than 2 fold over expressed. P-MWCNTs were also found induce 5.29 and 48.2 folds up-regulation of IL-8 and LDHA production. None of the increase of gene regulation was significant; however, the results could still suggest the oxidative environment induced by pristine MWCNTs.

Table 4-2 Alteration of gene regulation induced by pristine MWCNTs.

Symbol	Well	AVG ΔC_t (Ct(GOI) - Ave Ct (HKG))		$2^{-\Delta C_t}$		Fold Change	T-TEST	Fold Up- or Down-Regulation	Comments
		Test Sample	Control Sample	Test Sample	Control Sample	Test Sample /Control Sample	p value	Test Sample /Control Sample	
ADM	A01	4.29	3.82	5.1E-02	7.1E-02	0.72	0.598364	-1.38	OKAY
AKR1B1	A02	0.38	0.20	7.7E-01	8.7E-01	0.88	0.719760	-1.13	OKAY
AQP1	A03	12.46	12.01	1.8E-04	2.4E-04	0.73	0.584534	-1.36	OKAY
AQP2	A04	15.76	16.48	1.8E-05	1.1E-05	1.64	0.328817	1.64	B
AQP4	A05	14.29	15.18	5.0E-05	2.7E-05	1.86	0.628053	1.86	B
ARNT	A06	7.76	8.07	4.6E-03	3.7E-03	1.24	0.979642	1.24	OKAY
ATF4	A07	1.68	1.33	3.1E-01	4.0E-01	0.78	0.494652	-1.28	OKAY
ATF6	A08	5.10	4.46	2.9E-02	4.5E-02	0.64	0.076126	-1.56	OKAY
ATF6B	A09	5.65	5.55	2.0E-02	2.1E-02	0.93	0.782377	-1.07	OKAY
ATG12	A10	4.83	4.88	3.5E-02	3.4E-02	1.03	0.855253	1.03	OKAY
ATG5	A11	5.23	5.21	2.7E-02	2.7E-02	0.98	0.823480	-1.02	OKAY
ATG7	A12	6.53	6.35	1.1E-02	1.2E-02	0.88	0.667629	-1.13	OKAY
ATM	B01	7.32	7.54	6.3E-03	5.4E-03	1.16	0.712068	1.16	OKAY
ATR	B02	7.51	7.49	5.5E-03	5.6E-03	0.99	0.716943	-1.01	OKAY
BBC3	B03	7.62	7.83	5.1E-03	4.4E-03	1.16	0.760841	1.16	OKAY
BECN1	B04	5.09	4.93	2.9E-02	3.3E-02	0.89	0.608453	-1.12	OKAY
BID	B05	3.53	3.53	8.7E-02	8.7E-02	1.00	0.948733	1.00	OKAY
BNIP3L	B06	3.20	3.50	1.1E-01	8.9E-02	1.23	0.428197	1.23	OKAY

CA9	B07	8.93	10.05	2.1E-03	9.4E-04	2.17	0.165260	2.17	OKAY
CALR	B08	1.58	1.48	3.3E-01	3.6E-01	0.93	0.979217	-1.07	OKAY
CASP1	B09	12.35	12.45	1.9E-04	1.8E-04	1.07	0.799589	1.07	OKAY
CCL2	B10	8.05	8.22	3.8E-03	3.4E-03	1.12	0.611882	1.12	OKAY
CD40LG	B11	16.25	16.41	1.3E-05	1.2E-05	1.12	0.817028	1.12	B
CDKN1A	B12	3.75	4.07	7.5E-02	6.0E-02	1.25	0.482297	1.25	OKAY
CFTR	C01	14.80	14.84	3.5E-05	3.4E-05	1.03	0.911982	1.03	B
CHEK1	C02	5.61	5.68	2.0E-02	2.0E-02	1.05	0.944439	1.05	OKAY
CHEK2	C03	5.92	5.95	1.6E-02	1.6E-02	1.02	0.789231	1.02	OKAY
CRP	C04	16.25	16.48	1.3E-05	1.1E-05	1.18	0.712126	1.18	B
DDB2	C05	4.32	4.42	5.0E-02	4.7E-02	1.07	0.822287	1.07	OKAY
DDIT3	C06	7.71	6.08	4.8E-03	1.5E-02	**0.32**	0.706897	**-3.10**	OKAY
DNAJC3	C07	5.16	4.83	2.8E-02	3.5E-02	0.80	0.548226	-1.25	OKAY
EDN1	C08	2.01	2.47	2.5E-01	1.8E-01	1.38	0.663453	1.38	OKAY
EPO	C09	14.10	14.77	5.7E-05	3.6E-05	1.59	0.771351	1.59	B
FAS	C10	6.38	6.49	1.2E-02	1.1E-02	1.08	0.965248	1.08	OKAY
FTH1	C11	-4.60	-3.86	2.4E+01	1.5E+01	1.66	0.292030	1.66	OKAY
GADD45A	C12	7.19	7.19	6.8E-03	6.9E-03	1.00	0.873532	-1.00	OKAY
GADD45G	D01	11.82	12.27	2.8E-04	2.0E-04	1.37	0.704189	1.37	OKAY
GCLC	D02	1.44	1.33	3.7E-01	4.0E-01	0.92	0.801216	-1.08	OKAY
GCLM	D03	1.44	1.31	3.7E-01	4.0E-01	0.91	0.667602	-1.10	OKAY
GRB2	D04	4.35	4.32	4.9E-02	5.0E-02	0.98	0.946327	-1.02	OKAY
GSR	D05	4.80	4.12	3.6E-02	5.7E-02	0.62	0.254050	-1.60	OKAY
GSTP1	D06	-1.45	-1.18	2.7E+00	2.3E+00	1.20	0.351868	1.20	OKAY
HMOX1	D07	4.31	4.56	5.0E-02	4.2E-02	1.19	0.703629	1.19	OKAY

HSP90AA1	D08	-0.12	0.34	1.1E+00	7.9E-01	1.38	0.871684	1.38	OKAY
HSP90B1	D09	0.41	0.20	7.5E-01	8.7E-01	0.86	0.801942	-1.16	OKAY
HSPA4	D10	2.38	2.58	1.9E-01	1.7E-01	1.15	0.992299	1.15	OKAY
HSPA4L	D11	6.53	9.65	1.1E-02	1.2E-03	**8.66**	0.774197	**8.66**	OKAY
HSPA5	D12	6.29	6.22	1.3E-02	1.3E-02	0.96	0.835895	-1.04	OKAY
HUS1	E01	6.24	5.83	1.3E-02	1.8E-02	0.75	0.540410	-1.32	OKAY
IFNG	E02	16.25	15.23	1.3E-05	2.6E-05	0.49	0.330677	-2.02	B
IL1A	E03	11.56	11.83	3.3E-04	2.7E-04	1.20	0.695932	1.20	OKAY
IL1B	E04	12.77	12.75	1.4E-04	1.5E-04	0.98	0.697985	-1.02	OKAY
IL6	E05	14.59	14.79	4.1E-05	3.5E-05	1.15	0.724518	1.15	B
IL8	E06	8.22	10.62	3.4E-03	6.4E-04	**5.29**	0.853865	**5.29**	OKAY
LDHA	E07	-0.65	4.94	1.6E+00	3.3E-02	**48.20**	0.530184	**48.20**	OKAY
MCL1	E08	2.47	3.16	1.8E-01	1.1E-01	1.61	0.321185	1.61	OKAY
MMP9	E09	10.05	10.38	9.5E-04	7.5E-04	1.26	0.792421	1.26	OKAY
MRE11A	E10	4.99	4.69	3.2E-02	3.9E-02	0.81	0.378431	-1.23	OKAY
NBN	E11	4.43	4.28	4.7E-02	5.2E-02	0.90	0.509271	-1.11	OKAY
NFAT5	E12	5.71	6.04	1.9E-02	1.5E-02	1.26	0.826415	1.26	OKAY
NQO1	F01	-2.12	-1.90	4.3E+00	3.7E+00	1.16	0.618407	1.16	OKAY
PARP1	F02	3.56	3.07	8.5E-02	1.2E-01	0.71	0.208870	-1.41	OKAY
PRDX1	F03	2.64	7.06	1.6E-01	7.5E-03	**21.52**	0.631354	**21.52**	OKAY
PVR	F04	4.35	4.11	4.9E-02	5.8E-02	0.85	0.407713	-1.18	OKAY
RAD17	F05	5.29	5.69	2.6E-02	1.9E-02	1.33	0.951515	1.33	OKAY
RAD51	F06	6.60	6.62	1.0E-02	1.0E-02	1.01	0.764964	1.01	OKAY
RAD9A	F07	6.43	6.17	1.2E-02	1.4E-02	0.84	0.682718	-1.19	OKAY
RIPK1	F08	7.56	7.01	5.3E-03	7.8E-03	0.68	0.271310	-1.47	OKAY

SERPINE1	F09	3.28	4.00	1.0E-01	6.3E-02	1.64	0.475451	1.64	OKAY
SLC2A1	F10	5.88	5.93	1.7E-02	1.6E-02	1.03	0.758589	1.03	OKAY
SLC5A3	F11	7.28	7.01	6.4E-03	7.8E-03	0.83	0.647029	-1.21	OKAY
SQSTM1	F12	-0.61	-0.53	1.5E+00	1.4E+00	1.06	0.806264	1.06	OKAY
TLR4	G01	15.21	15.26	2.6E-05	2.5E-05	1.04	0.877080	1.04	B
TNF	G02	16.25	16.48	1.3E-05	1.1E-05	1.18	0.712126	1.18	B
TNFRSF10A	G03	6.70	6.15	9.7E-03	1.4E-02	0.69	0.250859	-1.46	OKAY
TNFRSF10B	G04	4.88	4.65	3.4E-02	4.0E-02	0.86	0.549037	-1.17	OKAY
TNFRSF1A	G05	2.23	2.10	2.1E-01	2.3E-01	0.92	0.576104	-1.09	OKAY
TP53	G06	1.84	1.70	2.8E-01	3.1E-01	0.91	0.756162	-1.10	OKAY
TXN	G07	-1.10	-0.91	2.1E+00	1.9E+00	1.14	0.656379	1.14	OKAY
TXNL4B	G08	5.71	5.63	1.9E-02	2.0E-02	0.94	0.821314	-1.06	OKAY
TXNRD1	G09	0.18	-0.07	8.8E-01	1.0E+00	0.84	0.389777	-1.19	OKAY
ULK1	G10	5.56	5.64	2.1E-02	2.0E-02	1.06	0.722594	1.06	OKAY
VEGFA	G11	6.02	6.06	1.5E-02	1.5E-02	1.03	0.733243	1.03	OKAY
XPC	G12	6.93	6.62	8.2E-03	1.0E-02	0.81	0.465680	-1.24	OKAY
ACTB	H01	-3.00	-3.54	8.0E+00	1.2E+01	0.69	0.199287	-1.45	OKAY
B2M	H02	1.62	1.85	3.3E-01	2.8E-01	1.18	0.408742	1.18	OKAY
GAPDH	H03	-2.01	-1.99	4.0E+00	4.0E+00	1.01	0.857257	1.01	OKAY
HPRT1	H04	3.40	3.68	9.5E-02	7.8E-02	1.21	0.479857	1.21	OKAY
RPLP0	H05	-3.31	-2.96	9.9E+00	7.8E+00	1.28	0.416727	1.28	OKAY

Fold-Regulation represents fold-change results in a biologically meaningful way.

Fold change values greater than one indicates a positive- or an up-regulation, and the fold-regulation is equal to the fold-change

Fold-change values less than one indicate a negative or down-regulation, and the fold-regulation is the negative inverse of the fold-change.

Fold-change and fold-regulation values greater than 2 are indicated in red; fold-change values less than 0.5 and fold-regulation values less than -2 are indicated in blue.

The p values are calculated based on a Student's t-test of the replicate 2^(- Delta Ct) values for each gene in the control group and treatment groups, and p values less than 0.05 are indicated in red.

A: This gene's average threshold cycle is relatively high (> 30) in either the control or the test sample, and is reasonably low in the other sample (< 30).

These data suggest that the gene's expression is relatively low in one sample and reasonably detected in the other sample suggesting that the actual fold-change value is at least as large as the calculated and reported fold-change result.

This fold-change result may also have greater variations if p value > 0.05; therefore, it is important to have a sufficient number of biological replicates to validate the result for this gene.

B: This gene's average threshold cycle is relatively high (> 30), meaning that its relative expression level is low, in both crontrol and test samples, and the p-value for the fold-change is either unavailable or relatively high (p > 0.05).

This fold-change result may also have greater variations; therefore, it is important to have a sufficient number of biological replicates to validate the result for this gene.

C: This gene's average threshold cycle is either not determined or greater than the defined cut-off (deault 35) in both samples meaning that its expression was undetected, making this fold-change result erroneous and un-interpretable.

Table 4-2 described the alteration of gene regulation induced by pristine MWCNTs. The meaning of AVG ΔCt (Ct(GOI) - Ave Ct (HKG)) has been explained on page 70. Fold changes provided the information about up or down regulation of the specific gene. P value showed the significancy of the fold change of genes. In most cases the comment reported is ‘okay’ which means most of the gene’s average threshold cycle is within 30 which is a reasonable cell cycle number.

From Table 4-2, it can be easily observed that, genes HSPA4L, IL8, LDHA, PRDX1 were all upregulated 8.66, 5.29, 48.2 and 21.52 folds respectively compared with negative control. However, none the change were significant. The great increase of LDHA and PRDX1 in gene expression could still suggest that pristine carbon nanotubes could potentially increase their expression although it is important to have a sufficient number of biological replicates to validate the result for them.

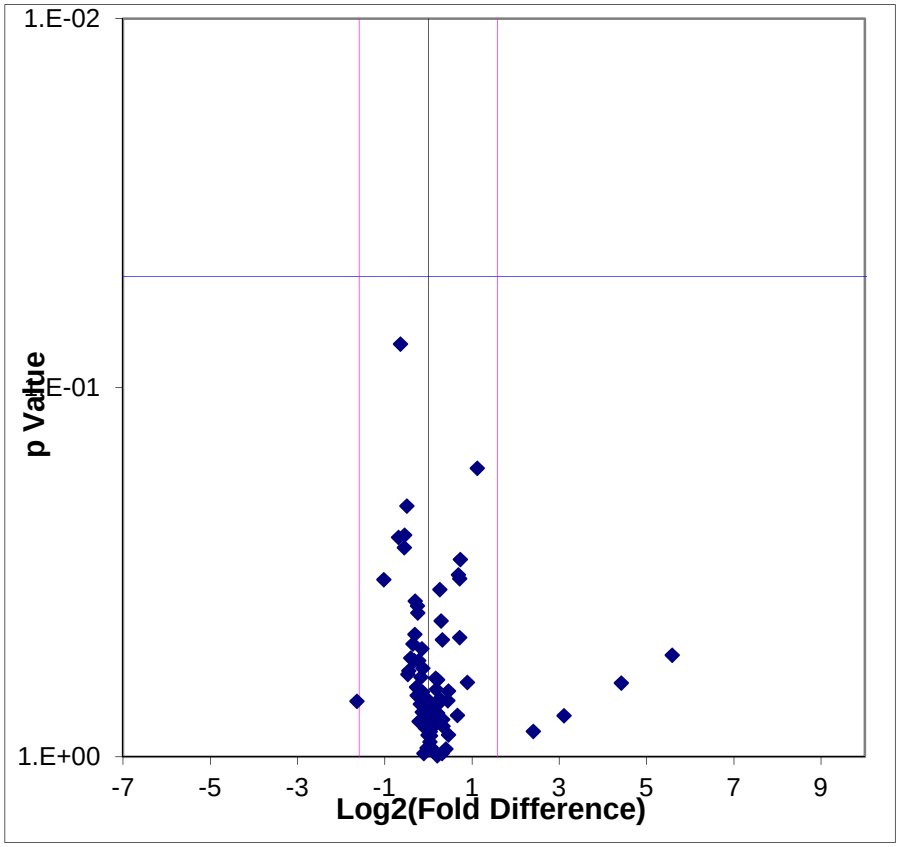

Figure 4-10 Total RNA array volcano plot. A549 cells were treated for 48 hours with pristine MWCNTs 50µg/mL. The x-axis represents the fold difference in RNA expression between control cells and those treated cells

Figure 4-10 is the volcano plot with data of pre normalisation. It was noted that several of RNAs were significantly up-regulated. After contacting the data analyst at Qaigen UK, it was advised that these results required to be normalised against house-keeping gene. All the data were normalised using the entire house-keeping gene including B2M, HPRT1, RPL13A, GAPDH and ACTB.

The template download from Qiagen website (http://www.sabiosciences.com/rt_pcr_product/HTML/PAHS-003Z.htmL) automatically displays the replicate Ct values for the chosen housekeeping genes in both samples.

The Volcano Plot graphs the log2 of the fold change in each gene's expression between the samples versus its p value from the t-test. The black line indicates fold changes of 1. The pink lines indicate the desired fold-change of 2 in gene expression. The blue line indicates the desired p value of the t-test threshold (0.05). In figure 4-10, only four dot located outside the pink line (on the right the pink line) which indicated that four genes were up-regulated. All the dots were underneath the blue line which means none of the change were significant.

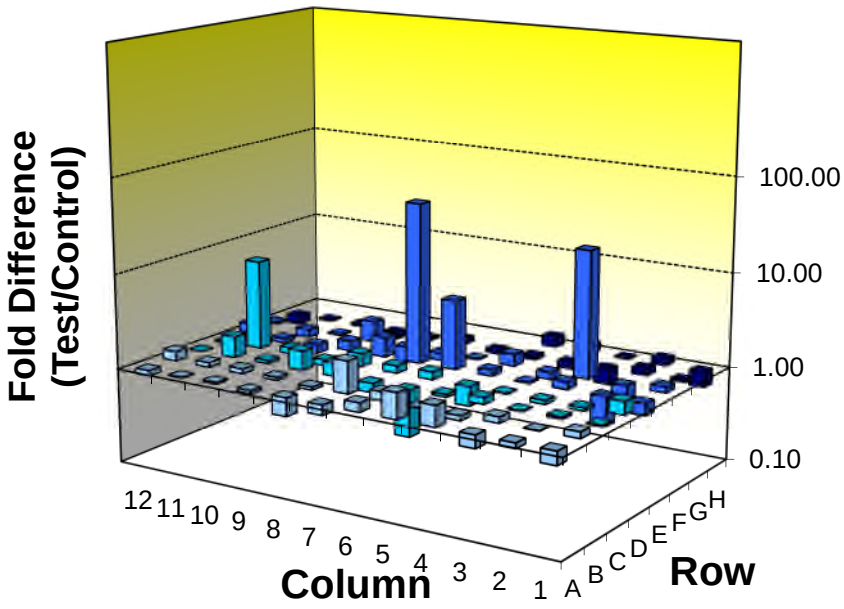

Figure 4-11 Total RNA array 3-D profile. A549 cells were treated for 48 hours with pristine MWCNTs 50µg/mL. The x-axis represents the fold difference in RNA expression between control cells and those treated cells.

The 3D profile graphs was also automatically generated from the data analysis template mentioned earlier. The 3D Profile graphs shows the fold difference in expression of each gene between the two samples in the 100 well ring format of the PCR Array. Columns pointing up (with z-axis values > 1) indicate an up-regulation of gene expression, and columns pointing down (with z-axis values <

1) indicate a down-regulation of gene expression in the test sample relative to the control sample.

The 3D profile made it more clear and obvious that certain genes were greatly up-regulated and none of the RNA was down-regulated.

4.2.8.3 Gene change induced by COOH-MWNCTs

Functionalized MWCNTs were found more genotoxic according to oxidative DNA damage experiment in A549 cells.

As shown in Table 4-3, much more genes are overexpressed in cells treated with COOH-MWCNTs than those treated with p-MWCNTs. In this experiment, genes ARNT, EPO, LDHA, ATG, CHECK1, GADD45G, HSPAL, IL-8 and PRDX1 were overexpressed more than 2 folds in treated cells. In addition, genes PROX1, ATG, HSPA and MMP were significantly increased by COOH-MWCNTs.

Among them, the genes whose expression increased in cells treated with pristine MWCNTs were also found over-expressed in cells treated with COOH-MWCNTs. The results suggested that pristine MWCNTs and COOH-MWCNTs had some common effects on cells, however, COOH functionalised MWCNTs were more geno-toxic by exhibiting more gene up-regulations.

Table 4-3 Alteration of gene regulation induced by COOH-MWCNTs.

Symbol	Well	AVG ΔC_t (Ct(GOI) - Ave Ct (HKG))		$2^{-\Delta C_t}$		Fold Change	T-TEST	Fold Up- or Down-Regulation	Comments
		Test Sample	Control Sample	Test Sample	Control Sample	Test Sample /Control Sample	p value	Test Sample /Control Sample	
ADM	A01	3.66	3.82	7.9E-02	7.1E-02	1.12	0.781541	1.12	OKAY
AKR1B1	A02	0.71	0.20	6.1E-01	8.7E-01	0.70	0.217341	-1.43	OKAY
AQP1	A03	11.41	12.01	3.7E-04	2.4E-04	1.52	0.456992	1.52	OKAY
AQP2	A04	17.45	16.48	5.6E-06	1.1E-05	0.51	0.774772	-1.96	B
AQP4	A05	13.92	15.18	6.5E-05	2.7E-05	2.40	0.327516	2.40	A
ARNT	A06	5.88	8.07	1.7E-02	3.7E-03	**4.55**	0.317719	**4.55**	OKAY
ATF4	A07	2.02	1.33	2.5E-01	4.0E-01	0.62	0.192927	-1.62	OKAY
ATF6	A08	4.17	4.46	5.6E-02	4.5E-02	1.22	0.400808	1.22	OKAY
ATF6B	A09	4.60	5.55	4.1E-02	2.1E-02	1.92	0.156078	1.92	OKAY
ATG12	A10	3.94	4.88	6.5E-02	3.4E-02	1.91	0.114520	1.91	OKAY
ATG5	A11	3.95	5.21	6.5E-02	2.7E-02	2.38	**0.007161**	2.38	OKAY
ATG7	A12	4.46	6.35	4.5E-02	1.2E-02	**3.69**	0.223349	**3.69**	OKAY
ATM	B01	5.97	7.54	1.6E-02	5.4E-03	2.97	0.100447	2.97	OKAY
ATR	B02	6.04	7.49	1.5E-02	5.6E-03	2.73	0.058693	2.73	OKAY
BBC3	B03	6.66	7.83	9.9E-03	4.4E-03	2.25	0.119271	2.25	OKAY
BECN1	B04	4.75	4.93	3.7E-02	3.3E-02	1.13	0.211146	1.13	OKAY
BID	B05	3.02	3.53	1.2E-01	8.7E-02	1.42	0.378193	1.42	OKAY
BNIP3L	B06	4.11	3.50	5.8E-02	8.9E-02	0.65	0.427111	-1.54	OKAY
CA9	B07	8.95	10.05	2.0E-03	9.4E-04	2.15	0.132307	2.15	OKAY
CALR	B08	1.48	1.48	3.6E-01	3.6E-01	1.00	0.917290	1.00	OKAY

CASP1	B09	12.13	12.45	2.2E-04	1.8E-04	1.24	0.907517	1.24	OKAY
CCL2	B10	8.22	8.22	3.3E-03	3.4E-03	0.99	0.844531	-1.01	OKAY
CD40LG	B11	17.70	16.41	4.7E-06	1.2E-05	0.41	0.200893	-2.46	B
CDKN1A	B12	3.18	4.07	1.1E-01	6.0E-02	1.86	0.089225	1.86	OKAY
CFTR	C01	15.32	14.84	2.4E-05	3.4E-05	0.71	0.804396	-1.40	A
CHEK1	C02	4.00	5.68	6.2E-02	2.0E-02	**3.19**	**0.047164**	**3.19**	OKAY
CHEK2	C03	5.08	5.95	3.0E-02	1.6E-02	1.83	0.089157	1.83	OKAY
CRP	C04	17.20	16.48	6.7E-06	1.1E-05	0.61	0.580509	-1.65	B
DDB2	C05	3.49	4.42	8.9E-02	4.7E-02	1.90	0.108486	1.90	OKAY
DDIT3	C06	5.20	6.08	2.7E-02	1.5E-02	1.83	0.283591	1.83	OKAY
DNAJC3	C07	4.55	4.83	4.3E-02	3.5E-02	1.22	0.339164	1.22	OKAY
EDN1	C08	1.99	2.47	2.5E-01	1.8E-01	1.39	0.626768	1.39	OKAY
EPO	C09	12.16	14.77	2.2E-04	3.6E-05	**6.10**	0.117451	**6.10**	A
FAS	C10	5.47	6.49	2.3E-02	1.1E-02	2.02	0.190663	2.02	OKAY
FTH1	C11	-3.76	-3.86	1.4E+01	1.5E+01	0.93	0.686185	-1.08	OKAY
GADD45A	C12	5.38	7.19	2.4E-02	6.9E-03	**3.50**	0.115399	**3.50**	OKAY
GADD45G	D01	10.17	12.27	8.7E-04	2.0E-04	**4.29**	0.061966	**4.29**	OKAY
GCLC	D02	1.41	1.33	3.8E-01	4.0E-01	0.94	0.695080	-1.06	OKAY
GCLM	D03	1.41	1.31	3.8E-01	4.0E-01	0.93	0.796435	-1.08	OKAY
GRB2	D04	3.57	4.32	8.4E-02	5.0E-02	1.68	0.108896	1.68	OKAY
GSR	D05	3.16	4.12	1.1E-01	5.7E-02	1.94	0.302309	1.94	OKAY
GSTP1	D06	-1.54	-1.18	2.9E+00	2.3E+00	1.28	0.381899	1.28	OKAY
HMOX1	D07	3.87	4.56	6.8E-02	4.2E-02	1.62	0.296914	1.62	OKAY
HSP90AA1	D08	0.63	0.34	6.4E-01	7.9E-01	0.82	0.478890	-1.23	OKAY
HSP90B1	D09	0.18	0.20	8.8E-01	8.7E-01	1.01	0.946457	1.01	OKAY
HSPA4	D10	1.15	2.58	4.5E-01	1.7E-01	2.69	**0.047869**	2.69	OKAY
HSPA4L	D11	5.17	9.65	2.8E-02	1.2E-03	**22.24**	0.274164	**22.24**	OKAY

HSPA5	D12	6.01	6.22	1.5E-02	1.3E-02	1.16	0.604680	1.16	OKAY
HUS1	E01	4.98	5.83	3.2E-02	1.8E-02	1.80	0.336651	1.80	OKAY
IFNG	E02	16.44	15.23	1.1E-05	2.6E-05	0.43	0.662561	-2.32	B
IL1A	E03	11.15	11.83	4.4E-04	2.7E-04	1.60	0.401914	1.60	OKAY
IL1B	E04	15.25	12.75	2.6E-05	1.5E-04	**0.18**	0.607219	**-5.69**	OKAY
IL6	E05	17.00	14.79	7.6E-06	3.5E-05	**0.22**	0.931150	**-4.61**	B
IL8	E06	6.80	10.62	8.9E-03	6.4E-04	**14.07**	0.141103	**14.07**	OKAY
LDHA	E07	-0.66	4.94	1.6E+00	3.3E-02	**48.56**	0.519129	**48.56**	OKAY
MCL1	E08	1.96	3.16	2.6E-01	1.1E-01	2.29	0.079347	2.29	OKAY
MMP9	E09	8.82	10.38	2.2E-03	7.5E-04	2.95	**0.037489**	2.95	OKAY
MRE11A	E10	4.11	4.69	5.8E-02	3.9E-02	1.50	0.437662	1.50	OKAY
NBN	E11	4.00	4.28	6.2E-02	5.2E-02	1.21	0.515214	1.21	OKAY
NFAT5	E12	4.38	6.04	4.8E-02	1.5E-02	**3.17**	0.159734	**3.17**	OKAY
NQO1	F01	-2.30	-1.90	4.9E+00	3.7E+00	1.31	0.287697	1.31	OKAY
PARP1	F02	3.12	3.07	1.1E-01	1.2E-01	0.96	0.799647	-1.04	OKAY
PRDX1	F03	2.28	7.06	2.1E-01	7.5E-03	**27.51**	0.343950	**27.51**	OKAY
PVR	F04	4.21	4.11	5.4E-02	5.8E-02	0.93	0.451232	-1.08	OKAY
RAD17	F05	4.29	5.69	5.1E-02	1.9E-02	2.64	0.076679	2.64	OKAY
RAD51	F06	5.53	6.62	2.2E-02	1.0E-02	2.13	0.101020	2.13	OKAY
RAD9A	F07	6.44	6.17	1.2E-02	1.4E-02	0.83	0.537322	-1.20	OKAY
RIPK1	F08	5.55	7.01	2.1E-02	7.8E-03	2.74	0.274367	2.74	OKAY
SERPINE1	F09	3.04	4.00	1.2E-01	6.3E-02	1.94	0.292145	1.94	OKAY
SLC2A1	F10	5.52	5.93	2.2E-02	1.6E-02	1.33	0.411943	1.33	OKAY
SLC5A3	F11	7.64	7.01	5.0E-03	7.8E-03	0.64	0.130826	-1.55	OKAY
SQSTM1	F12	-0.62	-0.53	1.5E+00	1.4E+00	1.07	0.775126	1.07	OKAY
TLR4	G01	14.69	15.26	3.8E-05	2.5E-05	1.49	0.310943	1.49	A
TNF	G02	18.88	16.48	2.1E-06	1.1E-05	**0.19**	0.075855	**-5.27**	B

TNFRSF10A	G03	6.20	6.15	1.4E-02	1.4E-02	0.97	0.803340	-1.03	OKAY
TNFRSF10B	G04	3.36	4.65	9.8E-02	4.0E-02	2.45	0.247295	2.45	OKAY
TNFRSF1A	G05	2.07	2.10	2.4E-01	2.3E-01	1.02	0.746688	1.02	OKAY
TP53	G06	1.98	1.70	2.5E-01	3.1E-01	0.82	0.538264	-1.22	OKAY
TXN	G07	-0.86	-0.91	1.8E+00	1.9E+00	0.97	0.921512	-1.03	OKAY
TXNL4B	G08	4.62	5.63	4.1E-02	2.0E-02	2.02	0.184666	2.02	OKAY
TXNRD1	G09	0.65	-0.07	6.4E-01	1.0E+00	0.61	0.131406	-1.65	OKAY
ULK1	G10	5.67	5.64	2.0E-02	2.0E-02	0.98	0.953436	-1.02	OKAY
VEGFA	G11	5.42	6.06	2.3E-02	1.5E-02	1.56	0.152361	1.56	OKAY
XPC	G12	4.71	6.62	3.8E-02	1.0E-02	**3.77**	0.346100	**3.77**	OKAY

For an interpretation of the table contents see the legend of table 4-2

Table 4-3 shows that gene ARNA, ATG7, CHEK1, EPO, GADD45A, GADD45G, HSPA4L, IL8, LDHA, MMP9, PRDX1 and XPC were 4.55, 3.69, 3.19, 6.10, 3.50, 4.29, 22.24, 14.07, 48.56, 3.17, 27.51 and 3.77 fold up-regulated. Gene IL1B, IL6 and TNF were 0.18, 0.22 and 0.19 fold down regulated. In addition, gene ATG5 and CHEK1 were significant showing increases of 2.39 and 3.19 fold, respectively.

Compared with pristine MWCNTs, functionalised MWCNTs induced more gene up and down-regulation. Similarily, most of gene expression cycle was within 30, which means the experiment was well controlled and reproducible. .

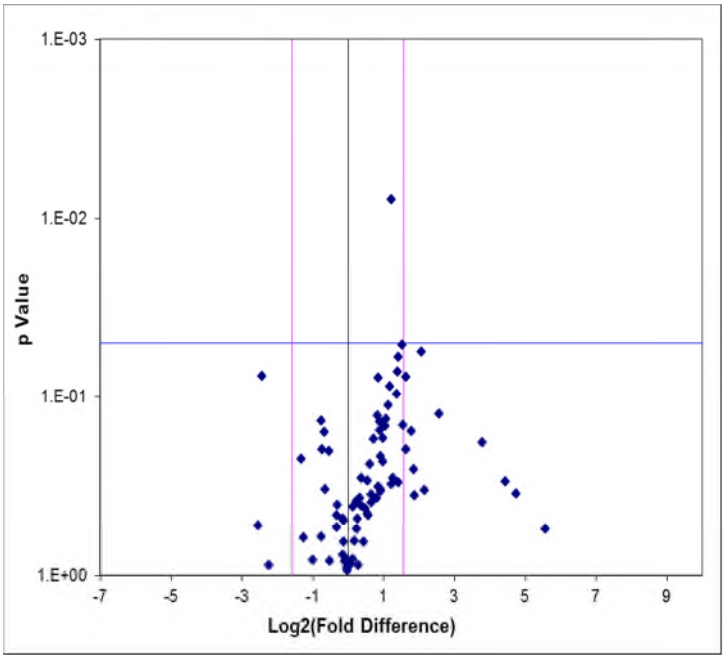

Figure 4-12 Figure Total RNA array volcano plot. A549 cells were treated for 48 hours with COOH-MWCNTs 50µg/mL. The x-axis represents the fold difference in RNA expression between control cells and those treated cells

This Volcano Plot (Figure 4-12) also demonstrates that log2 of the fold change in each gene's expression between the samples versus its p value from the t-test. Similarly as in Figure 4-10, the black line indicates fold changes of 1. The pink lines indicate the desired fold-change of 2 in gene expression. The blue line indicates the desired p value of the t-test threshold (0.05). The figure, clearly

shows that more dots are located on the right of the pink line compared with the volcano figure of pristine MWCNTs which means more genes were up-regulated. Three of the genes were down-regulated as three dots were on the left of the threshold.

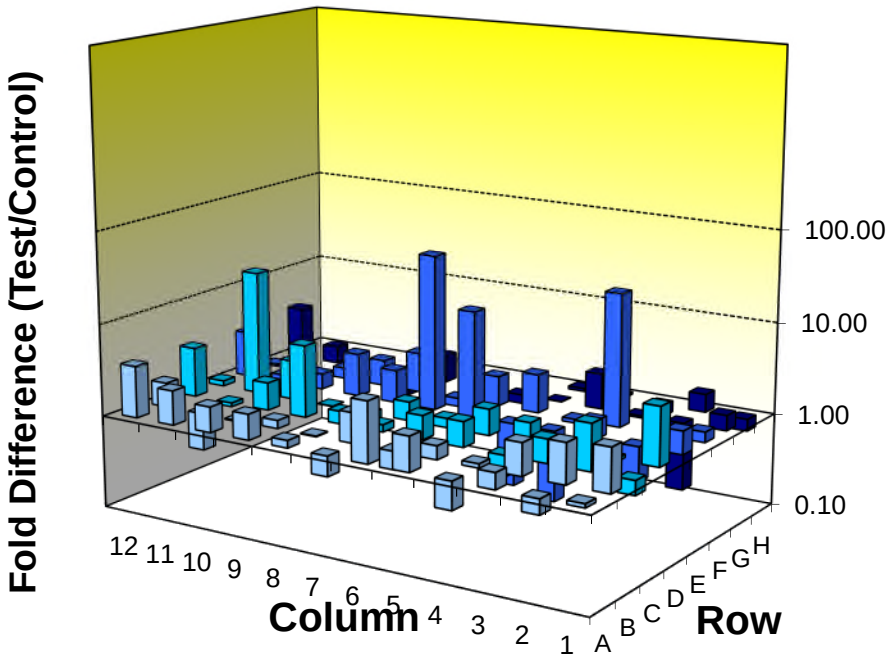

Figure 4-13 Total RNA array 3-D profile. A549 cells were treated for 48 hours with COOH-MWCNTs 50μg/mL. The x-axis represents the fold difference in RNA expression between control cells and those treated cells.

Same as the previous 3-D profile, each column represent one type of gene. Columns pointing up (with z-axis values > 1) indicate an up-regulation of gene expression, and columns pointing down (with z-axis values < 1) indicate a down-regulation of gene expression in the test sample relative to the control sample.

Compared with 3-D profile of pristine RNA, functionalised MWCNTs exhibited more columns pointing up higher than 10 folds, which indicated more gene up-regulation.

4.3 Discussion

MWCNTs are widely used for a variety of commercial products; however, the knowledge of the biological consequence of MWCNTs exposure in the environment is still poorly understood. In this study, the cytotoxic effects of functionalized and pristine MWCNTs were investigated using an experimental in vitro model consisting of human lung epithelial cells (A549). Different methods of measurement were applied in order to estimate the potential human exposure. Early and late cellular response to MWCNT was evaluated by the measurements of cell cytotoxicity, apoptosis and oxidative stress induced genotoxicity. In addition, non-toxic dose was also investigated in order to evaluate the feasible use of such materials therapeutically.

In our cell viability study, the cell proliferation reagent WST-1 was used to evaluate cell viability in response to pristine and functionalized MWCNTs. Figure 2 describes the cell viability in relation to concentrations. At 20µg/mL, the hydroxylated and carboxylated nanotubes were significantly more cytotoxic than pristine nanotubes. Toxicity is not significantly different at 50µg/mL but at 200µg/mL, the pristine MWCNTs became more toxic. Only higher concentrations (20-200 µg/mL) of MWCNTs were found to be toxic after 24 hours exposure employing the wst-1 assay; whilst all MWCNTs with lower concentrations (<10 µg/mL) didn't affect cell proliferation significantly. Results suggested that 0.8-10 µg/mL could be a safe dose for drug delivery. Similarly, in a study conducted by Srivastava, MWCNTs were found to be non-toxic of concentrations from 0.5 to 10 µg/mL following 24 and 48h exposure using the less sensitive MTT assay (Srivastava et al., 2011). Within the concentration range of 20-200µg/mL, we found that cell viability was altered by MWCNTs in a dose dependent manner. In addition, interestingly at concentration of 20µg/mL, non-functionalized MWCNT showed greater cell viability than either –OH and –COOH functionalized MWCNTs. This result was inverted when the concentration was increased to 200µg/mL. This could be attributed to functionalised MWCNTs exhibiting higher degree of aggregation than pristine MWCNTs in the medium. It has been reported that only those carbon nanotubes which are not aggregated and free in the medium are able to reach

the cytoplasm and subsequently the nucleus (Johnston et al., 2010). Furthermore, in our research all three MWCNTs used have the same dimensions in terms of length and of outside diameter but with different surface charge in the medium. Hence, the different cytotoxic effects found in this study could be attributed not only to the different level of aggregation, but also to the different charge resulting from the presence of hydroxyl or carboxyl group on the surface of MWCNT (Singh et al., 2012).

Apoptosis is one of the major factors, which determine the medical application of nanomaterials. Therefore, it is important to learn how modification of CNTs with functional groups would affect apoptotic pathway. The data presented in this study revealed that MWCNTs induced less apoptosis compared with functionalized MWCNTs (Figure 4-1), indicating that the presence of –OH and –COOH on MWCNTs promotes cell apoptosis. However, the extent of apoptosis was reduced when the functionalized MWCNTs' concentration increased to 200µg/mL. This reduction might be explained by the aggregation at 200µg/mL altered the pathway of cell death. According to the cell membrane integrity assay, cells didn't show significant membrane damage until the concentration was increased to 200µg/mL (Figure 4-3), suggesting different method of cell death among various concentrations. At lower concentrations, where carbon nanotubes were better dispersed, cell death was mainly due to apoptosis; when concentrations were increased to 200µg/mL cells underwent necrotic cell death illustrated by detection of cell aggregates in the medium.

Oxidative stress plays an essential role in toxicity induced by carbon nanotubes (Pichardo et al., 2012). During times of environmental stress, the highly increased ROS levels (Figure 4-4) can result in significant damage to cells by activating cell death. DNA damage was found in Met-5A and A549 cell lines using the comet assay (Cavallo et al., 2012), (Lindberg et al., 2013b) when exposed to MWCNTs. Our study showed that functionalized MWCNTs induced significantly higher amount of 8-oxo-dG indicating that functionalized forms of MWCNTs could lead to genotoxicity by damaging DNA (Figure 4-6). However, understanding of the toxic mechanisms underlying this toxicity still remains

incomplete. One view is that CNTs were taken up as nanoneedles which could puncture cell membrane directly and then move to the nucleus (Mu et al., 2009). A study carried out by Palomaki further showed that only long, needle-like CNT induced inflammatory activation (Palomäki et al., 2011). Another view is that the induction of oxidative stress is a main drive behind particle exposure-associated genotoxicity (Van Berlo et al., 2012). DNA damage can thus occur due to the direct action of reactive oxygen species such as hydroxyl radicals (Eastman and Barry, 1992). In our study, although total ROS generation didn't show significant difference among pristine and functionalised MWCNTs (Figure 4-4). In our experiment, functionalized MWNCTs induced more cell damage while ROS generation of them were not significantly higher than pristine form. It could be explained that functionalized MWCNTs have higher propensity to cross cell membranes (Mali et al., 2011), thereby they increase more genotoxicity as we observed.

The experiment of cell uptake showed different take-up efficiency of the three MWCNTs (Figure 4-7) and they are all dose-dependent. MWCNTs exerted highest take up efficiency which was 87.6% at 20μg/mL and 97.2%μg/mL respectively. OH-MWNCTs and COOH-MWCNTs exerted 81% and 72.7% at 20μg/mL, and increased to 94.2% and 91.8% respectively. In this case, high take-up efficiency was related to the degree of aggregation in the medium.

In this study pristine and functionalized (-OH, -COOH) multi-wall carbon nanotubes (MWCNTs) caused cell death with a concentration of or above 20 μg/mL. After 48 hours exposure, both apoptosis and DNA damage could be further observed. Functionalized MWCNTs exerted more genotoxicity compared with the pristine form according to apoptosis and 8-OHdG measurements. In addition, toxic effects of MWCNTs were also dependent on the dispersing agents. Cytotoxicity could be increased by the presence of BSA which could change dispersibility of MWCNTs in cell culture medium. In addition, it was also found that cell viability could be influenced by dispersion solvent and accumulation of 8-oxodG *in vitro* induced by MWCNTs.

Further work is needed to investigate cellular internalization of carbon nanotubes in order to gain better insight into the mechanism of toxicity. In addition, a normal lung fibroblast cell line as well as other cell lines (e.g. skin cell lines) may be employed for further study since different cell lines may show various sensitivities to nanoparticles (Hasan et al., 2012) and cancer cells might be more resistant to toxic factors. Some excellent efforts and progress has been made, but it still may be some time before more clinical applications of MWCNTs will be achieved by better understanding their health impact on humans.

Toxicology is the study of the adverse effects of chemicals, particularly drugs, on living organisms. The understanding of drug-body interactions is crucial to drug development. Drug absorption, distribution, metabolism, and excretion (ADME) is critical in all phases of drug development programs by providing key insights in how a drug will ultimately be treated or accepted by the body. In the late 1980s to the mid-1990s, 40% of all drug failures in clinical trials were due to unfavourable toxicology and ADME profiles. With the improvement of ADME and toxicology testing, the failure rate has now been reduced to 14%. QIAGEN's Toxicology and Drug ADME related PCR arrays can help analyse the toxicology and ADME profiles of drug candidates. Little work has been done on the involvement of RNA in therapeutic toxicity regulation. However, from what is established, the translation of carbon nanotubes toxicity is most likely via oxidative and inflammatory stresses. Oxidative stress triggers signalling pathways which lead to transcription of inflammatory cytokines and chemokines (Tripathi and Aggarwal, 2006).

Both pristine and COOH treated cells exhibited HSPA4, PRDX1, IL-8 which suggested environmental oxidative stress and inflammatory response. Among them, HSPA4 was significantly increased in COOH-MWCNTs treated cells. In addition, LDHA gene was also overexpressed in cells. Lactate dehydrogenase A catalyzes the inter-conversion of pyruvate and L-lactate with concomitant inter-conversion of NADH and NAD+. LDHA is found in most somatic tissues, it has long been known that many human cancers have higher LDHA levels

compared to normal tissues. It has also been shown that LDHA plays an important role in the development, invasion and metastasis of malignancies.

On the top of those genes, functionalized (-COOH) MWCNTs induced more up-regulated genes compared with p-MWCNTs. Among them, CHEK1.CHEK1 is a central component of genome surveillance pathways and is a key regulator of the cell cycle and cell survival. CHEK1 is required for the initiation of DNA damage checkpoints and has recently been shown to play a role in the normal cell cycle (Patil et al., 2013) CHEK1 impacts various stages of the cell cycle including the S phase, G2/M transition and M phase (Zhang and Hunter, 2014). The up-regulation of GADD45A and GADD45D indicated that COOH-MWNCTs also affected growth arrest and senescence. In addition, overexpressed ARNT, EPO, LDHA and MMP9 genes could suggest that treated cells were under hypoxia environment. In the experiment conducted by Wang the aggregated SWNTs showed significant effects on the hypoxia (Wang et al., 2014b). Figure 4-14 exhibited the model describing the inter-connected effects of MMP, ROS and O_2 consumption on mitochondrial dysfunction and hypoxia after treated with SWCNTs fractions. Hypoxia has also been found in Ehrlich ascites carcinoma cells after treatment with MWCNT.

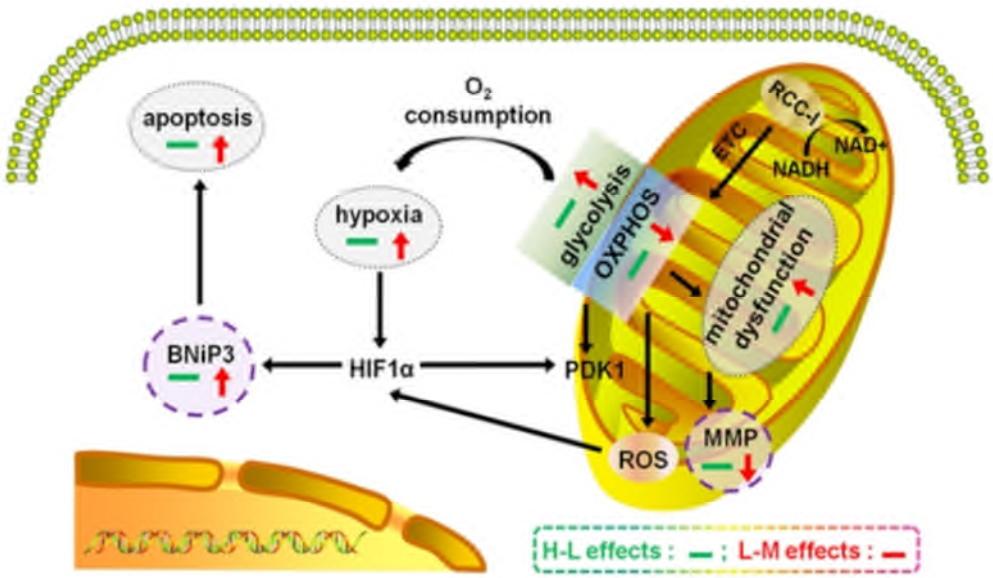

Figure 4-14 Schematics of the bio-effect of different SWCNT fractions. Models describing the interconnected effects of glycolysis/OXPHOS, MMP, RCC-I, HIF1α, BNiP3, PDK1, ROS and O2 consumption on mitochondrial dysfunction and hypoxia after treated with different SWNT fractions.

The present study shows that singly-dispersed fractions higher accumulated in cells with less mitochondria dysfunction and hypoxia. Particularly, hypoxia-relative gene MMP9 significantly increased in COOH-MWCNTs cells.

Carbon nanotubes were also found induce autophagy in cells (Park et al., 2014). MWCNTs seemed to trigger the activation of cell autophagy with the intracellular ATG16L1 level increase as a defence mechanism (Wang et al., 2014a). The result of significant up-regulation of gene ATG was in consistent with apoptosis detection (Table 4-1).

4.4 Conclusion

Pristine MWCNTs had lower IC50 than functional MWCNTs, which indicates that pristine MWCNTs were more toxic in terms of cell viability. However, LDH didn't showed any significant cell membrane damage at the same concentration, which could be explained that most of cells were dead through apoptosis instead of necrosis. In addition, both 8-oxo-dG and ROS generation suggested the oxidative environment induced by MWCNTs.

Functionalized MWCNTs exerted more oxidative DNA damage compared with the pristine form according to 8-OHdG measurements. These results were consistent with the .microRNA array detection. Functional MWCNTs induced more toxicity related gene alteration. Both pristine and COOH treated cells exhibited HSPA4, PRDX1, IL-8 which suggested environmental oxidative stress and inflammatory response. On the top of those genes, functionalized (-COOH) MWCNTs induced more up-regulated genes compared with p-MWCNTs including CHEK1, GADD45A, EPO, LDHA and MMP9. The results indicates that functional MWCNTs are more geno-toxic and induced higher level of oxidative stress, apoptosis, DNA damage and hypoxia environment.

In addition, according to the experiments of cell uptake, carbon nanotubes were not found inside of the cells but surrounded the cell surface. The flow cytometer also confirmed that MWCNTs were tended to attach to cells and pristine MWCNTs were found exhibiting significantly more attachments which was probably due to better dispersion of pristine MWCNTs.

In sum, pristine MWCNTs were more cytotoxic (more cell death) while functional MWCNTs were more genotoxic (higher standard of apoptosis and gene change)

Further work is needed to investigate cellular internalization of carbon nanotubes such as TEM and SEM. More cell lines need to be employed for further study since different cell lines may show various sensitivities to nanoparticles (Hasan et al., 2012) and cancer cells might be more resistant to toxic factors. Some excellent efforts and progress has been made, but it still

may be some time before more clinical applications of MWCNTs will be achieved by better understanding their health impact on humans.

Chapter 5

5 Mechanisms of carbon nanotube toxicity are cell line dependant

5.1 Introduction

Multi-walled Carbon nanotubes (MWCNT) are allotropes of carbon with a cylindrical nano structure. MWCNTs possess significant advantages including high surface area, well-defined morphologies as well as unique optical in addition to their superior mechanical strength and thermal conductivity (Fenoglio et al., 2006). Due to their unique and advanced properties, not traditionally observed in bulk materials, MWCNTs have received enormous interests and increasing attentions from industry and our society. They have already been successfully developed and applied to a broad range of fields, from aerospace to biological devices. However, safety fears and toxic concerns about MWCNTs, due to their structural similarity to asbestos fibres, have been raised globally with an ongoing debate, resulting in several government reports and/or guidance already, in order to minimise and manage the potential risk (HSE 2013).

Despite the fascinating advantages of MWCNTs, they have already shown a low compatibility in the biological and chemical environments (Erdely et al., 2013), generating some serious health and environment concerns (Jin et al., 2014). The toxicity of MWCNTs has also been explored and then found in many cell lines including A549 (a lung cancer cell line) (Fröhlich et al., 2013) and MCF-7 (a breast cancer cell line) (Muller et al., 2008); however, the toxicity data obtained using those cell lines are inconsistent. Furthermore, the mechanism behind the corresponding toxicity of MWCNTs is still ambiguous (Van Der Zande et al., 2011). The most popular hypothesis of underlying mechanism for the cytotoxicity and genotoxicity caused by carbon nanotubes mainly includes cell membrane damage and DNA damage (Cavallo et al., 2012), while the change of cell morphology (Subbiah et al., 2013) (Yan et al., 2013) has also

been suggested for the consequence of toxicity. Both mechanisms could lead to cell death, but in different forms which are necrosis and apoptosis, respectively.

Notwithstanding the existing great efforts on the cytotoxicity investigation of MWCNTs, the sensitivity of each cell line in terms of apoptosis and cellular morphology change to these nanomaterials still remains unclear. In this report, different levels of cellular response in relation to cell viability, apoptosis, DNA damage and cell morphology were investigated by studying the pristine multi-walled carbon nanotubes in A549 (a lung cancer cell line) and MRC-5 (a lung fibroblast) as well as MCF-7 (a breast cancer cell line) cell lines, in order to help to achieve a better understanding of the mechanisms of toxicity pathway behind.

5.2 Results

5.2.1 Cell culture

Human lung epithelial cell line (A549) and human lung fibroblast (MRC-5) were obtained as a gift from Dr Huijun Zhu. Both cell lines were cultured in F12/DMEM (invitrogen, United Kingdom) supplemented with 10% fetal calf serum (sigma, United Kingdom) at 37°C in 5% CO_2. Cells were seeded into 96-wll plates (sigma, United Kingdom) and cultured for 24 h before the exposure.
A549 (Figure 5-1) is a hypotriploid human cell line which was initiated through explant culture of carcinomatous tissue from a 58-year-old Caucasian male (Health Protection Agency Culture Collections, 2011).

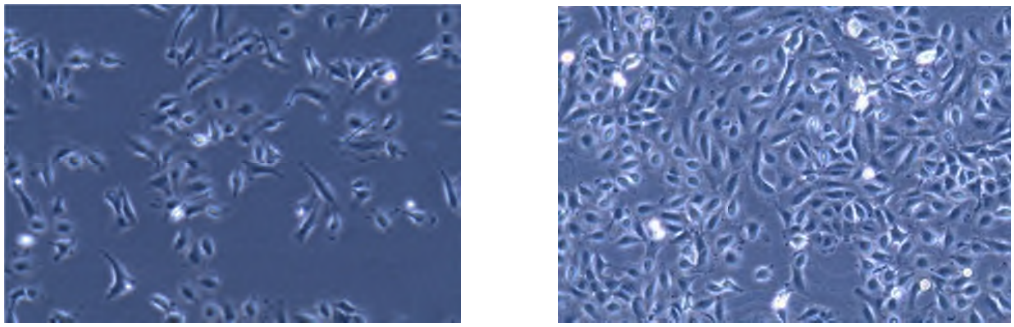

Figure 5-1 A549 cell line

A549 cell line is applied as it is a very sensitive cell line which has been used in many toxicological researches of carbon nanotubes (Breznan et al., 2015, Ursini et al., 2012a). In addition, lung cells are the most susceptible cells to inhaled carbon nanotubes.

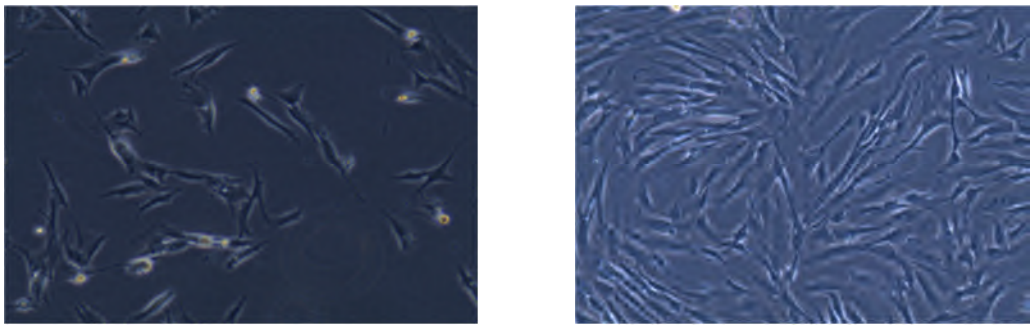

Figure 5-2 MRC-5 cell line

MRC-5 (Figure 5-2) is a normal human lung cell line derived from a normal lung tissue of a 14-week old. The cells are capable of 42-46 population doubling before the onset of senescence. MRC-5 cells were available in the lab and could serve the purpose of conducting comparative experiments on cancerous and normal cell lines. MRC-5 cells were also frequently used in toxicological research (Tan et al., 2014, Chueh et al., 2014, Pejin et al., 2014).

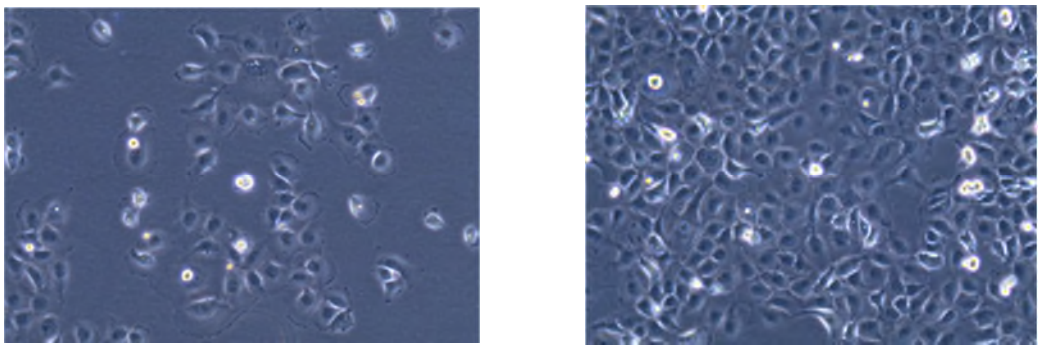

Figure 5-3 MCF-7 cell lines

MCF-7 (Figure 5-3) is epithelial breast cancer cell derived from 69 year female Caucasian suffering from a breast adenocarcinoma. These cells are suitable as

a transfection host and stably express green fluorescent protein so they are used in drug delivery study. Breast cancer cell line is a common used cell model applied in toxicological research (Fickova et al., 2015, Alqahtani et al., 2015).

5.2.2 Cell growth curves

The cell number as determined for the optimal seeding densities at 24, 48 and 72 hours were then used for cell growth doubling time calculations. The cell numbers at different time points are presented in Table 5-1. At 24h, cell number of A549, MCF-7 and MRC-5 were 1.8×10^4, 1.8×10^4 and 3.5×10^4 respectively. They were increased to 5.1×10^4, 5×10^4 and 4.6×10^4 at 48hour and then continually increased to 1.1×10^5, 1×10^5, 9.8×10^4 at 72 hour.

The doubling time graphs and calculations are presented in Figure 5-4. The doubling times were calculated as 19.98 hours for A549 cells, 21.06 hours for MCF-7 cells and 38.75 hours for MRC-5 cells. Data showed that at the chosen seeding densities, these cells were remained in exponential growth phase for up to 72 hour. Based on these calculations the chosen seeding densities were suitable for the nanoparticle cytotoxicity study.

Table 5-1 Optimal seeding density for cell growth. Cell counts were taken at intervals of 24 hours over 72 hour period using A549, MCF-7 and MRC-5 cell lines.

Time (hours)	**0**	**24**	**48**	**72**
A549 (cells/cm^2)	1×10^4	1.8×10^4	5.1×10^4	1.1×10^5
MCF-7 (cells/cm^2)	1×10^4	1.8×10^4	5×10^4	1×10^5
MRC-5 (cells/cm^2)	3×10^4	3.5×10^4	4.6×10^4	9.8×10^4

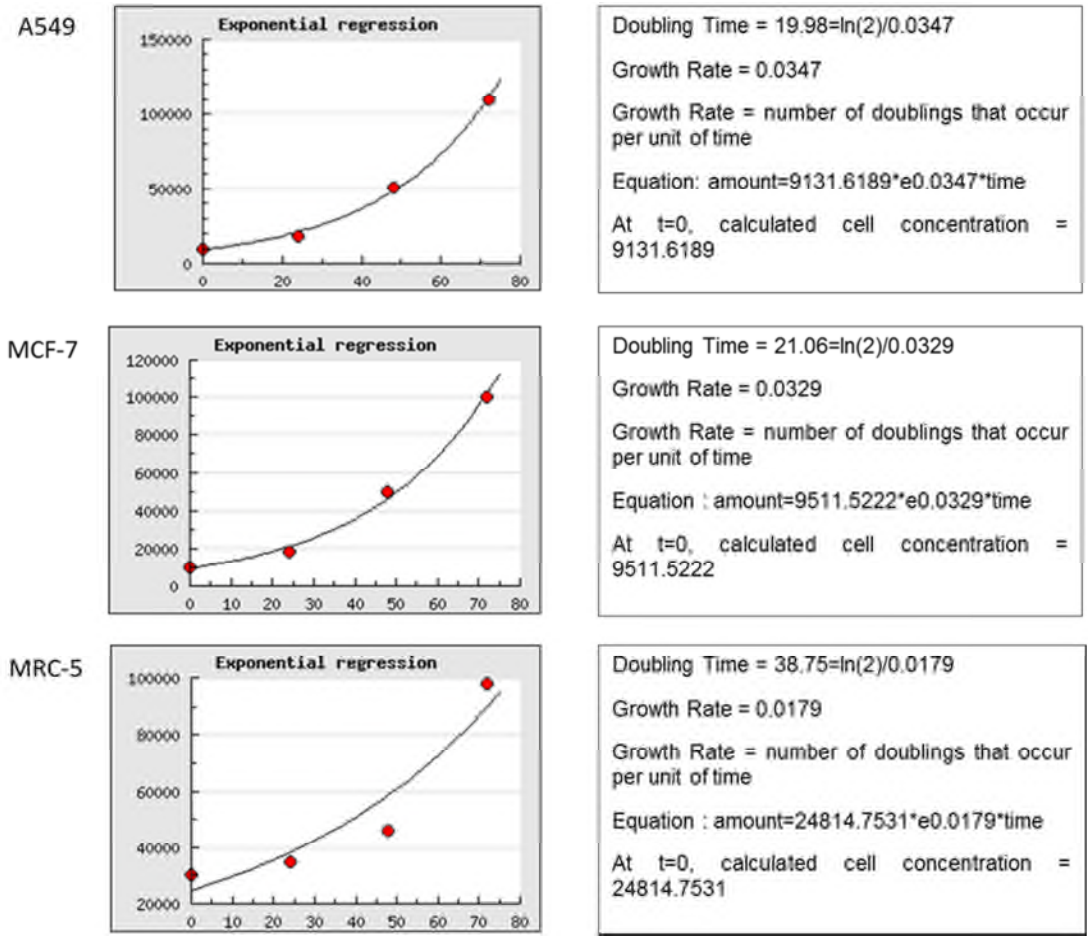

Figure 5-4 Cell growth curves and calculations for all cell lines. Using logarithmic calculations a doubling time is calculated based on growth rate of cells over.

The cell growth curves showed that different cell lines have their own growth pattern. Among them, MCF-7 cell lines and A549 cell lines share the similar growth pattern and their doubling time is also very similar whilst MRC-5 showed a slower growth period (Figure 5-4). The doubling time of MRC-5 was 1.94 and 1.79 times of A549 cell line and MCF-7 cell line.

5.2.3 Cell skeleton deformation

Cell skeleton deformation (Figure 5-5) observed by confocal microscope after staining actin and nucleus with fluorescent dyes (Alexa 633 and DAPI, respectively). Changes of the actin cytoskeletal organization of lung fibroblasts grown in the presence of 50 µg/mL pristine MWCNTs were observed after 48

hours' exposure. In our research, cells grown in the presence of pristine MWCNTs showed a weaker adherence to the underlying substrate than cells grown in the absence of pristine MWCNTs. Significant decrease in f-actin density of cytoskeleton organization and cell areas were noted during the entire time span investigated in MRC-5 cells after 48 hour' treatment (50μg/mL)

All the cells were deformed and very unhealthy by observation. Unlike the control cells, treated cells were separate from each other instead of attaching the adjacent cells.

MCF-7 was the most sensitive cell line to pristine MWCNT treatment *in vitro.* The treated MCF-7 cells were completely separated and the original cell structure was totally altered. At the same time, we also observed the loss of cell viability at this concentration through WST-1 assay (Figure 5-6).

MRC-5 cells basically maintained the original cell structure and morphology but with reduced protein. A549 cells

A549 cells also showed obvious change of cell morphology, but not as much as MCF-7 cell did.

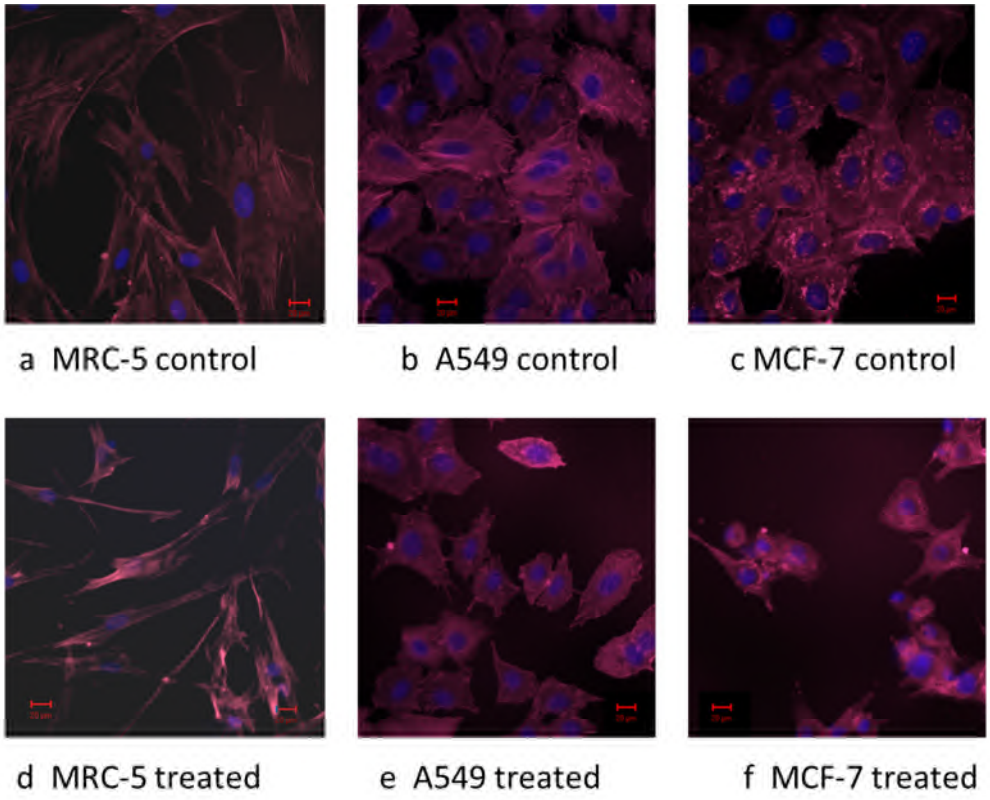

Figure 5-5 Confocal microscopy of cell morphology caused by pristine MWCNTs. Cell skeleton was labelled with Alexa 633 (1 μg/mL) and cell nuclear was labelled with DAPI (10 μg/mL). Cells were treated with 50 μg/mL pristine MWCNTs for 48 hours. a, MRC-5 (non-treated); b, A549 (non-treated); c, MCF-7 (non-treated); d, MRC-5 (treated); e, A549 (treated); f, MCF-7 (treated).

5.2.4 Cell viability

Cell Proliferation Reagent WST-1 was used to evaluate cell viability in response to pristine MWCNT challenge. The results showed a dose dependent cell death after 24 hours exposure in MCF-7 and MRC-5 cells (Figure 5-6). The data of cell viability of MRC-5 and MCF-7 are shown in 7.3.1B.1.1

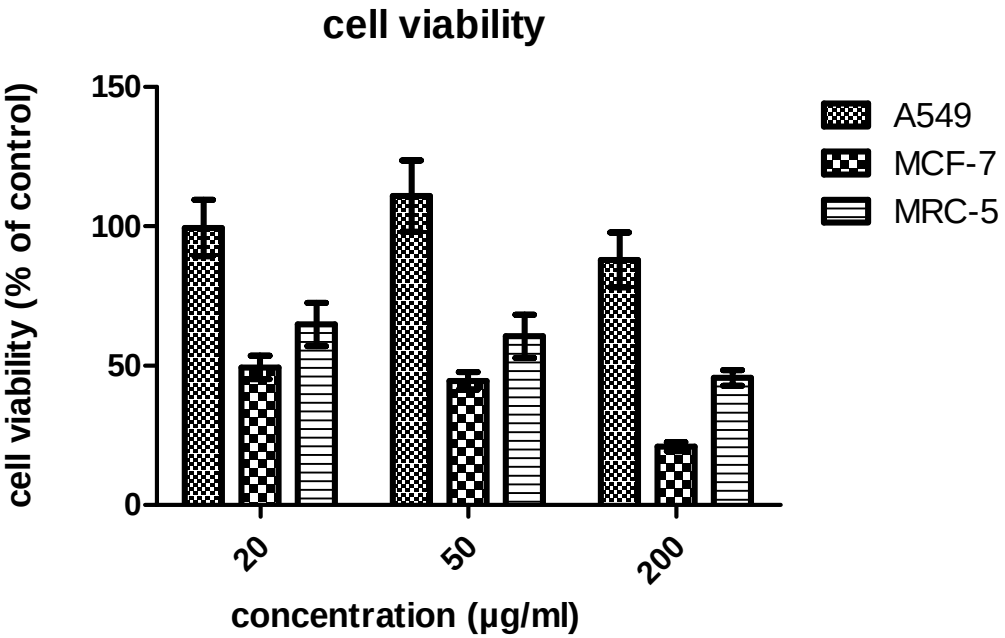

Figure 5-6 comparison of cell viability of A549, MCF-7, MRC-5 cell lines after 24 hours exposure to 20, 50 200 µg/mL pristine MWCNTs. Viability was detected by using WST-1 assay. Data are represented as mean of percentage of control ±SD of triplicate. $p<0.05$.

This figure is presented as percentage of control. All the data have been calculated using the control data of the same cell line. At 20µg/mL, MCF-7 and MRC-5 cell lines has lost about 50% and 40% respectively of cell viability whilst A549 cells didn't have significant change in cell number. Similarly, at 50µg/mL, the cell death of all three cell lines didn't experience significant cell death, however, the live cells of MCF-7 and MRC-5 cell lines had dropped to 20% and 50% respectively at 200µg/mL.

5.2.5 LDH release

LDH release was also assessed on all the three cell lines (Figure 5-7). Among these cell lines MCF-7 has been showed significantly higher LDH release, which is consistent with the results of viability detection as shown in Figure 5-6.

Both A549 and MRC-5 cells didn't show any significant cell membrane damage at all the concentrations. The result confirmed that MCF-7 cells are very

susceptible under the MWCNTs treated circumstance. The individual figures for membrane damage of MCF-7 and MRC-5 were showed in appendix (Figure_Apx 5)

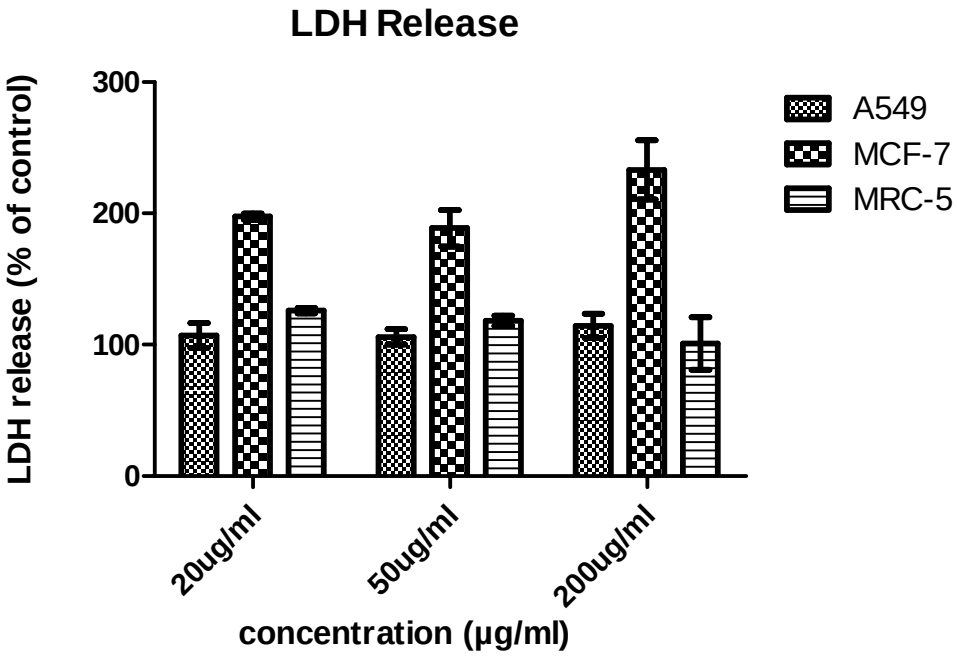

Figure 5-7 Comparison of cell membrane integrity of A549, MCF-7, MRC-5 cell lines after 24 hours exposure to pristine MWCNTs. Data are represented as mean of percentage of control ±SD of triplicate analysis.

5.2.6 Reactive oxygen species generation

The effects of carbon nanotubes on intracellular ROS were assessed after 6 hours' treatment with MWCNT (2, 20 and 50 µg/mL). As shown in Figure 5-8, the pristine MWCNTs at different concentrations could all induce an increase of ROS which was also dose-dependent. A549 and MCF-7 cell lines induced significantly more ROS compared with MRC-5 at concentration 20 and 50µg/mL of pristine MWCNTs. At 2µg/mL, no significant ROS production has been found among three cell lines.

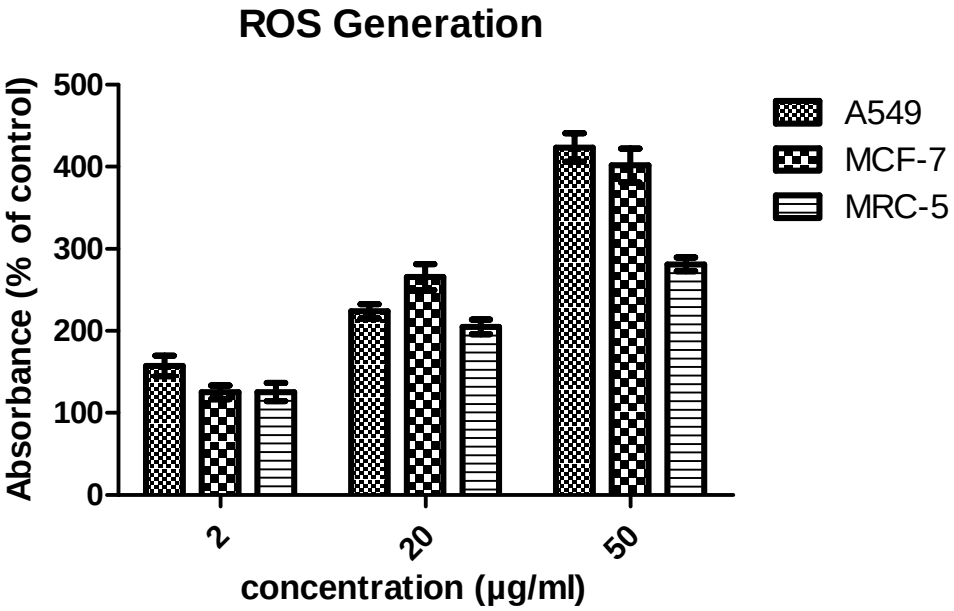

Figure 5-8 Comparison of ROS generation in A549, MCF-7, MRC-5 cell lines after 24 hours exposure to pristine MWCNTs. ROS generation was studied using dichlorofluorescein diacetate (DCFH-DA) dye assay. Data are represented as mean of percentage of control ±SD of triplicate analysis.

5.2.7 Apoptosis detection

Flow cytometer analysis of A549, MCF-7 and MRC-5 cell lines treated for 24 hours with pristine MWCNTs revealed an apoptosis induction from 20µg/mL. Both MCF-7 and A549 cell lines were found to exhibit significant apoptosis after treatment when compared to non-treated cells. MRC-5 aggregated in the cell medium, as such, they are not suitable for use of Annexin V assay (data not shown).

Both cell lines exerted apoptosis detection through AnnexinV detection; however A549 was apparent more susceptible to pristine MWCNT in terms of apoptosis. At 20µg/mL, pristine MWCNTs induced 8.5% and 7.7% of apoptotic cells, which was 1.51 and 1.77 times of negative control on A549 and MCF-7 cells respectively. When the concentration increased to 50µg/mL, the percentage of apoptotic cells of A549 have increased to 18.8%, which was 3.34 times of control while no significant increase has been found on MCF-7 cells.

Table 5-2 Cell apoptosis induced by MWCNTs (μg/mL) in A549 and MCF-7 cells

Cell line	Mean % apoptotic cells ±SD			
	20μg/mL MWCNT		50μg/mL MWCNT	
	Non-treated	Pristine MWCNT	Non-treated	Pristine MWCNT
A549	5.63±0.66	8.5±2.09	5.63±0.66	18.8±4.31
MCF-7	4.33±0..25	7.70±0.17	7.17±0.72	10.87±0.45

a, Apoptosis was evaluated by Annexin V-FITC, PI stain assay. Data are represented as mean ± SD of triplicate analysis.

5.2.8 DNA damage

In order to measure DNA damage caused by oxidative stress, 8-oxo-2'-deoxyguanosine (8-oxo-dG), a frequently used biomarker for oxidative DNA damage, was selected and then measured. Table 5-3 described the actual production of oxidative DNA and the unit is ng/mL. The negative control group of A549, MCF-7 and MRC-5 produced 0.57, 1.14 and 1.48ng/mL, respectively. The corresponding treated cells induced 0.88, 1.83 and 1.81ng/mL, respectively. The data were calculated using the equation extracted from standard curve (Figure 5-9a).

Detailed data of apoptosis detection of MCF-7 cells were described in Appendix B.1.3

Table 5-3 DNA damage in A549, MCF-7 and MRC-5 (ng/mL)

	A549	**MCF-7**	**MRC-5**
Negative control	0.57	1.41	1.48
Treated	0.88	1.83	1.81

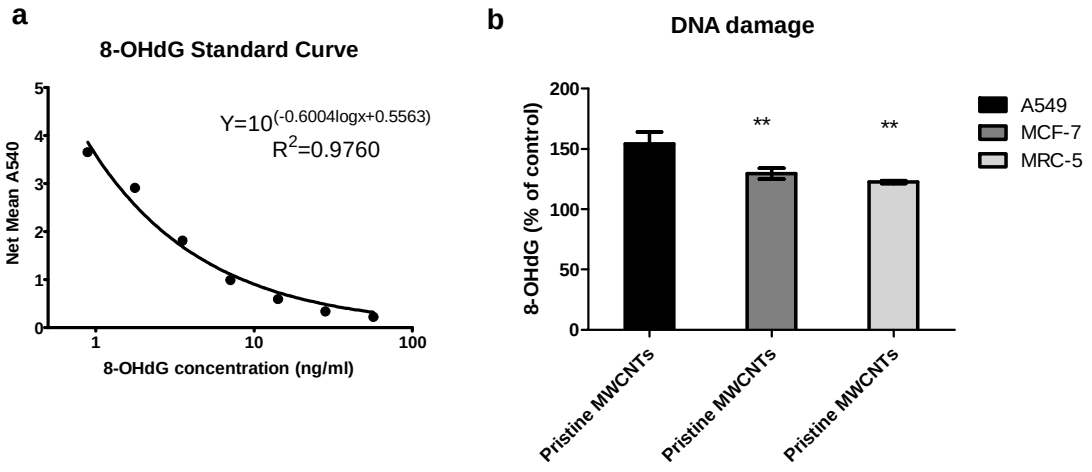

Figure 5-9 Comparison of DNA damage of A549, MCF-7, MRC-5 cell lines after 24 hours exposure to pristine MWCNTs at a concentration of 50 μg/mL. 8-OHdG was quantified by colorimetric antibody ELISA assay. Data are represented as mean ±SD of triplicate. $p<0.05$

The data of Figure 5-9 was presented as percentage of control. For example, oxo-dG in A549 cells were exhibited as percentage of this in untreated A549 cells. Through the figure, it was easily found that A549 cells were most sensitive to the exposure of pristine MWCNTs. Pristine MWCNTs resulted in 1.44, 1.31 and 1.23 fold greater levels of oxidative DNA damage compared with negative controls in A549, MCF-7 and MRC-5 cells, respectively. A549 cells showed the greatest difference in terms of DNA damage between control and treated groups (Table 5-3, Figure 5-9).

5.3 Discussion

MWCNTs are widely used for a variety of commercial products; however, the biological consequence of MWCNTs exposure in the environment is still poorly understood. Different methods of toxicity measurement have been applied in order to estimate the potential hazard of such nano-materials to human for different applications. In our study, the cellular responses to pristine MWCNTs with different timespan were evaluated in three cell lines (A549, MRC-5 and MCF-7) by the assessments of cell viability, LDH release, ROS generation, apoptosis, cell morphology and DNA damage. These multiple assays and evaluations could offer a more constructive guideline and solution for their future practice and applications, in terms of toxicity and hazard.

Notably, different degrees of sensitivity to cell viability were shown among lung cancer, lung fibroblast and breast cancer cell lines via WST-1 assay. A549 cells didn't show any significant cell death after the treatment with pristine MWCNTs at the concentrations of 20 and 50µg/mL; however, at the concentration of 200µg/mL, there was a significant toxicity of pristine MWCNTs to A549 cells. In comparison, both MRC-5 and MCF-7 cells had a loss of viability after exposing to pristine MWCNTs with a concentration from 20µg/mL. In particular, MCF-7 cells seem more sensitive to pristine MWCNTs than other two cell lines, in terms of viability (Figure 5-6).

By employing the LDH assay, a dose-dependent response was observed in all three cell lines (Figure 5-7). In other words, the higher concentration of pristine MWCNTs resulted in more LDH release. Again, MCF-7 was the most sensitive cell line and it showed more than two folds of LDH release compared with MRC-5 and A549 cell lines. It is in agreement with the result from Figure 5-6.

Oxidative stress plays a crucial role in toxicity induced by carbon nanotubes (Pichardo et al., 2012). The mechanisms of potential genotoxicity when MWCNTs exert in biological systems mainly contain two modes: 1) increased level of ROS; and 2) interference with cellular compounds (Lindberg et al., 2013a). During the period of environmental stress, the highly increased ROS

level can result in significant damage to cells by activating cell death and depletion of anti-oxidants. In our study, DCF-DA, a fluorescent dye, was used to measure the hydroxyl, peroxyl and other reactive oxygen species (ROS) within cells. The results of pristine MWCNTs-induced ROS generation are summarized in Figure 5-8. A549 cells showed a ROS generation after a 6-hour exposure of pristine MWCNTs with different concentrations (2, 20 and 50 μg/mL). Interestingly, as shown in Figure 5-9, the results of DNA damage assessment also suggested that the cells were under considerable oxidative stress following the treatment with 50 μg/mL pristine MWCNTs. In Figure 5-8, it is worth noting that the difference in total ROS production after a 6-hour treatment with pristine MWCNTs at all concentrations was not significant between MCF-7 and A549 cell lines. In comparison, MRC-5 cell lines were greatly less productive in terms of ROS generation. According to the cell growth curve (Figure 5-4), the doubling time of cell growth for MRC-5 cell lines is significantly longer than A549 and MCF-7 cell lines. Hence, the lower sensitivity of MRC-5 cell lines, in terms of ROS generation, cell viability and LDH release (combined with other results), could be attributed to their lower growth rate.

In the study of apoptosis detection, the Annexin V and PI staining were used to detect early sign of apoptosis induced by pristine MWCNTs. The flow cytometric analysis of A549 cells treated with pristine MWCNTs for 48 hours revealed an apoptosis induction (Table 5-2). As reported recently, apoptosis may be induced by nano-particles through ROS generation and oxidative stress (Ahamed, 2013). Previous research has suggested a apoptotic effect of MWCNTs in A549 cells (Ursini et al., 2012b); however, to the best of our knowledge the apoptosis detection in MCF-7 cells after the treatment with carbon nanotubes has not been reported yet. In our study, it was found that pristine MWCNTs induced a lower level of apoptosis in MCF-7 cells than that in A549 cells.

Carbon nanotubes could affect not only cell viability, ROS generation and apoptosis, but also cell spreading and the area of visible focal adhesion point (Kaiser et al., 2013). The actin cytoskeleton plays a critical role in the physiological maintenance (Lao et al., 2009). It was found that ARPE-19 cells

could become smaller and rounder after an incubation with MWCNTs (Yan et al., 2011). Similarly, in a study conducted by Kaiser (Kaiser et al., 2013), cells grown in the presence of 30 µg/mL single-walled CNTs (SWCNTs) for 5 days showed a reduced spreading area, compared to the control cultures grown. Cells exposed to SWCNTs reorganised their actin cytoskeleton, which resulted in decreased concentration of actin around cell edges. According to Kaiser et al. (2013), the possible reason behind it is that carbon nanotubes could adhere in a similar way as RGD-sequences (Arginine-Glycine-Aspartic acid) of the dissolved proteins to integrin, which results in a reduced cell spreading, as well as fewer and smaller focal adhesion points. In addition, it has been reported that SWCNTs can down regulate adhesion-associated genes and proteins, leading to thinner basement membrane and decreased adhesion ability of human HEK293 cell, which finally causes cellular apoptosis or death (Cui et al., 2005). As what has been seeing in Figure 5-5, cells grown in the presence of pristine MWCNTs showed a weaker adherence to the underlying substrate than cells grown in the absence of pristine MWCNTs. The result implies that the functions of cells were changed after exposing to pristine MWCNTs. More interestingly, in our study, A549 cells didn't show such obvious cell deformation following the same treatment compared to two other cell lines (*i.e.* MCF-7 and MRC-5).

DNA damage was found in Met-5A and A549 cell lines using the comet assay (Cavallo et al., 2012), (Lindberg et al., 2013b) when exposed to MWCNTs. Data on DNA damage of MCF-7 and MRC-5 cell lines caused by carbon nanotubes, however, is very limited. As it was explained earlier, in our research, 8-oxo-2'-deoxyguanosine (8-oxo-dG), a frequently used biomarker for oxidative DNA damage, was selected and then measured (Figure 5-9). We have found that A549 cells experienced the most severe DNA damage and many of them were dead through apoptosis. In comparison, MCF-7 cells were more affected by pristine MWCNTs in terms of viability, membrane damage and the change of cell morphology. These results could suggest that MCF-7 cells are more vulnerable to pristine MWCNTs, thus leading to death by means of necrosis. For MRC-5 cells, despite their low cell proliferation, no significant amount of

apoptotic cells was found after the treatment with pristine MWCNTs. It could indicate that pristine MWCNTs may preferentially induce toxicity in cancerous cells rather than healthy cells.

The mechanism to explain the different pathway of cell toxicity is still under investigation. A study conducted by Ursini et al. (2012) showed two cytotoxic mechanisms, by membrane damage for pristine MWCNTs and apoptosis for MWCNTs-OH (Ursini et al., 2012a). Based on our study, as discussed above, different mechanisms of cytotoxicity pathway to necrosis and apoptosis are summarized and proposed in Figure 5-10, as a result of the exposure of pristine MWCNTs to A549, MCF-7 and MRC-5 cells. For MCF-7 cells, most of them underwent necrosis whilst A549 cells suffered from apoptosis. It is worth noting that pristine MWCNTs (i.e. unmodified MWCNTs) induced significantly greater levels of cytotoxicity in cancer derived cells (e.g. MCF-7 and A549 cells) than non-immortalised cells (e.g. MRC-5 cells). This finding may be useful for the development and exploitation of carbon nanotubes as a chemotherapeutic agent in biomedical applications.

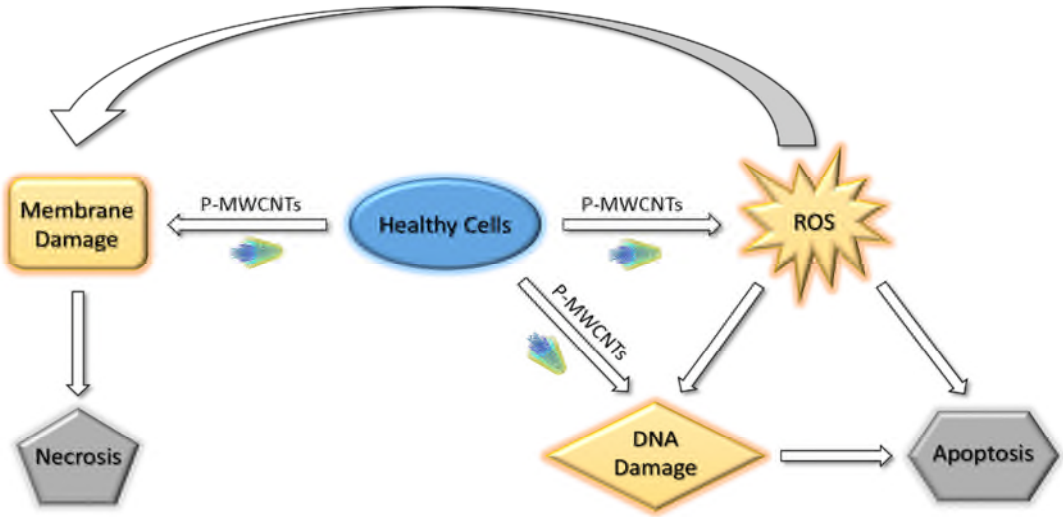

Figure 5-10 Schematic representation of different mechanisms of cytotoxicity pathway to necrosis and apoptosis, as a result of the exposure of pristine MWCNTs to A549, MCF-7 and MRC-5 cells.

5.4 Conclusion

Three different cell lines were applied in section. Among them, MCF-7 and A549 cells had similar growth speed while the doubling time of MRC-5 was 1.94 and 1.79 times of A549 cell line and MCF-7 cell line.

As mentioned before, different mechanisms of toxicity pathway could be presented on different cell lines. For example, MWCNTs were cytotoxic to the RLE lung epithelial cell line via an apoptotic mechanism and introduction of gene mutations but cytotoxic to A549 and BEAS by enhanced ROS production and the induction of an inflammatory response. In this chapter, toxicity of MWCNTs were detected on A549, MRC-5 and MCF-7 cell lines in order to better understand the cell line dependent toxicological mechanisms.

It was found that different cell lines showed different levels of cellular response to pristine MWCNTs. Among all three cell lines we studied, the MCF-7 breast cancer cell line was the most sensitive one to pristine MWCNTs in terms of cell viability, LDH release and the change of cell morphology. A549 cells lost viability via apoptosis after the exposure to pristine MWCNTs, which might be caused by ROS-induced DNA damage. In comparison, MRC-5 cells also showed a loss of cell viability but they exhibited a lower level degree of response to membrane damage and DNA damage assays, probably attributed to their low cell growth rate. However, a great reduction of F-actin was observed after the treatment with carbon nanotubes, which indicated that MRC-5 cells were in unhealthy state.

Importantly, it was also found that A549 cells were more sensitive to pristine MWCNTs in terms of DNA damage, however, both MRC-5 and MCF-7 cells showed more DNA damage caused by functional MWCNTs.

In sum, cell response to MWCNTs differs from cell line to cell line. In the other words, they rendered different level of sensitivity to WMNCTs and lost cell viability through different pathways.

Further study is needed to investigate the details of cell internalization of carbon nanotubes in order to gain a better insight into the mechanism of toxicity. In

addition, since gene regulation plays an important role in cytotoxicity, so the toxicity pathway could also be evaluated through the up or down regulation of RNA(s) which encodes the toxicity related protein(s).

Chapter 6

6 EGFP inhibited siRNA delivery using MWCNT

6.1 Introduction

Small interfering RNA (siRNA) are known to modulate enzymatic cleavage of homologous mRNA and subsequently interrupt gene expression (Mukerjee et al., 2011). siRNA based therapeutic agents may provide a promising way to overcome disease caused by abnormal gene over-expression, such as cancer, by the process of RNA interference. However, the delivery of siRNA into the cellular cytoplasm of target cells represents a major hurdle in treating disease due to its low charge density (Liu et al., 2007), hydrophilicity (Oliveira et al., 2007) and short biological half-life (Morrissey et al., 2005). This challenge can be addressed by encapsulation of siRNA in nanoparticles which can protect them from degradation (Yoo et al., 2011). Among nanomaterials, MWCNTs have gained significant interest as a promising tool for siRNA delivery as their needle-like shape provides capacity to cross cell membranes (Palomäki et al., 2011). It has been reported that needle like poly lactic-co-glycolic acid (PLGA) offer higher drug delivery efficiency with lower toxicity compared with their spherical counterparts (Hasan et al., 2012). Furthermore, siRNA can naturally wrap around CNTs through non-covalent π-π stacking interaction (Vardharajula et al., 2012).

The interaction between cells and MWCNTs is a critical issue that determines the transfection efficiency of drug and gene. Unfortunately, much about the interaction of MWCNTs with living cells is still unknown. In applications, chemical functionalisation of carbon nanotubes increased their ability of conjugation of biological components by acting as ligands which expedite their cellular internalisation through receptor mediated endocytosis (Das et al., 2013). Several studies have shown promising results using functionalised nanotubes for drug delivery. It has been reported that therapeutic silencing using ammonium functionalised MWCNTs-mediated siRNA delivery can lead to tumour growth arrest (Al-Jamal et al., 2011). Ammonium-functionalised

MWCNTs (MWNT-NH_{3+}) has been showed higher level of cellular internalization while exhibiting less toxicity compared to Pluronic F127 coated MWCNTs (Ali-Boucetta et al., 2011). However, the mechanisms and effects of different functionalisations on cell internalization efficiency remain unaddressed.

In this study, the eGFP inhibited siRNA delivery efficiency of -NH_2 functionalised MWCNTs on MCF-7 cells was investigated and the comparison with chemical Lipofectamine RNAiMAX has been studied in order to modulate the therapeutic performance of gene loaded MWCNTs.

6.2 Results

6.2.1 Cell viability

The MCF-7 cells were treated with -NH_2 functionalised MWCNTs (1µg/mL), siRNA-MWCNTs (1µg/mL) and Lipofectamine RNAiMAX for 72 hours. Untreated cells were used as a negative control.

Cell viability was measured using WST-1 in order to ensure that the long-term treatment will not influence cell growth. Results exhibited that among the three treatments only the Lipofectamine RNAiMAX significantly reduced the cell viability after 72 hours which indicates that Lipofectamine RNAiMAX is more toxic than NH_2-MWCNTs as delivery system (Figure 6-1).

Detailed data of cell viability evaluation of NH_2-MWCNTs has been shown in Appendix C.1.

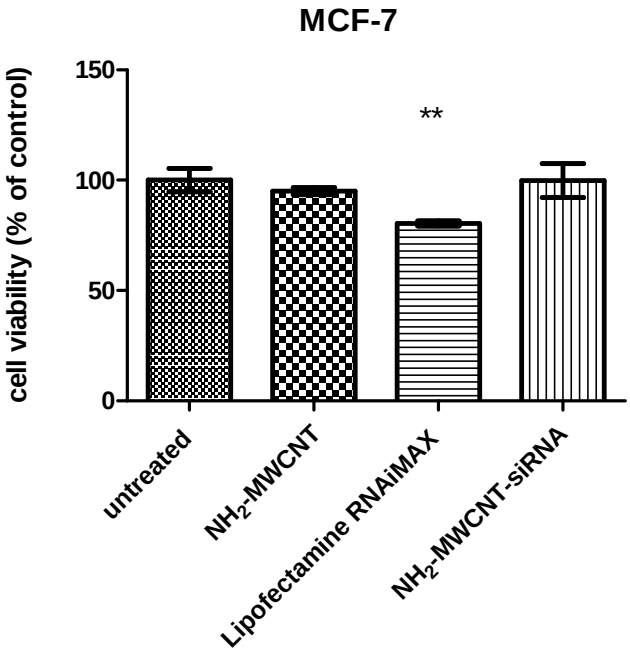

Figure 6-1 Cell viability of MCF-7 cells treated with MWCNT, siRNA-MWCNT and Lipofectamine RNAiMAX-siRNAfor 72h. Untreated cells are negative control. Data were presented as mean of percentage of negative control **p<0.01

6.2.2 The change of eGFP expression under confocal microscope

The cell line used here was eGFP transformed MCF-7 cells and the siRNA contained eGFP inhibited gene sequence; therefore, the efficiency of gene delivery by conjugating with MWCNTs was detected by decrease of green fluorescence.

The confocal microscope was used to observe green fluorescence of eGFP expressing MCF-7 cells (Figure 6-2). The images were chosen as representative areas. The expression of eGFP should be inhibited if the siRNA is sent to cells and successfully combined with corresponding cellular RNA, thereby; the delivery efficiency was evaluated through green fluorescence intensity detection.

In Figure 6-3, GFP expressed MCF-7 cells of negative control showed a clear fluorescence (image A and B). After the treatment with siRNA-NH_2-MWCNTs for 72 hours, the fluorescence is decreased. It could also be seen that cells

treated with Lipofectamine RNAiMAX-siRNA and NH_2-MWCNT-siRNA (image C and D) exhibited less fluorescence intensity

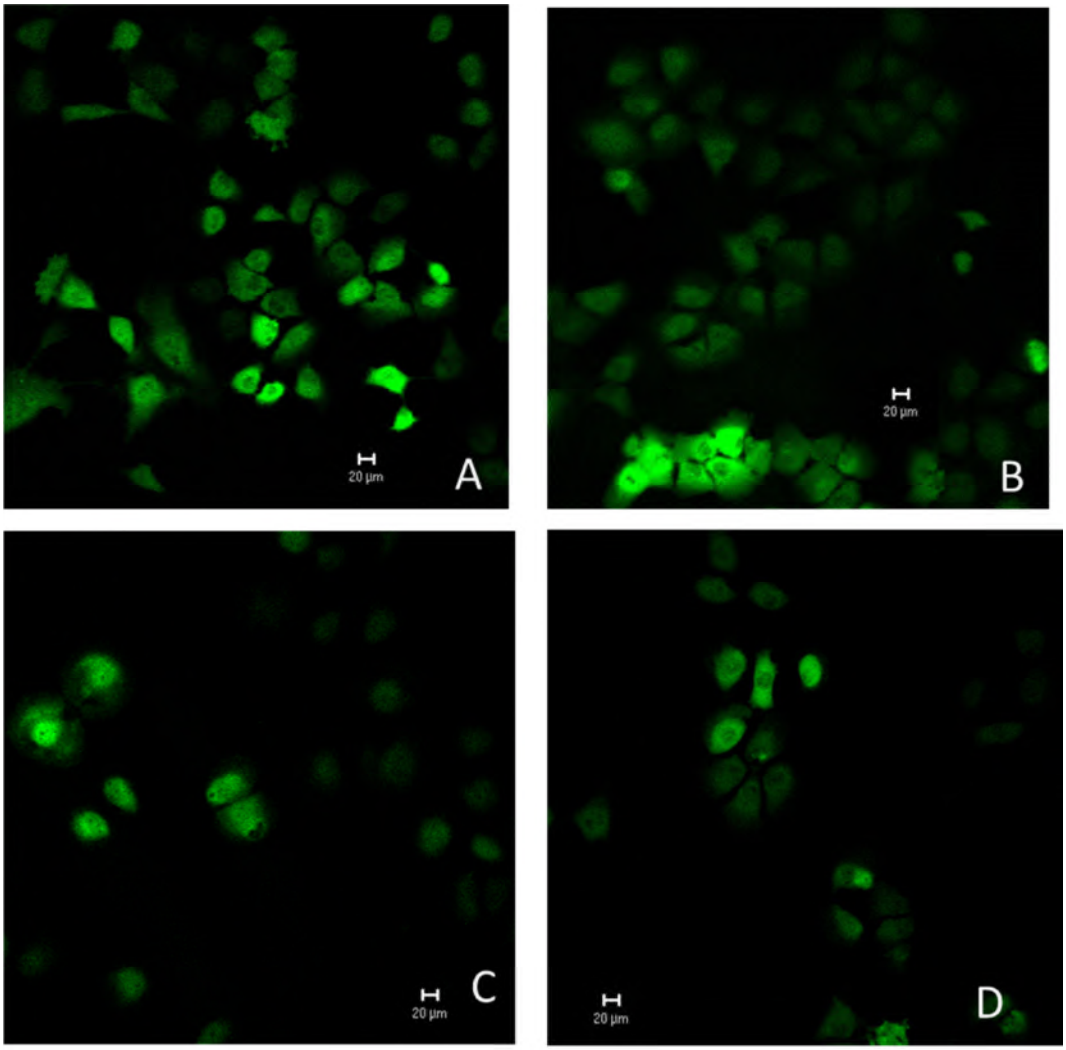

Figure 6-2 MCF-7 cells under confocal microscope A, negative control; B cells treated with NH2-MWCNT; C, Cells treated with Lipofectamine RNAiMAX-siRNA; D, Cells treated with NH2-MWCNT-siRNA

6.2.3 Green fluorescence inhibition assay (by plate reading)

Plate reading was conducted in conjunction with confocal microscope to back up the findings.

As seen in Figure 6-3, after 24 hours treatment, there's no significant change of intensity of green fluorescence from control under any treatment conditions. However, after 48 hours treatment siRNA-NH_2-MWCNTs treated cells exhibited

decreased intensity of fluorescence. Both siRNA-NH_2-MWCNTs and Lipofectamine RNAiMAX treated cells exhibited decrease of fluorescence intensity after 72 hours treatment. The fact that no significant difference between p-MWCNTs and negative control was observed indicates that p-MWNCTs do not affect cell viability and thus may represent a good gene delivery vector.

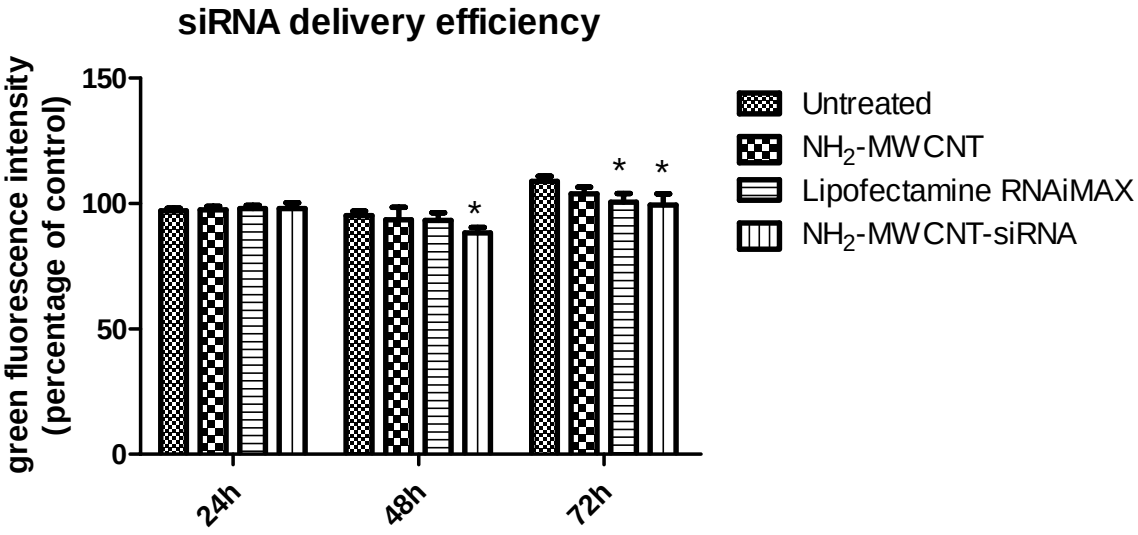

Figure 6-3 Green flurorescent intensity detection following 24, 48 and 72 hours treatment using plate reader. * P<0.05 vs control

6.3 Discussion

Small interfering RNAs (siRNAs) mediate gene silencing of a target protein by disrupting messenger RNAs in an efficient and sequence-specific manner (Zhang et al., 2014a). RNAi can specifically regulate gene expression, but efficient delivery of siRNA *in vivo* is difficult while it has been shown that modified carbon nanotubes (CNT) protect siRNA, facilitate entry into cells and enhance transdermal drugs delivery (Siu et al., 2014).

CNTs are considered as potential nanodrug delivery vectors due to prolonged circulation time, ease of crossing cell membranes, and translocation directly into the cytoplasm of target cells by an endocytosis-independent mechanism without inducing cell death (Mehra et al., 2014, Cai et al., 2005).

In this study, NH_2-MWCNTs have been used for conjugation with siRNA in eGFP expressed MCF-7 cells as CNTs functionalized through amidation were more efficient in siRNA complexation (Battigelli et al., 2013). Higher siRNA complexation was observed with the ammonium derivatives, compared to the guanidinium conjugates. Moreover, cellular uptake and western blotting studies confirmed the electrophoresis results that ammonium derivatives display the best siRNA uptake and gene silencing activity compared to the other conjugates studied here (Battigelli et al., 2013). In addition, the low cytotoxicity of all the derivatives revealed a promising relevance of these conjugates as gene delivery system. Silencing studies *in vivo* are currently under investigation (Battigelli et al., 2013).

In the previous chapters, concentrations of pristine, -OH and –COOH functional from 0 to 20µg/mL have very limited toxic effect Figure 4-1. A similar result has been confirmed in Figure 6-1 that NH_2-MWCNTs have exhibited no cell death at concentration 1µg/mL in cell viability. In the following experiments, cell fluorescence has been detected after treatment with siRNA-NH_2-MWCNTs using confocal microscopy and plate reader. Lipofectamine RNAiMAX has been used as a Lipofectamine RNAiMAX according to literature (Jensen et al., 2014, Yang et al., 2014). The results suggested that NH_2-MWCNTs-siRNA showed similar effect as Lipofectamine RNAiMAX but less cytotoxicity.

The selective and robust effect of RNA interference on gene expression, mediated by siRNA, makes it not only a valuable research tool, but also a promising therapeutic platform for the treatment of viral infections, dominant disorders, cancer, and neurological disorders(Ryther et al., 2005). In this chapter, we focused on the delivery of siRNA targeting the gene eGFP as a potential treatment for a range of cancers. The successful delivery of siRNA to target specific genes in mammalian model organisms has been achieved using a variety of methods, including liposomes, cationic lipids, polymers and nanoparticles. However, systemic toxicity remains a great concern with most of these delivery options. Thus, there is an ever-growing need to enhance the available tools that can lead to effective and safe gene delivery. The functionalized MWCNTs developed in this work present an alternative with reasonable biocompatibility, which can simultaneously serve as an imaging agent due to their unique Raman signature within biological environments (Neves et al., 2012). MWCNTs have an important advantage over SWNTs, for which any structural damage disrupts their mapping and progression over time. MWCNT–siRNA was not shown to cause cell death within 72 hours; this indicates that MWCNT–RNA does not have a deleterious effect on cells during their passage, although long-term effects remain to be investigated.

In terms of therapeutic efficacy, the achieved silencing effect was found lower than commercial transfection agents (Figure 6-3). Considering that most commercially available *in vitro* transfection agents are unsuitable for therapeutic applications due to their systemic toxicity, this indicates that MWCNTs may be successfully employed to deliver therapeutic moieties, such as siRNA, to cells for the treatment of cancerous disorders. Future work will need to be done to study the *in vivo* performance of this system and will allow for a comparison of the *in vivo* performance of MWCNTs with other carbon nanotube-based delivery systems in the literature.

6.4 Conclusions

On the basis of our experimental observations, we proposed a working model that describes our current understanding of gene delivery. The model has major impacts on both drug delivery and toxicity research of MWCNTs.

It suggested that NH_2-MWCNTs exerted less toxic but equal delivery ability compared with chemical agent. MWCNTs were not found exhibiting loss of cell viability according to WST-1 detection; however, Lipofectamine RNAiMAX exerted significant cell death which suggested not suitable as a drug/gene vector. The already used siRNA vection didn't decrease the intensity until 72 hours treatment. It suggested that NH_2-MWCNTs have a great delivery potential.

Future work is necessary to be conducted to evaluate the delivery efficiency on transcriptional stage. RNA expression of eGFP needs to be quantified through RT-PCR. In addition, long term *in vivo* experiments are also worth being conducted in order to confirm the delivery efficiency and mimic the long term effect in human body. Apoptosis and DNA detections are also necessary to be conducted for toxicity evaluations and to provide more information about application in medical area.

.

Chapter 7

7 General discussion

In recent years, interest has developed in exploring the potential biological applications of carbon nanotubes (CNTs), motivated by their unique physical properties including size, shape and structures (Chen et al., 2003, Kam et al., 2004, Bianco et al., 2005a). Among them CNTs, MWCNT mechanic stability is much higher than that of SWCNTs. In addition, the outer wall can be functionalised without changing the mechanical and electronic properties of the inner wall. These characteristics make them attractive for biomedical applications, although there has also been concern about potential harmful effects on living cells. These effects appear to depend on a variety of physicochemical properties including length and rigidity (Poland et al., 2008), aggregation behaviour (Wang et al., 2011), surface functionalisation (Crouzier et al., 2008) and cell lines.

The first part of this project examines the characterisation of pristine and functionalised MWCNTs and the relevance of bio-application (chapter 3). The second part assesses the cytotoxicity and genotoxicity of pristine and functionalized MWCNTs in different cell lines (chapter 4 and 5). After toxicity assessment, NH_2-MWCNTs have been investigated for siRNA delivery with non-cytotoxic concentration (chapter 6). Delivery efficiency has been compared with an established siRNA delivery system.

Concentrations of MWCNTs for toxicity evaluations were chosen based on literature reviews from 1 to 1000µg/mL (Liu et al., 2014). The concentration for the gene therapy was decided through result of toxicity detection and the concentration used for *in vivo* injection in literature (Iancu and Mocan, 2011).

7.1 MWCNTs toxicity *in vitro*

7.1.1 Influence of functional group in toxicity

The MWCNTs tested in this project are very similar in size range, which does not allow the results to be interpreted in direct relation to size specific effect of the primary particle sizes.

As the surface chemistry of MWCNTs is an important determinant of their toxicity, study of the difference of chemical property would provide some insights into their reactivity with biomolecules and cells in the testing systems. In our experiments, functionalised WMCNTs have been found to induce more DNA damage and apoptosis than pristine-MWCNTs. They also lead to more cell death at low concentrations (20 and 50µg/mL) compared with pristine MWCNTs.

It was found functionalisation did not only change the characteristics of MWCNT's surface but also their dispersibility in aqueous solution. SEM and TEM data suggest that MWCNTs form aggregates when suspended in culture medium. However, whether aggregates could induce or decrease toxicity is still ambiguous. Therefore, a series of experiments were conducted to investigate the alteration of toxicological response induced by aggregates. Aggregates were found to be less cytotoxic than better dispersed MWCNTs.

MWCNTs induced concentration dependent cytotoxicity as detected by the WST-1 assay at 24 h after treatment in A549 cells. These results are consistent with previous studies (Gilmour et al., 2013, Ursini et al., 2012a) which also found MWCNTs induced concentration-dependent toxicity. Taking all of the multi parametric endpoint cytotoxicity/stress test results into account it appeared that the apoptosis is the mechanism of MWCNTs cytotoxicity in A549 cell line. It may be attributable to a cell-type specific response. Toxicity mechanisms in different cell lines need further investigation.

7.1.2 Cell line dependent toxicity

Different mechanisms of toxicity could be present in different cell lines. MWCNTs were cytotoxic to the RLE lung epithelial cell line via an apoptotic mechanism and introduction of gene mutations but cytotoxic to A549 and BEAS by enhanced ROS production and the induction of an inflammatory response.

The cell line dependency of toxicity mechanisms was investigated using three cell lines-A549, MRC-5 and MCF-7. The MCF-7 breast cancer cell line was the most sensitive to pristine MWCNTs in terms of cell viability, LDH release and the change of cell morphology. A549 cells lost viability mainly through apoptosis after the exposure to pristine MWCNTs, which might be caused by ROS-induced oxidative DNA damage. In comparison, MRC-5 cells also also showed loss of cell viability and poor attachment to the flasks as a large reduction of F-actin was observed after treatment with pristine MWCNTs. However, they exhibited a lower level degree of response to membrane damage, ROS production and DNA damage assays compared with A549 and MCF-7 cell lines.

For A549 cells, pristine MWCNTs exerted more cell death than functional MWCNTs while functional MWCNTs induced more apoptosis and DNA damage than the pristine version. MCF-7 and MRC-5 cells were more sensitive to pristine MWCNTs in regards to cell death, apoptosis and DNA damage.

7.1.3 Gene regulation

A RNA array assay was employed to study the mechanisms of MWCNT mediated toxicity. Total RNA analysis of both pristine and –COOH functionalised MWCNT treated cells indicated altered gene expression following treatment. The change in RNA regulation suggests that the identified RNA may influence the activation of signalling pathways to combat both oxidative and hypoxic stress and lead to the transcription of inflammatory factors. DNA damage, heat shock protein and autophagy related were also found increase after treatment with MWCNTs in this experiment.

In addition, through the result of RNA array, COOH functionalised MWCNTs were found induced a greater number of up-regulation of genes compared with

pristine MWCNTs. This result is also in consistent with the previous oxidative DNA damage findings.

7.2 siRNA delivery

Gene therapy has drawn significant attention as a potential method for treating both acute and chronic diseases. Current research efforts have focused on developing carriers that effectively compact and protect naked DNA, RNA and siRNA and exhibit limited risk to human health (Choi et al., 2014). Since MWCNTs were previously suggested to have potential as gene carrier (Hollanda et al., 2014) and exhibited no significant cell death at concentration of 1 µg/mL when they were conjugated with GFP siRNA. According to joint detection using flow cytometer, confocal microscope and plate reader, NH_2-MWCNTs showed less toxic effects than Lipofectamine RNAiMAX-siRNA without compromising their delivery efficiency. These experiments suggested successful siRNA delivery into MCF-7 cell line.

7.3 Conclusions

This project aimed to investigate the in vitro toxicity of MWCNTs to assess their potential medical application. The results achieved suggest 1) Functionalised WMCNTs exhibited more aggregates than pristine MWCNTs; 2) Functionalised MWNCTs exhibited more apoptosis, DNA damage and toxicological alteration of RNA regulation than pristine forms; 3) Toxicity pathways of MWNCTs are cell dependent; 4) Low concentration of MWCNTs could successfully deliver siRNA into cells without compromising their viability.

The study also highlights the importance of aggregation in assessment of toxicity. BSA was used to make MWCNTs better dispersed in the cell culture medium and lead to more toxicity of functionalised MWCNTs.

Importantly, this study explored new avenues to study the mechanisms of toxicity pathways. The RNA assay allows the identification of factors that regulate the cellular response to MWCNTs at transcription level. The results suggested that A549 cells were under oxidative and hypoxia stress upon

treatment with MWCNTs. interestingly, COOH-functionalised MWCNTs are more genotoxic.

Ultimately, the MWNCTs were also found less toxic than Lipofectamine RNAiMAX-siRNA in siRNA delivery, which confirmed it potential application in medical area.

7.3.1 Outlook and future study

The outlook for nanotechnology medical applications is potentially very exciting. The dose control and characterisation of MWCNTs is a major step to minimise their toxicity while potentiating their medical applications. Alongside the development of methods such as cell viability and apoptosis cellular changes caused by toxic MWCNTs can potentially be detected earlier. From these assays detecting cellular and RNA changes, the overall long term effect of MWCNTs can be predicted effectively.

The results obtained so far provide some new insights about toxicity assessment of MWCNTs with tendency to aggregate in the testing system. Potentially the use of RNA arrays can specify and reveal in depth information about molecular mechanism of toxicity. Some studies are being conducted in the field of toxicology using such technique (Choi et al., 2012). These forms of studies have the potential to identify long term health effects that may occur due to exposures to MWCNTs.

Some aspects of the original objectives were not achieved. Such as identification of specific uptake pathways and the mechanism of toxicity, although uptake has been identified and observed the mechanisms is still unknown. The toxicity of low concentration MWCNTs in terms of cytotoxicity and RNA regulations was also not fully detailed.

The genotoxicity of MWCNTs were investigated by oxidative DNA damage detection and RNA array. The endpoints of genotoxicity of MWCNTs are DNA damage, DNA mutation and chromosome damages thereby, genotoxicity could be deeply investigated through looking at the other two sides of endpoints by Bacterial Reverse Mutation Assay (Ames Test), Mammalian Forward Mutation

Assay (Mouse Lymphoma Assay), Chromosome Aberration Analysis, Micronucleus Analysis or Senescence Bypass Assays.

Although long term effect could be predicted through RNA regulation, it is still important and necessary to monitor long term treatment *in vivo*, which will provide more reliable and accurate information on long term and side effect of MWCNTs.

Dermal toxicity of MWCNTs is also very important as nanomaterials' potential in cosmetic. The toxicity study for dermal sensitivity detection includes chicken eye isolation and irritation assays, which could be performed on 3-D dermal model.

Pharmacokinetics plays an important role in drug development. The most important parameters of pharmacokinetics are absorption, distribution, metabolisation and excretion which describe how the body affects a specific drug after administration. Until their distribution and toxicoketic profiles are fully understood, their translation into the clinic will be hindered. The majority of intravenously injected CNTs in mice mainly seem to be emptied in the urine, with far less found in the liver, spleen, and lungs (Firme Iii and Bandaru, 2010). However, other studies indicate that the liver and spleen were the main sites of CNT accumulation. Studies have also found CNTs deposit mostly in the excretory systems like the bladder, kidney, and intestine (Schipper et al., 2008). A contributing factor to this tendency was that CNTs could often be trapped in capillaries, a mechanical cause of toxicity that may explain distribution of residual CNTs. For example; the liver might be a preferred site for CNT accumulation due to its greater vascularity (Liu et al., 2008). More studies could be done here to clarify the pharmacokinetics of MWCNTs, the understanding of which will facilitate the clinical applications.

REFERENCES

http://bonnerlab.wordpress.ncsu.edu/research, accessed on 23/3/2015

http://www.sabiosciences.com/rt_pcr_product/HTML/PAHS-003Z.htmL, accessed on 06/01/2015

http://www.dojindo.com/Shared/Flyer/CK04_MTT_MTS_WST1.pdf, accessed on 01/04/2014

ABE, S., HYONO, A. & YONEZAWA, T. 2014. Influence of surface properties on SEM observation for carbon nanotubes with pretreatment using room temperature ionic liquids. Journal of Solution Chemistry, 43, 1645-1654.

ADELI, M., SOLEYMAN, R., BEIRANVAND, Z. & MADANI, F. 2013. Carbon nanotubes in cancer therapy: A more precise look at the role of carbon nanotube-polymer interactions. Chemical Society Reviews, 42, 5231-5256.

AHAMED, M. 2013. Silica nanoparticles-induced cytotoxicity, oxidative stress and apoptosis in cultured A431 and A549 cells. Human and Experimental Toxicology, 32, 186-195.

AHAMED, M., POSGAI, R., GOREY, T. J., NIELSEN, M., HUSSAIN, S. M. & ROWE, J. J. 2010. Silver nanoparticles induced heat shock protein 70, oxidative stress and apoptosis in Drosophila melanogaster. Toxicology and Applied Pharmacology, 242, 263-269.

AL-JAMAL, K. T., GHERARDINI, L., BARDI, G., NUNES, A., GUO, C., BUSSY, C., HERRERO, M. A., BIANCO, A., PRATO, M., KOSTARELOS, K. & PIZZORUSSO, T. 2011. Functional motor recovery from brain ischemic insult by carbon nanotube-mediated siRNA silencing. Proceedings of the National Academy of Sciences of the United States of America, 108, 10952-10957.

ALI-BOUCETTA, H., AL-JAMAL, K. T., MÜLLER, K. H., LI, S., PORTER, A. E., EDDAOUDI, A., PRATO, M., BIANCO, A. & KOSTARELOS, K. 2011. Cellular uptake and cytotoxic impact of chemically functionalized and polymer-coated carbon nanotubes. Small, 7, 3230-3238.

ALI-BOUCETTA, H., NUNES, A., SAINZ, R., HERRERO, M. A., TIAN, B., PRATO, M., BIANCO, A. & KOSTARELOS, K. 2013. Asbestos-like Pathogenicity of Long Carbon Nanotubes Alleviated by Chemical Functionalization. Angewandte Chemie International Edition, n/a-n/a.

ALQAHTANI, S., SIMON, L., ASTETE, C. E., ALAYOUBI, A., SYLVESTER, P. W., NAZZAL, S., SHEN, Y., XU, Z., KADDOUMI, A. & SABLIOV, C. M. 2015. Cellular uptake, antioxidant and antiproliferative activity of entrapped α-tocopherol and γ-tocotrienol in poly (lactic-co-glycolic) acid

(PLGA) and chitosan covered PLGA nanoparticles (PLGA-Chi). Journal of Colloid and Interface Science, 445, 243-251.

ANBARASAN, B., VIGNESH BABU, S., ELANGO, K., SHRIYA, B. & RAMAPRABHU, S. 2015. PH responsive release of doxorubicin to the cancer cells by functionalized multi-walled carbon nanotubes. Journal of Nanoscience and Nanotechnology, 15, 4799-4805.

AVOURIS, P. 2002. Carbon nanotube electronics. Chemical Physics, 281, 429-445.

BARDI, G., TOGNINI, P., CIOFANI, G., RAFFA, V., COSTA, M. & PIZZORUSSO, T. 2009. Pluronic-coated carbon nanotubes do not induce degeneration of cortical neurons in vivo and in vitro. Nanomedicine: Nanotechnology, Biology, and Medicine, 5, 96-104.

BATTIGELLI, A., WANG, J. T. W., RUSSIER, J., DA ROS, T., KOSTARELOS, K., AL-JAMAL, K. T., PRATO, M. & BIANCO, A. 2013. Ammonium and guanidinium dendron-carbon nanotubes by amidation and click chemistry and their use for siRNA delivery. Small, 9, 3610-3619.

BEERS JR, R. F. & SIZER, I. W. 1952. A spectrophotometric method for measuring the breakdown of hydrogen peroxide by catalase. The Journal of biological chemistry, 195, 133-140.

BEYERSMANN, D. & HARTWIG, A. 2008. Carcinogenic metal compounds: Recent insight into molecular and cellular mechanisms. Archives Of Toxicology, 82, 493-512.

BIANCO, A., KOSTARELOS, K., PARTIDOS, C. D. & PRATO, M. 2005a. Biomedical applications of functionalised carbon nanotubes. Chemical Communications, 571-577.

BIANCO, A., KOSTARELOS, K. & PRATO, M. 2005b. Applications of carbon nanotubes in drug delivery. Current Opinion in Chemical Biology, 9, 674-679.

BREZNAN, D., DAS, D., MACKINNON-ROY, C., SIMARD, B., KUMARATHASAN, P. & VINCENT, R. 2015. Non-specific interaction of carbon nanotubes with the resazurin assay reagent: Impact on in vitro assessment of nanoparticle cytotoxicity. Toxicology in Vitro, 29, 142-147.

BROWN, D. M., KINLOCH, I. A., BANGERT, U., WINDLE, A. H., WALTER, D. M., WALKER, G. S., SCOTCHFORD, C. A., DONALDSON, K. & STONE, V. 2007. An in vitro study of the potential of carbon nanotubes and nanofibres to induce inflammatory mediators and frustrated phagocytosis. Carbon, 45, 1743-1756.

BUSSY, C., PINAULT, M., CAMBEDOUZOU, J., LANDRY, M. J., JEGOU, P., MAYNE-L'HERMITE, M., LAUNOIS, P., BOCZKOWSKI, J. & LANONE, S. 2012. Critical role of surface chemical modifications induced by length

shortening on multi-walled carbon nanotubes-induced toxicity. Particle and Fibre Toxicology, 9.

CAI, D., MATARAZA, J. M., QIN, Z. H., HUANG, Z., HUANG, J., CHILES, T. C., CARNAHAN, D., KEMPA, K. & REN, Z. 2005. Highly efficient molecular delivery into mammalian cells using carbon nanotube spearing. Nature Methods, 2, 449-454.

CARLBERG, I. & MANNERVIK, B. 1975. Purification and characterization of the flavoenzyme glutathione reductase from rat liver. Journal of Biological Chemistry, 250, 5475-5480.

CASEY, A., DAVOREN, M., HERZOG, E., LYNG, F. M., BYRNE, H. J. & CHAMBERS, G. 2007. Probing the interaction of single walled carbon nanotubes within cell culture medium as a precursor to toxicity testing. Carbon, 45, 34-40.

CASTRANOVA, V., SCHULTE, P. A. & ZUMWALDE, R. D. 2013. Occupational nanosafety considerations for carbon nanotubes and carbon nanofibers. Accounts of Chemical Research, 46, 642-649.

CAVALLO, D., FANIZZA, C., URSINI, C. L., CASCIARDI, S., PABA, E., CIERVO, A., FRESEGNA, A. M., MAIELLO, R., MARCELLONI, A. M., BURESTI, G., TOMBOLINI, F., BELLUCCI, S. & IAVICOLI, S. 2012. Multi-walled carbon nanotubes induce cytotoxicity and genotoxicity in human lung epithelial cells. Journal Of Applied Toxicology, 32, 454-464.

CHEN, C., XIE, X. X., ZHOU, Q., ZHANG, F. Y., WANG, Q. L., LIU, Y. Q., ZOU, Y., TAO, Q., JI, X. M. & YU, S. Q. 2012. EGF-functionalized single-walled carbon nanotubes for targeting delivery of etoposide. Nanotechnology, 23.

CHEN, R. J., BANGSARUNTIP, S., DROUVALAKIS, K. A., WONG SHI KAM, N., SHIM, M., LI, Y., KIM, W., UTZ, P. J. & DAI, H. 2003. Noncovalent functionalization of carbon nanotubes for highly specific electronic biosensors. Proceedings of the National Academy of Sciences of the United States of America, 100, 4984-4989.

CHENG, Q., BLAIS, M. O., HARRIS, G. & JABBARZADEH, E. 2013. PLGA-carbon nanotube conjugates for intercellular delivery of caspase-3 into osteosarcoma cells. PLoS ONE, 8.

CHO, S. Y., YUN, Y. S., KIM, E. S., KIM, M. S. & JIN, H. J. 2011. Stem cell response to multiwalled carbon nanotube-incorporated regenerated silk fibroin films. Journal of Nanoscience and Nanotechnology, 11, 801-805.

CHOI, H. J., YUN, H. S., KANG, H. J., BAN, H. J., KIM, Y., NAM, H. Y., HONG, E. J., JUNG, S. Y., JUNG, S. E., JEON, J. P. & HAN, B. G. 2012. Human transcriptome analysis of acute responses to glucose ingestion reveals the role of leukocytes in hyperglycemia-induced inflammation. Physiological Genomics, 44, 1179-1187.

CHOI, Y. S., LEE, M. Y., DAVID, A. E. & PARK, Y. S. 2014. Nanoparticles for gene delivery: Therapeutic and toxic effects. Molecular and Cellular Toxicology, 10, 1-8.

CHUEH, P. J., LIANG, R. Y., LEE, Y. H., ZENG, Z. M. & CHUANG, S. M. 2014. Differential cytotoxic effects of gold nanoparticles in different mammalian cell lines. Journal of Hazardous Materials, 264, 303-312.

CIOFANI, G., RAFFA, V., PENSABENE, V., MENCIASSI, A. & DARIO, P. 2009. Dispersion of multi-walled carbon nanotubes in aqueous pluronic F127 solutions for biological applications. Fullerenes Nanotubes and Carbon Nanostructures, 17, 11-25.

COLVIN, V. L. 2003. The potential environmental impact of engineered nanomaterials. Nature Biotechnology, 21, 1166-1170.

CROUZIER, T., NIMMAGADDA, A., NOLLERT, M. U. & MCFETRIDGE, P. S. 2008. Modification of single walled carbon nanotube surface chemistry to improve aqueous solubility and enhance cellular interactions. Langmuir, 24, 13173-13181.

CUI, D., TIAN, F., OZKAN, C. S., WANG, M. & GAO, H. 2005. Effect of single wall carbon nanotubes on human HEK293 cells. Toxicology Letters, 155, 73-85.

CUNHA, C., PANSERI, S., IANNAZZO, D., PIPERNO, A., PISTONE, A., FAZIO, M., RUSSO, A., MARCACCI, M. & GALVAGNO, S. 2012. Hybrid composites made of multiwalled carbon nanotubes functionalized with Fe3O4 nanoparticles for tissue engineering applications. Nanotechnology, 23, 465102.

DAS, M., SINGH, R. P., DATIR, S. R. & JAIN, S. 2013. Surface Chemistry Dependent "switch" Regulates the Trafficking and Therapeutic Performance of Drug-Loaded Carbon Nanotubes. Bioconjugate Chemistry, 24, 626-639.

DESAI, M. P., LABHASETWAR, V., WALTER, E., LEVY, R. J. & AMIDON, G. L. 1997. The mechanism of uptake of biodegradable microparticles in Caco-2 cells is size dependent. Pharmaceutical Research, 14, 1568-1573.

DI SOTTO, A., CHIARETTI, M., CARRU, G. A., BELLUCCI, S. & MAZZANTI, G. 2009. Multi-walled carbon nanotubes: Lack of mutagenic activity in the bacterial reverse mutation assay. Toxicology Letters, 184, 192-197.

DONALDSON, K., AITKEN, R., TRAN, L., STONE, V., DUFFIN, R., FORREST, G. & ALEXANDER, A. 2006. Carbon nanotubes: A review of their properties in relation to pulmonary toxicology and workplace safety. Toxicological Sciences, 92, 5-22.

DONALDSON, K., POLAND, C. A., MURPHY, F. A., MACFARLANE, M., CHERNOVA, T. & SCHINWALD, A. 2013. Pulmonary toxicity of carbon

nanotubes and asbestos - Similarities and differences. Advanced Drug Delivery Reviews, 65, 2078-2086.

DOSQUET, C., WEILL, D. & WAUTIER, J. L. 1995. Cytokines and thrombosis. J Cardiovasc Pharmacol, 25 Suppl 2, S13-9.

DU, J., WANG, S., YOU, H. & ZHAO, X. 2013. Understanding the toxicity of carbon nanotubes in the environment is crucial to the control of nanomaterials in producing and processing and the assessment of health risk for human: A review. Environmental Toxicology And Pharmacology, 36, 451-462.

EASTMAN, A. & BARRY, M. A. 1992. The origins of DNA breaks: A consequence of DNA damage, DNA repair, or apoptosis? Cancer Investigation, 10, 229-240.

ELGRABLI, D., ABELLA-GALLART, S., AGUERRE-CHARIOL, O., ROBIDEL, F., ROGERIEUX, F., BOCZKOWSKI, J. & LACROIX, G. 2007. Effect of BSA on carbon nanotube dispersion for in vivo and in vitro studies. Nanotoxicology, 1, 266-278.

ERDELY, A., DAHM, M., CHEN, B. T., ZEIDLER-ERDELY, P. C., FERNBACK, J. E., BIRCH, M. E., EVANS, D. E., KASHON, M. L., DEDDENS, J. A., HULDERMAN, T., BILGESU, S. A., BATTELLI, L., SCHWEGLER-BERRY, D., LEONARD, H. D., MCKINNEY, W., FRAZER, D. G., ANTONINI, J. M., PORTER, D. W., CASTRANOVA, V. & SCHUBAUER-BERIGAN, M. K. 2013. Carbon nanotube dosimetry: From workplace exposure assessment to inhalation toxicology. Particle and Fibre Toxicology, 10.

FENOGLIO, I., ALDIERI, E., GAZZANO, E., CESANO, F., COLONNA, M., SCARANO, D., MAZZUCCO, G., ATTANASIO, A., YAKOUB, Y., LISON, D. & FUBINI, B. 2012. Thickness of multiwalled carbon nanotubes affects their lung toxicity. Chemical Research in Toxicology, 25, 74-82.

FENOGLIO, I., TOMATIS, M., LISON, D., MULLER, J., FONSECA, A., NAGY, J. B. & FUBINI, B. 2006. Reactivity of carbon nanotubes: Free radical generation or scavenging activity? Free Radical Biology and Medicine, 40, 1227-1233.

FICKOVA, M., MACHO, L. & BRTKO, J. 2015. A comparison of the effects of tributyltin chloride and triphenyltin chloride on cell proliferation, proapoptotic p53, Bax, and antiapoptotic Bcl-2 protein levels in human breast cancer MCF-7 cell line. Toxicology in Vitro, 29, 727-731.

FIRME III, C. P. & BANDARU, P. R. 2010. Toxicity issues in the application of carbon nanotubes to biological systems. Nanomedicine: Nanotechnology, Biology and Medicine, 6, 245-256.

FOLKMANN, J. K., RISOM, L., JACOBSEN, N. R., WALLIN, H., LOFT, S. & MØLLER, P. 2009. Oxidatively damaged DNA in rats exposed by oral

gavage to C60 fullerenes and single-walled carbon nanotubes. Environmental Health Perspectives, 117, 703-708.

FRÖHLICH, E., BONSTINGL, G., HÖFLER, A., MEINDL, C., LEITINGER, G., PIEBER, T. R. & ROBLEGG, E. 2013. Comparison of two in vitro systems to assess cellular effects of nanoparticles-containing aerosols. Toxicology in vitro : an international journal published in association with BIBRA, 27, 409-417.

FUJITA, K., FUKUDA, M., ENDOH, S., KATO, H., MARU, J., NAKAMURA, A., UCHINO, K., SHINOHARA, N., OBARA, S., NAGANO, R., HORIE, M., KINUGASA, S., HASHIMOTO, H. & KISHIMOTO, A. 2013. Physical properties of single-wall carbon nanotubes in cell culture and their dispersal due to alveolar epithelial cell response. Toxicology Mechanisms and Methods, 23, 598-609.

GILMOUR, A. D., GREEN, R. A. & THOMSON, C. E. 2013. A low-maintenance, primary cell culture model for the assessment of carbon nanotube toxicity. Toxicological and Environmental Chemistry, 95, 1129-1144.

GIRIFALCO, L. A., HODAK, M. & LEE, R. S. 2000. Carbon nanotubes, buckyballs, ropes, and a universal graphitic potential. Physical Review B - Condensed Matter and Materials Physics, 62, 13104-13110.

HABIG, W. H., PABST, M. J. & JAKOBY, W. B. 1974. Glutathione S transferases. The first enzymatic step in mercapturic acid formation. Journal of Biological Chemistry, 249, 7130-7139.

HAMILTON JR, R. F., WU, Z., MITRA, S., SHAW, P. K. & HOLIAN, A. 2013. Effect of MWCNT size, carboxylation, and purification on in vitro and in vivo toxicity, inflammation and lung pathology. Particle and Fibre Toxicology, 10.

HASAN, W., CHU, K., GULLAPALLI, A., DUNN, S. S., ENLOW, E. M., LUFT, J. C., TIAN, S., NAPIER, M. E., POHLHAUS, P. D., ROLLAND, J. P. & DESIMONE, J. M. 2012. Delivery of multiple siRNAs using lipid-coated PLGA nanoparticles for treatment of prostate cancer. Nano Letters, 12, 287-292.

HAUSER-KAWAGUCHI, A. M. N. & LUYT, L. G. 2015. Nanomedicine—nanoparticles in cancer imaging and therapy. Cancer Metastasis - Biology and Treatment.

HE, H., PHAM-HUY, L. A., DRAMOU, P., XIAO, D., ZUO, P. & PHAM-HUY, C. 2013. Carbon nanotubes: Applications in pharmacy and medicine. BioMed Research International, 2013.

HE, X., YOUNG, S. H., SCHWEGLER-BERRY, D., CHISHOLM, W. P., FERNBACK, J. E. & MA, Q. 2011. Multiwalled carbon nanotubes induce a fibrogenic response by stimulating reactive oxygen species production, activating NF-κB signaling, and promoting fibroblast-to-myofibroblast transformation. Chemical Research in Toxicology, 24, 2237-2248.

HERRMANN, M., LORENZ, H. M., VOLL, R., GRUNKE, M., WOITH, W. & KALDEN, J. R. 1994. A rapid and simple method for the isolation of apoptotic DNA fragments. Nucleic Acids Research, 22, 5506-5507.

HERZOG, E., BYRNE, H. J., DAVOREN, M., CASEY, A., DUSCHL, A. & OOSTINGH, G. J. 2009. Dispersion medium modulates oxidative stress response of human lung epithelial cells upon exposure to carbon nanomaterial samples. Toxicology and Applied Pharmacology, 236, 276-281.

HITOSHI, K., KATOH, M., SUZUKI, T., ANDO, Y. & NADAI, M. 2012. Single-walled carbon nanotubes downregulate stress-responsive genes in human respiratory tract cells. Biological and Pharmaceutical Bulletin, 35, 455-463.

HOLLANDA, L. M., LOBO, A. O., LANCELLOTTI, M., BERNI, E., CORAT, E. J. & ZANIN, H. 2014. Graphene and carbon nanotube nanocomposite for gene transfection. Materials Science and Engineering C, 39, 288-298.

HUSSAIN, S., SANGTIAN, S., ANDERSON, S. M., SNYDER, R. J., MARSHBURN, J. D., RICE, A. B., BONNER, J. C. & GARANTZIOTIS, S. 2014. Inflammasome activation in airway epithelial cells after multi-walled carbon nanotube exposure mediates a profibrotic response in lung fibroblasts. Particle and Fibre Toxicology, 11.

HUTVÁGNER, G. & ZAMORE, P. D. 2002. A microRNA in a multiple-turnover RNAi enzyme complex. Science, 297, 2056-2060.

IANCU, C. & MOCAN, L. 2011. Advances in cancer therapy through the use of carbon nanotube-mediated targeted hyperthermia. International journal of nanomedicine, 6, 1675-1684.

JENSEN, K., ANDERSON, J. A. & GLASS, E. J. 2014. Comparison of small interfering RNA (siRNA) delivery into bovine monocyte-derived macrophages by transfection and electroporation. Veterinary Immunology and Immunopathology, 158, 224-232.

JEYAMOHAN, P., HASUMURA, T., NAGAOKA, Y., YOSHIDA, Y., MAEKAWA, T. & SAKTHI KUMAR, D. 2013. Accelerated killing of cancer cells using a multifunctional single-walled carbon nanotube-based system for targeted drug delivery in combination with photothermal therapy. International Journal of Nanomedicine, 8, 2653-2667.

JIANG, X., WANG, G., LIU, R., WANG, Y., WANG, Y., QIU, X. & GAO, X. 2013. RNase non-sensitive and endocytosis independent siRNA delivery system: Delivery of siRNA into tumor cells and high efficiency induction of apoptosis. Nanoscale, 5, 7256-7264.

JIN, L., SON, Y., DEFOREST, J. L., KANG, Y. J., KIM, W. & CHUNG, H. 2014. Single-walled carbon nanotubes alter soil microbial community composition. Science of the Total Environment, 466-467, 533-538.

JOHNSTON, H. J., HUTCHISON, G. R., CHRISTENSEN, F. M., PETERS, S., HANKIN, S., ASCHBERGER, K. & STONE, V. 2010. A critical review of the biological mechanisms underlying the in vivo and in vitro toxicity of carbon nanotubes: The contribution of physico-chemical characteristics. Nanotoxicology, 4, 207-246.

KAGAN, V. E., TYURINA, Y. Y., TYURIN, V. A., KONDURU, N. V., POTAPOVICH, A. I., OSIPOV, A. N., KISIN, E. R., SCHWEGLER-BERRY, D., MERCER, R., CASTRANOVA, V. & SHVEDOVA, A. A. 2006. Direct and indirect effects of single walled carbon nanotubes on RAW 264.7 macrophages: Role of iron. Toxicology Letters, 165, 88-100.

KAISER, J. P., BUERKI-THURNHERR, T. & WICK, P. 2013. Influence of single walled carbon nanotubes at subtoxical concentrations on cell adhesion and other cell parameters of human epithelial cells. Journal of King Saud University - Science, 25, 15-27.

KAM, N. W. S., JESSOP, T. C., WENDER, P. A. & DAI, H. 2004. Nanotube molecular transporters: Internalization of carbon nanotube-protein conjugates into mammalian cells. Journal of the American Chemical Society, 126, 6850-6851.

KANEKO, Y., SHOJO, H., BURNS, J., STAPLES, M., TAJIRI, N. & BORLONGAN, C. V. 2014. DJ-1 ameliorates ischemic cell death in vitro possibly via mitochondrial pathway. Neurobiology of Disease, 62, 56-61.

KANG, S., HERZBERG, M., RODRIGUES, D. F. & ELIMELECH, M. 2008. Antibacterial Effects of Carbon Nanotubes: Size Does Matter! Langmuir, 24, 6409-6413.

KATO, T., TOTSUKA, Y., ISHINO, K., MATSUMOTO, Y., TADA, Y., NAKAE, D., GOTO, S., MASUDA, S., OGO, S., KAWANISHI, M., YAGI, T., MATSUDA, T., WATANABE, M. & WAKABAYASHI, K. 2013. Genotoxicity of multi-walled carbon nanotubes in both in vitro and in vivo assay systems. Nanotoxicology, 7, 452-461.

KIM, J. S., LEE, K., LEE, Y. H., CHO, H. S., KIM, K. H., CHOI, K. H., LEE, S. H., SONG, K. S., KANG, C. S. & YU, I. J. 2011a. Aspect ratio has no effect on genotoxicity of multi-wall carbon nanotubes. Archives of Toxicology, 85, 775-786.

KIM, J. S., SONG, K. S., LEE, J. H. & YU, I. J. 2011b. Evaluation of biocompatible dispersants for carbon nanotube toxicity tests. Archives of Toxicology, 85, 1499-1508.

KIM, K. H., YEON, S. M., KIM, H. G., LEE, H., KIM, S. K., HAN, S. H., MIN, K. J., BYUN, Y., LEE, E. H., LEE, K. S., YUK, S. H., HA, U. H. & JUNG, Y. W. 2013. Single-Walled Carbon Nanotubes Induce Cell Death and Transcription of TNF-α in Macrophages Without Affecting Nitric Oxide Production. Inflammation, 1-11.

KISIN, E. R., MURRAY, A. R., KEANE, M. J., SHI, X. C., SCHWEGLER-BERRY, D., GORELIK, O., AREPALLI, S., CASTRANOVA, V., WALLACE, W. E., KAGAN, V. E. & SHVEDOVA, A. A. 2007. Single-walled carbon nanotubes: Geno- and cytotoxic effects in lung fibroblast V79 cells. Journal of Toxicology and Environmental Health - Part A: Current Issues, 70, 2071-2079.

KLUMPP, C., KOSTARELOS, K., PRATO, M. & BIANCO, A. 2006a. Functionalized carbon nanotubes as emerging nanovectors for the delivery of therapeutics. Biochimica et Biophysica Acta - Biomembranes, 1758, 404-412.

KLUMPP, C., KOSTARELOS, K., PRATO, M. & BIANCO, A. 2006b. Functionalized carbon nanotubes as emerging nanovectors for the delivery of therapeutics. Biochimica et Biophysica Acta (BBA) - Biomembranes, 1758, 404-412.

KREUTER, J., RAMGE, P., PETROV, V., HAMM, S., GELPERINA, S. E., ENGELHARDT, B., ALYAUTDIN, R., VON BRIESEN, H. & BEGLEY, D. J. 2003. Direct evidence that polysorbate-80-coated poly(butylcyanoacrylate) nanoparticles deliver drugs to the CNS via specific mechanisms requiring prior binding of drug to the nanoparticles. Pharmaceutical Research, 20, 409-416.

LAM, C. W., JAMES, J. T., MCCLUSKEY, R. & HUNTER, R. L. 2004. Pulmonary toxicity of single-wall carbon nanotubes in mice 7 and 90 days after intractracheal instillation. Toxicological Sciences, 77, 126-134.

LAO, F., CHEN, L., LI, W., GE, C., QU, Y., SUN, Q., ZHAO, Y., HAN, D. & CHEN, C. 2009. Fullerene nanoparticles selectively enter oxidation-damaged cerebral microvessel endothelial cells inhibit JNK-related apoptosis. ACS Nano, 3, 3358-3368.

LAVERNY, G., CASSET, A., PUROHIT, A., SCHAEFFER, E., SPIEGELHALTER, C., DE BLAY, F. & PONS, F. 2013. Immunomodulatory properties of multi-walled carbon nanotubes in peripheral blood mononuclear cells from healthy subjects and allergic patients. Toxicology Letters, 217, 91-101.

LEE, B. W., KADOYA, C., HORIE, M., MIZUGUCHI, Y., HASHIBA, M., KAMBARA, T., OKADA, T., MYOJO, T., OYABU, T., OGAMI, A., MORIMOTO, Y., TANAKA, I., UCHIDA, K., ENDOH, S. & NAKANISHI, J. 2013. Analysis of pulmonary surfactant in rat lungs after intratracheal instillation of short and long multi-walled carbon nanotubes. Inhalation Toxicology, 25, 609-620.

LI, C. & CHOU, T.-W. 2003. Single-walled carbon nanotubes as ultrahigh frequency nanomechanical resonators. Physical Review B, 68, 073405.

LI, J., YAP, S. Q., YOONG, S. L., NAYAK, T. R., CHANDRA, G. W., ANG, W. H., PANCZYK, T., RAMAPRABHU, S., VASHIST, S. K., SHEU, F. S.,

TAN, A. & PASTORIN, G. 2012. Carbon nanotube bottles for incorporation, release and enhanced cytotoxic effect of cisplatin. Carbon, 50, 1625-1634.

LI, J. G., LI, Q. N., XU, J. Y., CAL, X. O., LIU, R. L., LI, Y. J., MA, J. F. & LI, W. X. 2009. The pulmonary toxicity of multi-wall carbon nanotubes in mice 30 and 60 days after inhalation exposure. Journal Of Nanoscience And Nanotechnology, 9, 1384-1387.

LI, M., LU, W., ZHANG, F., DING, Q., WU, X., TAN, Z., WU, W., WENG, H., WANG, X., SHI, W., DONG, P., GU, J. & LIU, Y. 2014. Anti-tumor effects of DDP-PLLA-CNTs on human cholangiocarcinoma cell line in vitro. National Medical Journal of China, 94, 3163-3166.

LI, R., WANG, X., JI, Z., SUN, B., ZHANG, H., CHANG, C. H., LIN, S., MENG, H., LIAO, Y. P., WANG, M., LI, Z., HWANG, A. A., SONG, T. B., XU, R., YANG, Y., ZINK, J. I., NEL, A. E. & XIA, T. 2013. Surface charge and cellular processing of covalently functionalized multiwall carbon nanotubes determine pulmonary toxicity. ACS Nano, 7, 2352-2368.

LIN, A. C. 2007. Size matters: Regulating nanotechnology. Harvard Environmental Law Review, 31, 349-408.

LINDBERG, H. K., FALCK, G. C. M., SINGH, R., SUHONEN, S., JÄRVENTAUS, H., VANHALA, E., CATALÁN, J., FARMER, P. B., SAVOLAINEN, K. M. & NORPPA, H. 2013a. Genotoxicity of short single-wall and multi-wall carbon nanotubes in human bronchial epithelial and mesothelial cells in vitro. Toxicology, 313, 24-37.

LINDBERG, H. K., FALCK, G. C. M., SINGH, R., SUHONEN, S., JÄRVENTAUS, H., VANHALA, E., CATALÁN, J., FARMER, P. B., SAVOLAINEN, K. M. & NORPPA, H. 2013b. Genotoxicity of short single-wall and multi-wall carbon nanotubes in human bronchial epithelial and mesothelial cells in vitro. Toxicology.

LINDBERG, H. K., FALCK, G. C. M., SUHONEN, S., VIPPOLA, M., VANHALA, E., CATALÁN, J., SAVOLAINEN, K. & NORPPA, H. 2009. Genotoxicity of nanomaterials: DNA damage and micronuclei induced by carbon nanotubes and graphite nanofibres in human bronchial epithelial cells in vitro. Toxicology Letters, 186, 166-173.

LIU, D., WANG, L., WANG, Z. & CUSCHIERI, A. 2012. Different cellular response mechanisms contribute to the length-dependent cytotoxicity of multi-walled carbon nanotubes. Nanoscale Research Letters, 7, 1-21.

LIU, H. L., ZHANG, Y. L., YANG, N., ZHANG, Y. X., LIU, X. Q., LI, C. G., ZHAO, Y., WANG, Y. G., ZHANG, G. G., YANG, P., GUO, F., SUN, Y. & JIANG, C. Y. 2011. A functionalized single-walled carbon nanotubeinduced autophagic cell death in human lung cells through Akt-TSC2-mTOR signaling. Cell Death and Disease, 2.

LIU, J., RINZLER, A. G., DAI, H., HAFNER, J. H., KELLEY BRADLEY, R., BOUL, P. J., LU, A., IVERSON, T., SHELIMOV, K., HUFFMAN, C. B., RODRIGUEZ-MACIAS, F., SHON, Y. S., LEE, T. R., COLBERT, D. T. & SMALLEY, R. E. 1998. Fullerene pipes. Science, 280, 1253-1256.

LIU, X., HOWARD, K. A., DONG, M., ANDERSEN, M. Ø., RAHBEK, U. L., JOHNSEN, M. G., HANSEN, O. C., BESENBACHER, F. & KJEMS, J. 2007. The influence of polymeric properties on chitosan/siRNA nanoparticle formulation and gene silencing. Biomaterials, 28, 1280-1288.

LIU, Z., DAVIS, C., CAI, W., HE, L., CHEN, X. & DAI, H. 2008. Circulation and long-term fate of functionalized, biocompatible single-walled carbon nanotubes in mice probed by Raman spectroscopy. Proceedings of the National Academy of Sciences of the United States of America, 105, 1410-1415.

LIU, Z., DONG, X., SONG, L., ZHANG, H., LIU, L., ZHU, D., SONG, C. & LENG, X. 2014. Carboxylation of multiwalled carbon nanotube enhanced its biocompatibility with L02 cells through decreased activation of mitochondrial apoptotic pathway. Journal of Biomedical Materials Research - Part A, 102, 665-673.

MA-HOCK, L., STRAUSS, V., TREUMANN, S., KÜTTLER, K., WOHLLEBEN, W., HOFMANN, T., GRÖTERS, S., WIENCH, K., VAN RAVENZWAAY, B. & LANDSIEDEL, R. 2013. Comparative inhalation toxicity of multi-wall carbon nanotubes, graphene, graphite nanoplatelets and low surface carbon black. Particle and Fibre Toxicology, 10.

MA, X., SHU, C., GUO, J., PANG, L., SU, L., FU, D. & ZHONG, W. 2014. Targeted cancer therapy based on single-wall carbon nanohorns with doxorubicin in vitro and in vivo. Journal of Nanoparticle Research, 16.

MAGREZ, A., KASAS, S., SALICIO, V., PASQUIER, N., SEO, J. W., CELIO, M., CATSICAS, S., SCHWALLER, B. & FORRÓ, L. 2006. Cellular toxicity of carbon-based nanomaterials. Nano Letters, 6, 1121-1125.

MALI, N., JADHAV, S., KARPE, M. & KADAM, V. 2011. Carbon nanotubes as carriers for delivery of bioactive and therapeutic agents: An overview. International Journal of Pharmacy and Pharmaceutical Sciences, 3, 45-52.

MANKE, A., WANG, L. & ROJANASAKUL, Y. 2013. Pulmonary toxicity and fibrogenic response of carbon nanotubes. Toxicology Mechanisms and Methods, 23, 196-206.

MAO, H., KAWAZOE, N. & CHEN, G. 2013. Uptake and intracellular distribution of collagen-functionalized single-walled carbon nanotubes. Biomaterials, 34, 2472-2479.

MARTÍN, O., GUTIERREZ, H. R., MAROTO-VALIENTE, A., TERRONES, M., BLANCO, T. & BASELGA, J. 2013a. An efficient method for the

carboxylation of few-wall carbon nanotubes with little damage to their sidewalls. Materials Chemistry and Physics, 140, 499-507.

MARTÍN, O., GUTIERREZ, H. R., MAROTO-VALIENTE, A., TERRONES, M., BLANCO, T. & BASELGA, J. 2013b. An efficient method for the carboxylation of few-wall carbon nanotubes with little damage to their sidewalls. Materials Chemistry and Physics.

MAUTER, M. S. & ELIMELECH, M. 2008. Environmental applications of carbon-based nanomaterials. Environmental Science and Technology, 42, 5843-5859.

MCCARTHY, N. 2012. Nanotechnology: Size matters. Nat Rev Cancer, 12, 7-7.

MEHRA, N. K., MISHRA, V. & JAIN, N. K. 2014. A review of ligand tethered surface engineered carbon nanotubes. Biomaterials, 35, 1267-1283.

MISEWICH, J. A., MARTEL, R., AVOURIS, P., TSANG, J. C., HEINZE, S. & TERSOFF, J. 2003. Electrically induced optical emission from a carbon nanotube FET. Science, 300, 783-786.

MITCHELL, L. A., LAUER, F. T., BURCHIEL, S. W. & MCDONALD, J. D. 2009. Mechanisms for how inhaled multiwalled carbon nanotubes suppress systemic immune function in mice. Nature Nanotechnology, 4, 451-456.

MORRISSEY, D. V., BLANCHARD, K., SHAW, L., JENSEN, K., LOCKRIDGE, J. A., DICKINSON, B., MCSWIGGEN, J. A., VARGEESE, C., BOWMAN, K., SHATTER, C. S., POLISKY, B. A. & ZINNEN, S. 2005. Activity of stabilized short interfering RNA in a mouse model of hepatitis B virus replication. Hepatology, 41, 1349-1356.

MU, Q., BROUGHTON, D. L. & YAN, B. 2009. Endosomal leakage and nuclear translocation of multiwalled carbon nanotubes: Developing a model for cell uptake. Nano Letters, 9, 4370-4375.

MUKERJEE, A., SHANKARDAS, J., RANJAN, A. P. & VISHWANATHA, J. K. 2011. Efficient nanoparticle mediated sustained RNA interference in human primary endothelial cells. Nanotechnology, 22.

MULLER, J., DECORDIER, I., HOET, P. H., LOMBAERT, N., THOMASSEN, L., HUAUX, F., LISON, D. & KIRSCH-VOLDERS, M. 2008. Clastogenic and aneugenic effects of multi-wall carbon nanotubes in epithelial cells. Carcinogenesis, 29, 427-433.

MULLER, J., HUAUX, F., MOREAU, N., MISSON, P., HEILIER, J.-F., DELOS, M., ARRAS, M., FONSECA, A., NAGY, J. B. & LISON, D. 2005. Respiratory toxicity of multi-wall carbon nanotubes. Toxicology And Applied Pharmacology, 207, 221-231.

MÜLLER, R. H., GOHLA, S. & KECK, C. M. 2011. State of the art of nanocrystals - Special features, production, nanotoxicology aspects and

intracellular delivery. European Journal of Pharmaceutics and Biopharmaceutics, 78, 1-9.

NAGAI, H., OKAZAKI, Y., CHEW, S. H., MISAWA, N., YAMASHITA, Y., AKATSUKA, S., ISHIHARA, T., YAMASHITA, K., YOSHIKAWA, Y., YASUI, H., JIANG, L., OHARA, H., TAKAHASHI, T., ICHIHARA, G., KOSTARELOS, K., MIYATA, Y., SHINOHARA, H. & TOYOKUNI, S. 2011. Diameter and rigidity of multiwalled carbon nanotubes are critical factors in mesothelial injury and carcinogenesis. Proceedings of the National Academy of Sciences, 108, E1330–E1338.

NEVES, V., HEISTER, E., COSTA, S., TÎLMACIU, C., FLAHAUT, E., SOULA, B., COLEY, H. M., MCFADDEN, J. & SILVA, S. R. P. 2012. Design of double-walled carbon nanotubes for biomedical applications. Nanotechnology, 23.

NUNES, A., AL-JAMAL, K. T. & KOSTARELOS, K. 2012. Therapeutics, imaging and toxicity of nanomaterials in the central nervous system. Journal Of Controlled Release, 161, 290-306.

OGASAWARA, Y., UMEZU, N. & ISHII, K. 2012. [DNA damage in human pleural mesothelial cells induced by exposure to carbon nanotubes]. Nihon eiseigaku zasshi. Japanese journal of hygiene, 67, 76-83.

OLIVEIRA, S., VAN ROOY, I., KRANENBURG, O., STORM, G. & SCHIFFELERS, R. M. 2007. Fusogenic peptides enhance endosomal escape improving siRNA-induced silencing of oncogenes. International Journal Of Pharmaceutics, 331, 211-214.

OSSWALD, S., HAVEL, M. & GOGOTSI, Y. 2007. Monitoring oxidation of multiwalled carbon nanotubes by Raman spectroscopy. Journal of Raman Spectroscopy, 38, 728-736.

OVERCHUK, M., PRYLUTSKA, S., BILYY, R., PRYLUTSKY, Y. & RITTER, U. The interaction of the carbon nanoparticles with human cell plasma membrane. 2013.

PALOMÄKI, J., VÄLIMÄKI, E., SUND, J., VIPPOLA, M., CLAUSEN, P. A., JENSEN, K. A., SAVOLAINEN, K., MATIKAINEN, S. & ALENIUS, H. 2011. Long, needle-like carbon nanotubes and asbestos activate the NLRP3 inflammasome through a similar mechanism. ACS Nano, 5, 6861-6870.

PANYAM, J. & LABHASETWAR, V. 2003. Biodegradable nanoparticles for drug and gene delivery to cells and tissue. Advanced Drug Delivery Reviews, 55, 329-347.

PARK, E. J., ZAHARI, N. E. M., LEE, E. W., SONG, J., LEE, J. H., CHO, M. H. & KIM, J. H. 2014. SWCNTs induced autophagic cell death in human bronchial epithelial cells. Toxicology in Vitro, 28, 442-450.

PATIL, M., PABLA, N. & DONG, Z. 2013. Checkpoint kinase 1 in DNA damage response and cell cycle regulation. Cellular and Molecular Life Sciences, 70, 4009-4021.

PATLOLLA, A., KNIGHTEN, B. & TCHOUNWOU, P. 2010a. Multi-walled carbon nanotubes induce cytotoxicity, genotoxicity and apoptosis in normal human dermal fibroblast cells. Ethnicity & Disease, 20, S1-65-72.

PATLOLLA, A. K., HUSSAIN, S. M., SCHLAGER, J. J., PATLOLLA, S. & TCHOUNWOU, P. B. 2010b. Comparative study of the clastogenicity of functionalized and nonfunctionalized multiwalled carbon nanotubes in bone marrow cells of Swiss-Webster mice. Environmental Toxicology, 25, 608-621.

PEJIN, B., IODICE, C., TOMMONARO, G., BOGDANOVIC, G., KOJIC, V. & DE ROSA, S. 2014. Further in vitro evaluation of cytotoxicity of the marine natural product derivative 4′-leucine-avarone. Natural Product Research, 28, 347-350.

PESCATORI, M., BEDOGNETTI, D., VENTURELLI, E., MÉNARD-MOYON, C., BERNARDINI, C., MURESU, E., PIANA, A., MAIDA, G., MANETTI, R., SGARRELLA, F., BIANCO, A. & DELOGU, L. G. 2013. Functionalized carbon nanotubes as immunomodulator systems. Biomaterials, 34, 4395-4403.

PICHARDO, S., GUTIÉRREZ-PRAENA, D., PUERTO, M., SÁNCHEZ, E., GRILO, A., CAMEÁN, A. M. & JOS, Á. 2012. Oxidative stress responses to carboxylic acid functionalized single wall carbon nanotubes on the human intestinal cell line Caco-2. Toxicology In Vitro, 26, 672-677.

POLAND, C. A., DUFFIN, R., KINLOCH, I., MAYNARD, A., WALLACE, W. A. H., SEATON, A., STONE, V., BROWN, S., MACNEE, W. & DONALDSON, K. 2008. Carbon nanotubes introduced into the abdominal cavity of mice show asbestos-like pathogenicity in a pilot study. Nature Nanotechnology, 3, 423-428.

POPOV, V. N. 2004. Carbon nanotubes: properties and application. Materials Science and Engineering: R: Reports, 43, 61-102.

PRATO, M., KOSTARELOS, K. & BIANCO, A. 2008. Functionalized carbon nanotubes in drug design and discovery. Accounts of Chemical Research, 41, 60-68.

QI, P., VERMESH, O., GRECU, M., JAVEY, A., WANG, Q., DAI, H., PENG, S. & CHO, K. J. 2003. Toward large arrays of multiplex functionalized carbon nanotube sensors for highly sensitive and selective molecular detection. Nano Letters, 3, 347-351.

RASTOGI, R., KAUSHAL, R., TRIPATHI, S. K., SHARMA, A. L., KAUR, I. & BHARADWAJ, L. M. 2008. Comparative study of carbon nanotube dispersion using surfactants. Journal of Colloid and Interface Science, 328, 421-428.

REN, J., SHEN, S., WANG, D., XI, Z., GUO, L., PANG, Z., QIAN, Y., SUN, X. & JIANG, X. 2012. The targeted delivery of anticancer drugs to brain glioma by PEGylated oxidized multi-walled carbon nanotubes modified with angiopep-2. Biomaterials, 33, 3324-3333.

RYTHER, R. C. C., FLYNT, A. S., PHILLIPS III, J. A. & PATTON, J. G. 2005. siRNA therapeutics: Big potential from small RNAs. Gene Therapy, 12, 5-11.

SAFARI, J. & ZARNEGAR, Z. 2014. Advanced drug delivery systems: Nanotechnology of health design A review. Journal of Saudi Chemical Society, 18, 85-99.

SARIGIANNIS, D. A., CIMINO REALE, G., COLLOTTA, A., RODA, E., MUSTARELLI, P., COCCINI, T. & MANZO, L. Genomic-level effects of carbon nanotubes. 2012.

SATO, Y., YOKOYAMA, A., SHIBATA, K. I., AKIMOTO, Y., OGINO, S. I., NODASAKA, Y., KOHGO, T., TAMURA, K., AKASAKA, T., UO, M., MOTOMIYA, K., JEYADEVAN, B., ISHIGURO, M., HATAKEYAMA, R., WATARI, F. & TOHJI, K. 2005. Influence of length on cytotoxicity of multi-walled carbon nanotubes against human acute monocytic leukemia cell line THP-1 in vitro and subcutaneous tissue of rats in vivo. Molecular BioSystems, 1, 176-182.

SAXENA, R. K., WILLIAMS, W., MCGEE, J. K., DANIELS, M. J., BOYKIN, E. & GILMOUR, M. I. 2007. Enhanced in vitro and in vivo toxicity of poly-dispersed acid-functionalized single-wall carbon nanotubes. Nanotoxicology, 1, 291-300.

SCHEINBERG, D. A., MCDEVITT, M. R., DAO, T., MULVEY, J. J., FEINBERG, E. & ALIDORI, S. 2013. Carbon nanotubes as vaccine scaffolds. Advanced Drug Delivery Reviews, 65, 2016-2022.

SCHIPPER, M. L., NAKAYAMA-RATCHFORD, N., DAVIS, C. R., KAM, N. W. S., CHU, P., LIU, Z., SUN, X., DAI, H. & GAMBHIR, S. S. 2008. A pilot toxicology study of single-walled carbon nanotubes in a small sample of mice. Nature Nanotechnology, 3, 216-221.

SHENG, S. L., LIU, J. J., DAI, Y. H., SUN, X. G., XIONG, X. P. & HUANG, G. 2012. Knockdown of lactate dehydrogenase A suppresses tumor growth and metastasis of human hepatocellular carcinoma. FEBS Journal, 279, 3898-3910.

SHVEDOVA, A. A., CASTRANOVA, V., KISIN, E. R., SCHWEGLER-BERRY, D., MURRAY, A. R., GANDELSMAN, V. Z., MAYNARD, A. & BARON, P. 2003. Exposure to carbon nanotube material: Assessment of nanotube cytotoxicity using human keratinocyte cells. Journal of Toxicology and Environmental Health - Part A, 66, 1909-1926.

SHVEDOVA, A. A., KISIN, E. R., MERCER, R., MURRAY, A. R., JOHNSON, V. J., POTAPOVICH, A. I., TYURINA, Y. Y., GORELIK, O., AREPALLI, S.,

SCHWEGLER-BERRY, D., HUBBS, A. F., ANTONINI, J., EVANS, D. E., KU, B. K., RAMSEY, D., MAYNARD, A., KAGAN, V. E., CASTRANOVA, V. & BARON, P. 2005. Unusual inflammatory and fibrogenic pulmonary responses to single-walled carbon nanotubes in mice. American Journal of Physiology - Lung Cellular and Molecular Physiology, 289, L698-L708.

SHVEDOVA, A. A., KISIN, E. R., MURRAY, A. R., GORELIK, O., AREPALLI, S., CASTRANOVA, V., YOUNG, S. H., GAO, F., TYURINA, Y. Y., OURY, T. D. & KAGAN, V. E. 2007. Vitamin E deficiency enhances pulmonary inflammatory response and oxidative stress induced by single-walled carbon nanotubes in C57BL/6 mice. Toxicology and Applied Pharmacology, 221, 339-348.

SIMON-DECKERS, A., GOUGET, B., MAYNE-L'HERMITE, M., HERLIN-BOIME, N., REYNAUD, C. & CARRIÈRE, M. 2008. In vitro investigation of oxide nanoparticle and carbon nanotube toxicity and intracellular accumulation in A549 human pneumocytes. Toxicology, 253, 137-146.

SINGH, R. P., DAS, M., THAKARE, V. & JAIN, S. 2012. Functionalization density dependent toxicity of oxidized multiwalled carbon nanotubes in a murine macrophage cell line. Chemical Research in Toxicology, 25, 2127-2137.

SIU, K. S., CHEN, D., ZHENG, X., ZHANG, X., JOHNSTON, N., LIU, Y., YUAN, K., KOROPATNICK, J., GILLIES, E. R. & MIN, W. P. 2014. Non-covalently functionalized single-walled carbon nanotube for topical siRNA delivery into melanoma. Biomaterials, 35, 3435-3442.

SKOREK, R., ZAWISZA, B., MARGUÍ, E., QUERALT, I. & SITKO, R. 2013. Dispersive micro solid-phase extraction using multiwalled carbon nanotubes for simultaneous determination of trace metal ions by energy-dispersive x-ray fluorescence spectrometry. Applied Spectroscopy, 67, 204-209.

SMART, S. K., CASSADY, A. I., LU, G. Q. & MARTIN, D. J. 2006. The biocompatibility of carbon nanotubes. Carbon, 44, 1034-1047.

SOENEN, S. J. H., ILLYES, E., VERCAUTEREN, D., BRAECKMANS, K., MAJER, Z., DE SMEDT, S. C. & DE CUYPER, M. 2009. The role of nanoparticle concentration-dependent induction of cellular stress in the internalization of non-toxic cationic magnetoliposomes. Biomaterials, 30, 6803-6813.

SOFUNI, T., HONMA, M., HAYASHI, M., SHIMADA, H., TANAKA, N., WAKURI, S., AWOGI, T., YAMAMOTO, K. I., NISHI, Y. & NAKADATE, M. 1996. Detection of in vitro clastogens and spindle poisons by the mouse lymphoma assay using the micro well method: interim report of an international collaborative study. Mutagenesis, 11, 349-355.

SONG, M., ZENG, L., YUAN, S., YIN, J., WANG, H. & JIANG, G. 2013. Study of cytotoxic effects of single-walled carbon nanotubes functionalized with

different chemical groups on human MCF7 cells. Chemosphere, 92, 576-582.

SRIVASTAVA, R. K., PANT, A. B., KASHYAP, M. P., KUMAR, V., LOHANI, M., JONAS, L. & RAHMAN, Q. 2011. Multi-walled carbon nanotubes induce oxidative stress and apoptosis in human lung cancer cell line-A549. Nanotoxicology, 5, 195-207.

STOKER, E., PURSER, F., KWON, S., PARK, Y. B. & LEE, J. S. 2008. Alternative estimation of human exposure of single-walled carbon nanotubes using three-dimensional tissue-engineered human lung. International Journal of Toxicology, 27, 441-448.

SUBBIAH, R., RAMASUNDARAM, S., DU, P., KIM, H., SUNG, D., PARK, K., LEE, N. E., YUN, K. & CHOI, K. J. 2013. Evaluation of cytotoxicity, biophysics and biomechanics of cells treated with functionalized hybrid nanomaterials. Journal of the Royal Society Interface, 10.

SWEENEY, S., BERHANU, D., MISRA, S. K., THORLEY, A. J., VALSAMI-JONES, E. & TETLEY, T. D. 2014. Multi-walled carbon nanotube length as a critical determinant of bioreactivity with primary human pulmonary alveolar cells. Carbon, 78, 26-37.

TAGMATARCHIS, N. & PRATO, M. 2004. Functionalization of carbon nanotubes via 1,3-dipolar cycloadditions. Journal of Materials Chemistry, 14, 437-439.

TAHERMANSOURI, H. & GHOBADINEJAD, H. 2013. Functionalization of short multi-walled carbon nanotubes with creatinine and aromatic aldehydes via microwave and thermal methods and their influence on the MKN45 and MCF7 cancer cells. Comptes Rendus Chimie, 16, 838-844.

TAN, J. M., FOO, J. B., FAKURAZI, S. & HUSSEIN, M. Z. 2015. Release behaviour and toxicity evaluation of levodopa from carboxylated single-walled carbon nanotubes. Beilstein Journal of Nanotechnology, 6, 243-253.

TAN, J. M., KARTHIVASHAN, G., ARULSELVAN, P., FAKURAZI, S. & HUSSEIN, M. Z. 2014. In vitro nanodelivery of silibinin as an anticancer drug under pH response. Journal of Drug Delivery Science and Technology, 24, 579-584.

TASIS, D., TAGMATARCHIS, N., GEORGAKILAS, V. & PRATO, M. 2003. Soluble carbon nanotubes. Chemistry - A European Journal, 9, 4000-4008.

TEHRANI, M. S., AZAR, P. A., NAMIN, P. E. & DEHAGHI, S. M. 2013. Removal of Lead Ions from Wastewater Using Functionalized Multiwalled Carbon Nanotubes with Tris (2-Aminoethyl) Amine.

THONGKUMKOON, P., SANGWIJIT, K., CHAIWONG, C., THONGTEM, S., SINGJAI, P. & YU, L. D. 2014. Direct nanomaterial-DNA contact effects on DNA and mutation induction. Toxicology Letters, 226, 90-97.

TIAN, L., LIN, Z. Q., LIN, B. C., LIU, H. L., YAN, J. & XI, Z. G. 2013. Single wall carbon nanotube induced inflammation in cruor-fibrinolysis system. Biomedical and environmental sciences : BES, 26, 338-345.

URSINI, C. L., CAVALLO, D., FRESEGNA, A. M., CIERVO, A., MAIELLO, R., BURESTI, G., CASCIARDI, S., TOMBOLINI, F., BELLUCCI, S. & IAVICOLI, S. 2012a. Comparative cyto-genotoxicity assessment of functionalized and pristine multiwalled carbon nanotubes on human lung epithelial cells. Toxicology in Vitro, 26, 831-840.

URSINI, C. L., CAVALLO, D., FRESEGNA, A. M., CIERVO, A., MAIELLO, R., CASCIARDI, S., TOMBOLINI, F., BURESTI, G. & IAVICOLI, S. 2012b. Study of cytotoxic and genotoxic effects of hydroxyl-functionalized multiwalled carbon nanotubes on human pulmonary cells. Journal of Nanomaterials, 2012.

UUSITALO, L. M. & HEMPEL, N. 2012. Recent advances in intracellular and in vivo ROS sensing: Focus on nanoparticle and nanotube applications. International Journal of Molecular Sciences, 13, 10660-10679.

VAN BERLO, D., CLIFT, M., ALBRECHT, C. & SCHINS, R. 2012. Carbon nanotubes: An insight into the mechanisms of their potential genotoxicity. Swiss Medical Weekly, 142.

VAN DER ZANDE, M., JUNKER, R., WALBOOMERS, X. F. & JANSEN, J. A. 2011. Carbon nanotubes in animal models: A systematic review on toxic potential. Tissue Engineering - Part B: Reviews, 17, 57-69.

VARDHARAJULA, S., ALI, S. Z., TIWARI, P. M., EROĞLU, E., VIG, K., DENNIS, V. A. & SINGH, S. R. 2012. Functionalized carbon nanotubes: Biomedical applications. International Journal of Nanomedicine, 7, 5361-5374.

VASHIST, S. K., ZHENG, D., PASTORIN, G., AL-RUBEAAN, K., LUONG, J. H. T. & SHEU, F. S. 2011. Delivery of drugs and biomolecules using carbon nanotubes. Carbon, 49, 4077-4097.

WADA, H., KANEKO, T., OHIWA, M., TANIGAWA, M., TAMAKI, S., MINAMI, N., TAKAHASHI, H., DEGUCHI, K., NAKANO, T. & SHIRAKAWA, S. 1992. Plasma cytokine levels in thrombotic thrombocytopenic purpura. Am J Hematol, 40, 167-70.

WALKER, P. R., KOKILEVA, L., LEBLANC, J. & SIKORSKA, M. 1993. Detection of the initial stages of DNA fragmentation in apoptosis. BioTechniques, 15, 1032-1040.

WANG, F. D., ZHANG, H., JIN, C., LIANG, H., TANG, Y. & YANG, Y. J. 2014a. Nanotoxicity of multiwall carbon nanotubes to a549 cells in vitro. Nano, 9.

WANG, J., SUN, P., BAO, Y., DOU, B., SONG, D. & LI, Y. 2012. Vitamin E renders protection to PC12 cells against oxidative damage and apoptosis induced by single-walled carbon nanotubes. Toxicology in Vitro, 26, 32-41.

WANG, L. R., XUE, X., HU, X. M., WEI, M. Y., ZHANG, C. Q., GE, G. L. & LIANG, X. J. 2014b. Structure-dependent mitochondrial dysfunction and hypoxia induced with single-walled carbon nanotubes. Small, 10, 2859-2869.

WANG, X., XIA, T., ADDO NTIM, S., JI, Z., LIN, S., MENG, H., CHUNG, C. H., GEORGE, S., ZHANG, H., WANG, M., LI, N., YANG, Y., CASTRANOVA, V., MITRA, S., BONNER, J. C. & NEL, A. E. 2011. Dispersal state of multiwalled carbon nanotubes elicits profibrogenic cellular responses that correlate with fibrogenesis biomarkers and fibrosis in the murine lung. ACS Nano, 5, 9772-9787.

WEN, S., LIU, H., CAI, H., SHEN, M. & SHI, X. 2013. Targeted and pH-responsive delivery of doxorubicin to cancer cells using multifunctional dendrimer-modified multi-walled carbon nanotubes. Advanced Healthcare Materials, 2, 1267-1276.

WICK, P., MANSER, P., LIMBACH, L. K., DETTLAFF-WEGLIKOWSKA, U., KRUMEICH, F., ROTH, S., STARK, W. J. & BRUININK, A. 2007. The degree and kind of agglomeration affect carbon nanotube cytotoxicity. Toxicology Letters, 168, 121-131.

WIN-SHWE, T. T. & FUJIMAKI, H. 2011. Nanoparticles and Neurotoxicity. International Journal of Molecular Sciences, 12, 6267-6280.

XIAO, H., ZHU, B., WANG, D., PANG, Y., HE, L., MA, X., WANG, R., JIN, C., CHEN, Y. & ZHU, X. 2012. Photodynamic effects of chlorin e6 attached to single wall carbon nanotubes through noncovalent interactions. Carbon, 50, 1681-1689.

YAN, L., LI, G. X., ZHANG, S., SUN, F., HUANG, X. J., ZHANG, Q., DAI, L. M., LU, F. & LIU, Y. 2013. Cytotoxicity and genotoxicity of multi-walled carbon nanotubes with human ocular cells. Chinese Science Bulletin, 58, 2347-2352.

YAN, L., ZHANG, S., ZENG, C., XUE, Y., ZHOU, Z., LU, F., CHEN, H., QU, J., DAI, L. & LIU, Y. 2011. Cytotoxicity of single-walled carbon nanotubes with human ocular cells.

YANG, H. Y., VONK, L. A., LICHT, R., VAN BOXTEL, A. M. G., BEKKERS, J. E. J., KRAGTEN, A. H. M., HEIN, S., VARGHESE, O. P., HOWARD, K. A., CUMHUR ÖNER, F., DHERT, W. J. A. & CREEMERS, L. B. 2014. Cell type and transfection reagent-dependent effects on viability, cell content, cell cycle and inflammation of RNAi in human primary mesenchymal cells. European Journal of Pharmaceutical Sciences, 53, 35-44.

YE, S. F., WEN, W., WANG, Y. F., LIN, C. L., WU, Y. H. & ZHANG, Q. Q. 2010. Multi-walled carbon nanotubes induces nuclear factor-κB activation in A549 Cells. Gaodeng Xuexiao Huaxue Xuebao/Chemical Journal of Chinese Universities, 31, 497-501.

YE, S. F., WU, Y. H., HOU, Z. Q. & ZHANG, Q. Q. 2009. ROS and NF-κB are involved in upregulation of IL-8 in A549 cells exposed to multi-walled carbon nanotubes. Biochemical and Biophysical Research Communications, 379, 643-648.

YOO, J.-W., DOSHI, N. & MITRAGOTRI, S. 2011. Adaptive micro and nanoparticles: Temporal control over carrier properties to facilitate drug delivery. Advanced Drug Delivery Reviews, 63, 1247-1256.

YOONG, S. L., WONG, B. S., ZHOU, Q. L., CHIN, C. F., LI, J., VENKATESAN, T., HO, H. K., YU, V., ANG, W. H. & PASTORIN, G. 2014. Enhanced cytotoxicity to cancer cells by mitochondria-targeting MWCNTs containing platinum(IV) prodrug of cisplatin. Biomaterials, 35, 748-759.

ZHANG, J., LI, X. & HUANG, L. 2014a. Non-viral nanocarriers for siRNA delivery in breast cancer. Journal of Controlled Release, 190, 440-450.

ZHANG, L., HOU, P. X., LI, S., SHI, C., CONG, H. T., LIU, C. & CHENG, H. M. 2014b. In situ TEM observations on the sulfur-assisted catalytic growth of single-wall carbon nanotubes. Journal of Physical Chemistry Letters, 5, 1427-1432.

ZHANG, Y. & HUNTER, T. 2014. Roles of Chk1 in cell biology and cancer therapy. International Journal of Cancer, 134, 1013-1023.

ZHU, L., CHANG, D. W., DAI, L. & HONG, Y. 2007. DNA damage induced by multiwalled carbon nanotubes in mouse embryonic stem cells. Nano Letters, 7, 3592-3597.

APPENDICES

Appendix A **MTT assay**

MTT assay is a colorimetric assay for assessing cell viability. NADPH-dependent cellular oxidoreductase enzymes may reflect the number of viable cells present. These enzymes are capable of reducing the terazolium dye to its insoluble formazan which has a purple colour. Usually a solubilisation solution (dimethyl sulfoxide, an acidified ethanol solution, or a solution of the detergent sodium dodecyl sulphate in diluted hydrochloric acid) is added to dissolve the insoluble purple formazan product into a coloured solution (Figure_Apx 1). We could also observe the MWCNT on the bottom of each well, which will interfere with the absorbance.

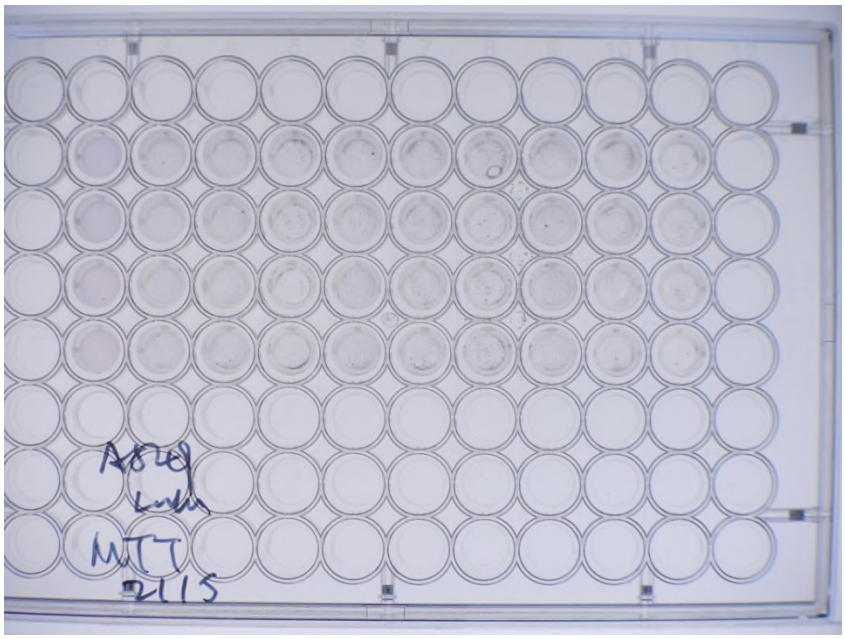

Figure_Apx 1 Picture of MTT formazan

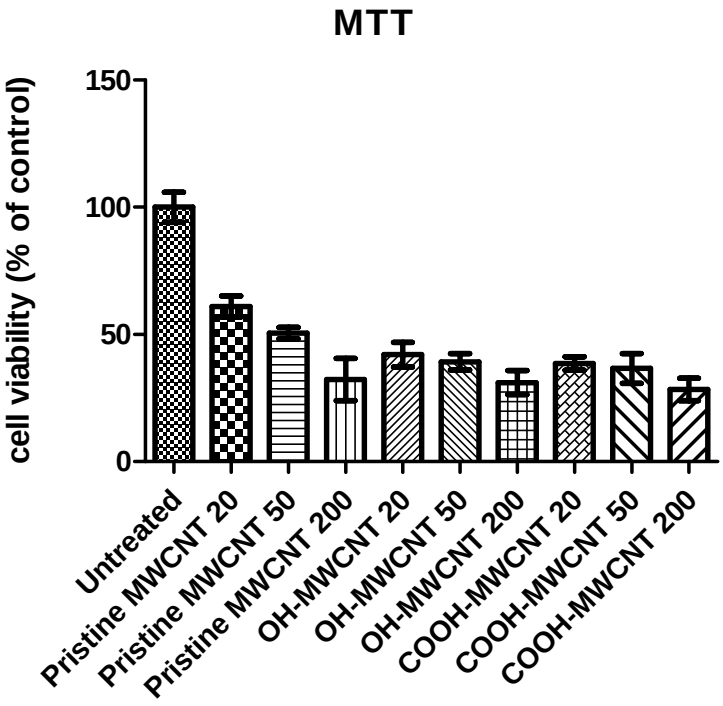

Figure_Apx 2 Cell viability of A549 cells using MTT

MTT assay showed big error bar on cells viability after treatment with carbon nanotubes which interfere with the absorbance at 570nm. In this sense, MTT assay is not suitable for cell viability test.

Appendix B **Cytotoxicity of MCF-7 and MRC-5**

B.1.1 Cell viability of MCF-7 and MRC-5 cells

The data of cell viability of MCF-7 and MRC-5 cell lines were converted to percentage of negative control. Both cell lines were treated at the exactly as condition as A549 using the same reagents.

Figure_Apx 3 described that all three type of MWCNTs could significant induce cell death in MCF-7 cells. Cell viability of MCF-7 exhibited dose dependent matter. After 24 hours' incubation with WMCNTs, cell viability dropped to less than 50% at both 50 and 200µg/mL. Pristine MWCNTs induced significantly more cell death than functionalised MWCNTs.

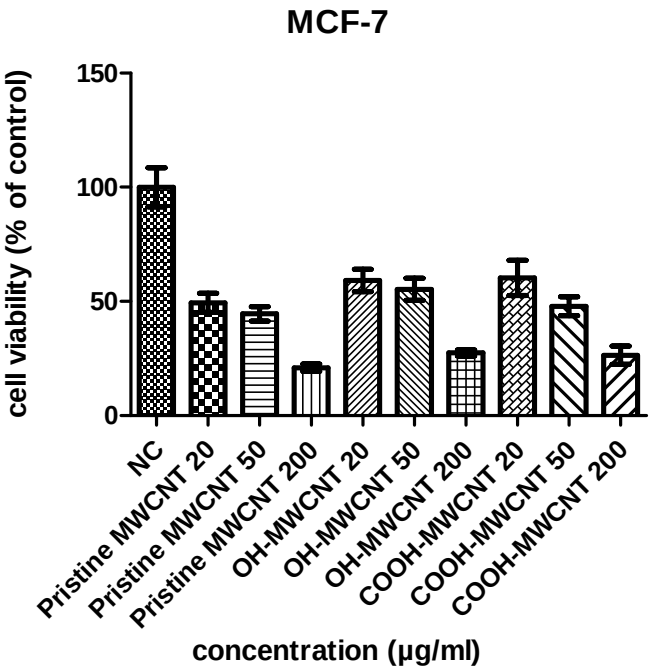

Figure_Apx 3 Results of cell viability assay study. MCF-7 cells was evaluated after 24 hours exposure to pristine MWCNTs, OH-MWCNTs and COOH-MWCNTs with concentrations from 20 to 200 µg/mL. Viability was detected by using WST-1 assay. Data are represented as mean of percentage of control±SD of triplicate. * p<0.05, **p<0.01, ***p<0.001.

Figure_Apx 4 described the cell loss of MRC-5 cells induced by three types of MWCNTs. MRC-5 cell line also exhibited a dose dependent pattern to MWCNTs. At 20 and 50 µg/mL, viability of treated MRC-5 cells was all beyond 50% of control. When the concentrations were increased to 200µg/mL, cell viability dropped to less than half of the non-treated cells. In addition, similar to MCF-7 cells, MRC-5 cells were also more sensitive to pristine MWCNTs, which means that, pristine MWNCTs induced significant more cell death than functionalised MWCNTs.

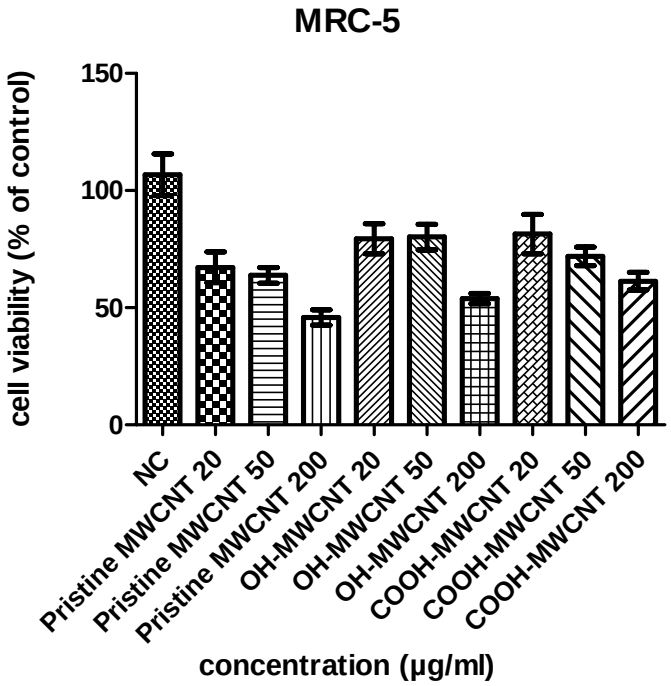

Figure_Apx 4 Results of cell viability assay study. MRC-5 cells was evaluated after 24 hours exposure to pristine MWCNTs, OH-MWCNTs and COOH-MWCNTs with concentrations from 20 to 200 µg/mL. Viability was detected by using WST-1 assay. Data are represented as mean of percentage of control±SD of triplicate. * p<0.05, **p<0.01, ***p<0.001.

B.1.2 Membrane damage of MCF-7 and MRC-5 cell line

The data of cell membrane damage of MCF-7 and MRC-5 were also converted to percentage of negative control.

This figure described that all three types of MWCNTs could induced significant higher level of LDH release than negative control. Among them, MCF-7 cells were most sensitive to pristine MWCNTs which induced 2 times more LDH release than negative control.

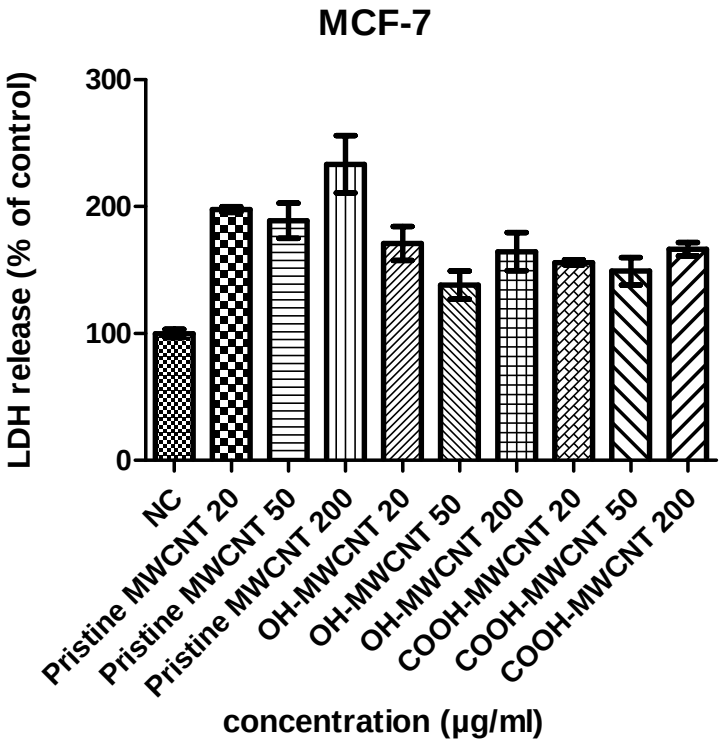

Figure_Apx 5 LDH release assay. Cytotoxicity of all the cell lines was evaluated after 24 hours exposure to pristine MWCNTs, OH-MWCNTs and COOH-MWCNTs with concentrations from 20 to 200 µg/mL. Viability was detected by using LDH assay. Data are represented as mean±SD of triplicate. * p<0.05, **p<0.01, ***p<0.001. ROS generation

MRC-5 cells didn't exhibited significant LDH release induced by functionalised MWCNTs. But pristine MWCNTs at 20 and 50µg/mL induced significant more LDH release than negative control.

Both Figure_Apx 4 and Figure_Apx 5 exhibited that MCF-7 and MRC-5 cells are more sensitive to pristine MWCNTs rather than functionalised MWCNTs.

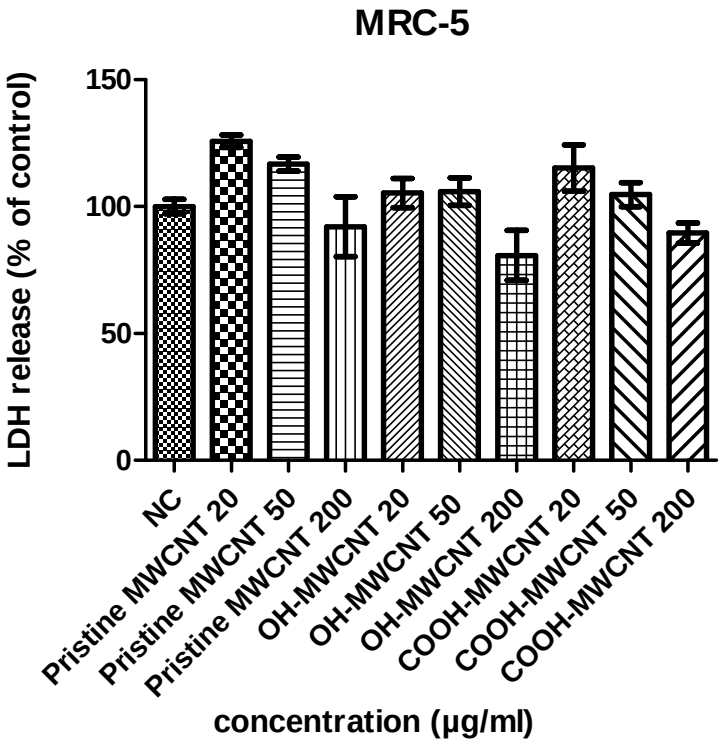

LDH release assay. Cytotoxicity of all the cell lines was evaluated after 24 hours exposure to pristine MWCNTs, OH-MWCNTs and COOH-MWCNTs with concentrations from 20 to 200 µg/mL. Viability was detected by using LDH assay. Data are represented as mean±SD of triplicate. * p<0.05, **p<0.01, ***p<0.001. ROS generation

B.1.3 Apoptosis detection in MCF-7 cell line

As MCF-7 cells were stably transformed with enhanced green fluorescent protein, we choose to use Annexin V-PE, 7-AAD instead of using Annexin V-FITC, PI for apoptosis detection to avoid the interference with green fluorescent protein from apoptotic cells.

Different form the apoptosis pattern in A549 cells, MWNCTs induced overall less apoptosis in MCF-7 cells. In A549 cells, pristine MWCNTs exerted least apoptosis. However, in contrast, pristine MWCNT induced most cell apoptosis in MCF-7 cells.

At 20μg/mL, MCF-7 cells treated with pristine MWCNT, OH-MWCNT and COOH-MWCNT showed 1.77, 1.51 and 1.49 times apoptosis of untreated cells. At 50μg/mL, we didn't see significant difference among different types of carbon nanotubes. However, the overall percentage of apoptosis is significantly lower than that of A549 cells.

Table_Apx 1 Cell apoptosis induced by three types of MWCNTs in MCF-7

	Non-treated	**Pristine MWCNT**	**OH-MWCNT**	**COOH-MWCNT**
20μg/mL	4.33%±0..25%	7.70%±0.17%	6.56%±0.20%	6.47%±0.29%
50μg/mL	7.17%±0.72%	10.87%±0.45%	10.37%±0.35%	10.6%±0.61%

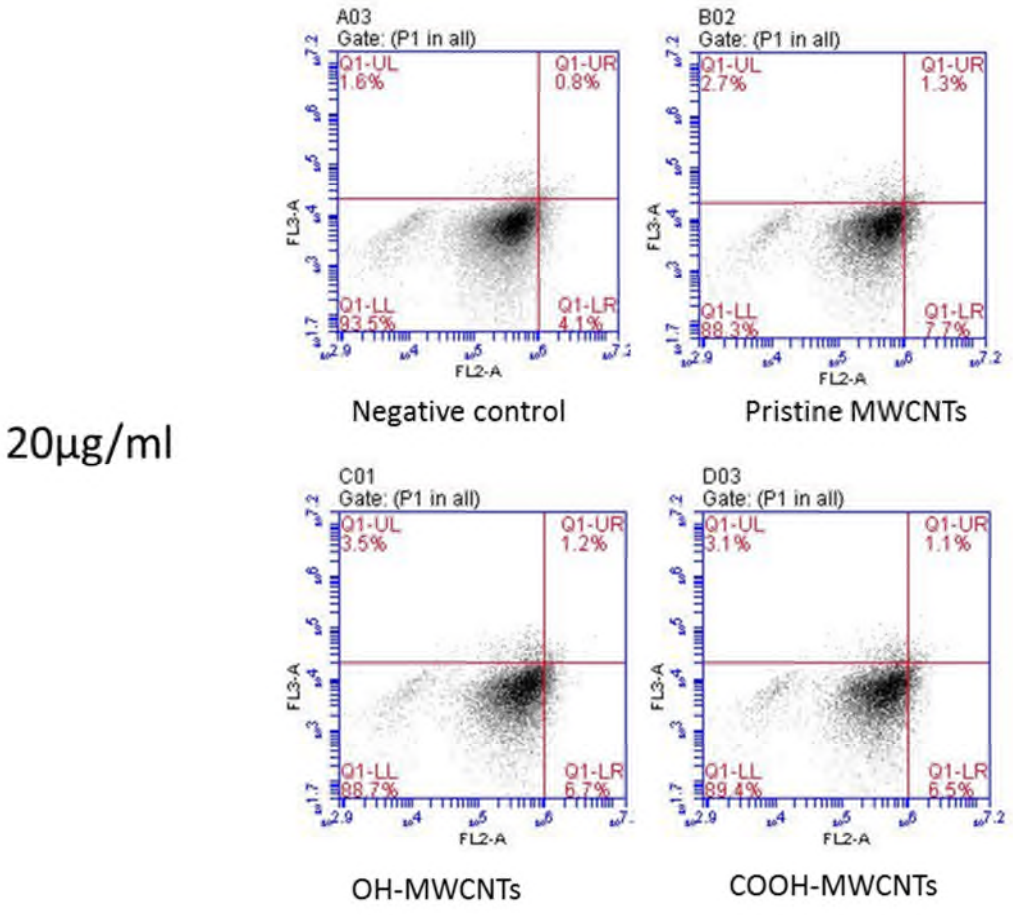

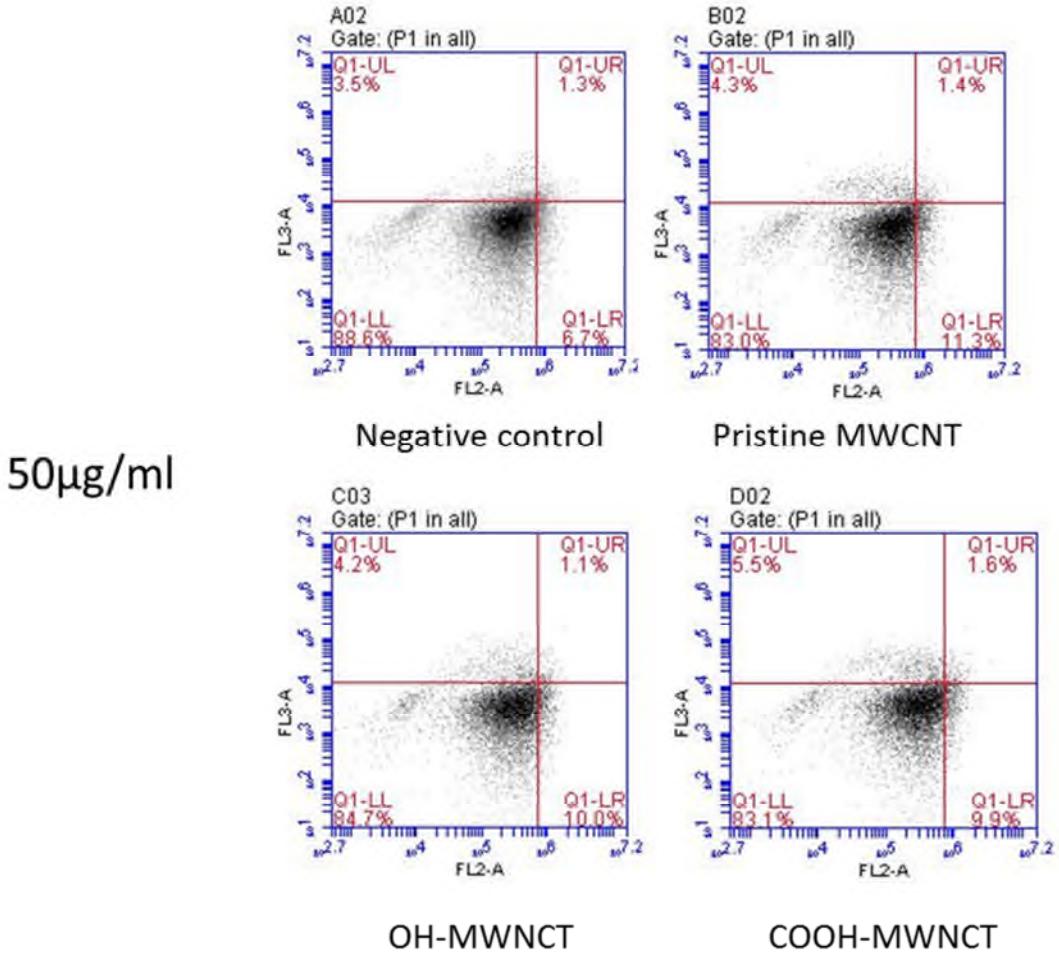

Figure_Apx 6 Flow cytometry Annexin V-PE, 7-AAd apoptosis detection after 48 hours exposure to 20, 50µg/mL MWCNTs in MCF-7

Appendix C **Cytotoxicity of NH_2-MWCNT applied in siRNA delivery**

C.1 Cell viability of NH2-MWCNT compared with pristine and functionalized MWCNTs

The cell viability has been evaluated using four types of MWCNTs on A549 cells. Here, we mainly aim to look at the toxicity of NH_2-MWCNTs. At 20 and 50µg/mL, there's no significant difference among all the MWCNTs. However, at 200µg/mL, NH_2-MWCNTs exhibited more toxicity than the other two functionalised MWCNT but less toxicity than pristine one. As explained in chapter four,

functionalized carbon nanotubes are more easily aggregated, in which case, decrease the efficient dose in the medium, subsequently, cause less cell death.

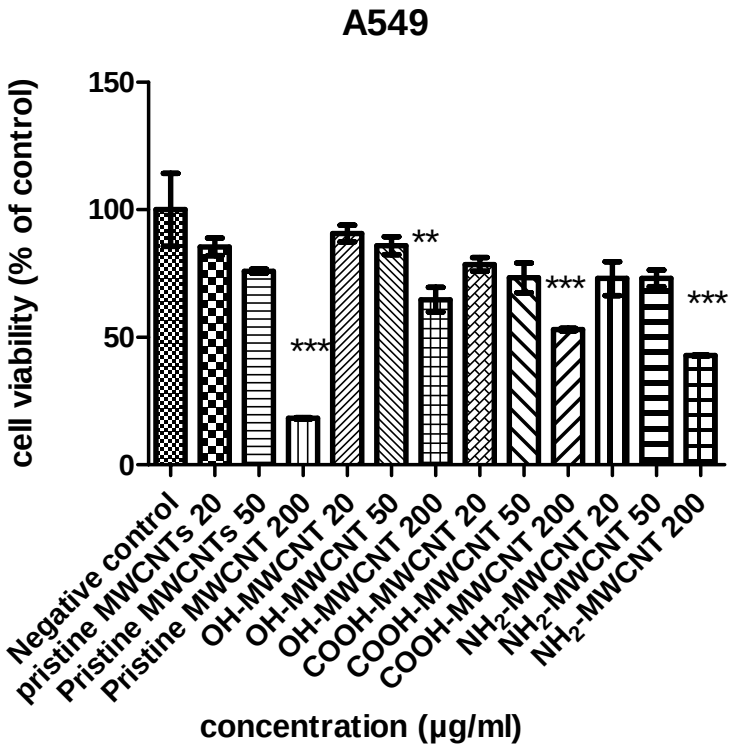

Figure_Apx 7 Cytotoxicity of A549 cells was evaluated after 24 hrs exposure to pristine MWCNTs, OH-MWCNTs and COOH-MWCNTs with concentrations from 20 to 200 µg/mL. Viability was detected by using WST-1 assay. Data are represented as mean±SD of triplicate.